Czech Technical University in Prague

Faculty of Electrical Engineering
Department of Control Engineering

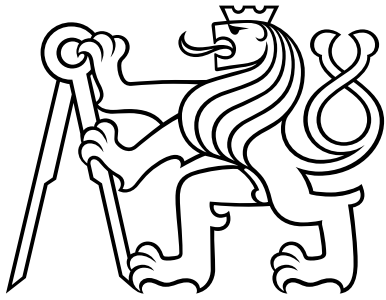

Doctoral Thesis

Consensus and Synchronization

in Distributed Estimation and Adaptive Control

by Ing. Štefan Knotek

presented to the Faculty of Electrical Engineering,
Czech Technical University in Prague,
in partial fulfillment of the requirements
for the degree of
Doctor of Philosophy

Ph.D. program: Electrical Engineering and Information Technology
Branch of study: Control Engineering and Robotics
Supervisor: Prof. Ing. Michael Šebek, DrSc.
Co-supervisor: Doc. Kristian Hengster-Movric, Ph.D.

October 2020

Acknowledgement

Writing of this doctoral thesis would not be possible without all the great people at the Department of Control Engineering that supported me and helped me throughout my doctoral studies. They taught me not only science but also life and guided me towards my research. Thanks to them, I had a wonderful time during my studies, and it stays forever in my memories.

First of all, I would like to thank my supervisor, Professor Michael Šebek, and supervisor specialist, Kristian Hengster-Movric, for their trust, belief, and support in pursuing new research topics. They provided me everything I needed to work on my research topic and to continue my studies. Big thanks also belong to my previous colleagues Ivo Herman and Dan Martinec, for helping me out at the beginning of my studies and guiding me toward my first research achievements. I am thankful to Martin Hromčík and Jiří Dostál for opportunities to collaborate on industrial-grade projects. Martin's optimism and humor made the research and collaboration on the projects more joy than hard work. Nonetheless, excellent team-building activities organized by Jirka will forever stay in my memories. I am graceful to Zdeněk Hurák and the members of the AA4CC group, Martin Gurtner, Tomáš Michálek, Jiří Zemánek, to name only a few, for accepting me as a member and a colleague. I will always remember the fun we had during our talks with Martin Gurtner, Pavel Otta, Filip Svoboda, and Jaroslav Tabaček. Also, I will never forget my colleagues and friends Daniel Wagner, Zhongzhe Dong, and Xueji Zhang, which showed me that hard work always pays out.

Last but not least, I would like to thank my family and my girlfriend, Aneta, for their immense love, care, and support during my Ph.D. studies. My deepest gratitude belongs to my parents, as they taught me never to give up on my goals and dreams no matter where they led me.

Declaration

This doctoral thesis is submitted in partial fulfillment of the requirements for the degree of doctor (Ph.D.). The work submitted in this dissertation is the result of my own investigation, except where otherwise stated. I declare that I worked out this thesis independently and I quoted all used sources of information in accord with Methodical instructions of CTU in Prague about ethical principles for writing academic thesis. Moreover I declare that it has not already been accepted for any degree and is also not being concurrently submitted for any other degree.

Czech Technical University in Prague
October 2020

Štefan Knotek

Abstract

This thesis brings two complementary approaches for distributed control and estimation in spatially interconnected multi-agent systems. In particular, the first approach brings a distributed estimation scheme for large-scale systems. The plant is considered affected by process disturbance, and measurements are corrupted by measurement noise. The proposed approach fuses measurements of differing reliability so that all nodes reach consensus on the plant's state estimate. This architecture is flexible to addition of new nodes and, to a certain extent, robust to node or communication link failures. This follows from a protocol allowing existence of nodes that do not measure anything but contribute to the data fusion in the sensor network. Hence, in spite of limited observability by each of the nodes, data fusion over sensor network allows each node to obtain the full estimate of the plant's state. Structured Lyapunov functions are used to prove the convergence of the estimator. Resulting estimation error covariances are analyzed in detail.

The second approach introduces a fully distributed adaptive protocol for consensus and synchronization in multi-agent systems on directed communication networks. Agents are modeled as general linear time-invariant systems. The proposed protocol introduces a novel adaptation scheme allowing control coupling gains to decay to their reference values. This approach improves upon existing adaptive consensus protocols, which may result in overly large or even unbounded coupling gains. The protocol design in this paper does not rely on any centralized information; hence it is fully distributed. Nevertheless, the price to pay for this is the need to estimate those reference values. Convergence of the overall network dynamics is guaranteed for correctly estimated references; otherwise, the trajectory of the system is only uniformly ultimately bounded. Two estimation algorithms are proposed: one based on the interval-halving method and the other based on a distributed estimation of Laplacian eigenvalues.

Keywords

Adaptive control, consensus, cooperative control, distributed control, distributed estimation, multi-agent systems, sensor fusion, sensor networks.

Abstrakt

Táto práca sa zaoberá dvoma komplementárnymi prístupmi pre distribuované riadenie a odhadovanie na priestorovo rozprostrených multiagentových systémoch. Prvý prístup sa venuje distribuovanému odhadovaniu veľkého systému pri predpoklade, že na stavy systému a merania pôsobí šum. Princíp navrhovanej metódy spočíva vo fúzii meraní s rôznou presnosťou tak, aby všetci agenti v sieti dosiahli konsensus na odhade stavu pozorovaného systému. Táto architektúra umožňuje existenciu agentov ktorí nič nemerajú, avšak prispievajú k šíreniu informácií v sieti, a zároveň dovoľuje pridávanie nových agentov do siete, čo vedie ku zvýšeniu odolnosti voči zlyhaniu komunikačnej linky alebo samotného agenta. Vďaka tomu, aj napriek obmedzenej pozorovateľnosti odhadovaného systému z pohľadu každého agenta, vedie fúzia dát zo siete k úplnej rekonštrukcii stavu pozorovaného systému každým agentom samostatne. Na preukázanie konvergencie odhadov agentov sú použité štruktúrované Lyapunove funkcie. Výsledné kovariancie chýb odhadu sú podrobené detailnej analýze.

Druhý prístup prezentuje plne distribuovaný adaptívny protokol pre konsensus a synchronizáciu multiagentových systémov na orientovaných grafoch. Navrhovaný distribuovaný protokol prináša novú adaptačnú schému, ktorá umožňuje aby riadiace väzobné zosilnenia klesali ku ich referenčným hodnotám. Tento prístup rieši problémy súčasných distribuovaných adaptívnych protokolov, ktoré môžu dosahovať veľmi veľké alebo dokonca neobmedzené väzobné zosilnenia. Návrh samotného adaptívneho protokolu nevyžaduje žiadnu centralizovanú informáciu, preto je plne distribuovaný. Avšak, daň za to spočíva v potrebe odhadovať referenčné hodnoty pre väzobné zosilnenia. Pri správnom odhade týchto referencii je zaručená stabilita protokolu, v opačnom prípade je trajektória samotnej siete obmedzená v určitom pásme. Pre odhad referencií sú vyvinuté dva algoritmy: prvý je založený na metóde polovičného delenia intervalu, zatiaľ čo druhý je založený na distribuovanom odhade vlastných čísel Laplasiánu.

Kľúčové slová

Adaptívne riadenie, distribuované odhadovanie, distribuované riadenie, fúzia senzorov, konsensus, kooperatívne riadenie, multiagentové systémy, senzorové siete.

List of Abbreviations

ACP	adaptive consensus protocol
ARE	algebraic Riccati equation
DACP	distributed adaptive consensus protocol
DKF	distributed Kalman filter
DLO	distributed Luenberger observer
JCF	Jordan canonical form
LMI	linear matrix inequality
LQR	linear-quadratic regulator
LTI	linear time-invariant
MCF	modal canonical form
NCS	networked control system
NN	neural network
UUB	uniform ultimate boundedness
WGN	zero-mean white Gaussian noise

List of Symbols

The following list specifies the most important symbols used in this doctoral thesis. Symbols excluded from this list are defined later in the text. Note that some symbols might have multiple meanings depending on the context.

Uppercase Latin letters

A	system matrix
B	system input matrix
C	system output matrix
C_i	system output matrix of node (sensor) i
D	graph degree matrix
E	graph adjacency matrix
$\mathcal{E}$	set of arcs (edges)
$\mathbb{E}(\nu)$	expected value of ν
G	graph pinning matrix
$\mathcal{G}$	graph
H	pinned Laplacian matrix
I	identity matrix
$\Im(a)$	imaginary part of a complex number a
K	state feedback gain matrix
L	graph Laplacian matrix
$\Re(a)$	real part of a complex number a
$\mathbb{R}$	set of real number
$\mathcal{V}$	set of nodes
$\mathcal{V}_i$	set of (in-)neighbors of node i

$V(x)$	Lyapunov function of state x
P	matrix solution of the algebraic Riccati equation
Q	matrix weighting the state error in the algebraic Riccati equation
R	matrix weighting the control effort in the algebraic Riccati equation

Lowercase Latin letters

c	coupling gain
c_i	coupling gain associated with node i
c_{ij}	coupling gain associated with arc $j \to i$
d_i	(in-)degree of node i
e_{ij}	ijth element of the adjacency matrix, E
f_s	sampling frequency
$f(x)$	function of the state vector x
i, j	indices of nodes in the network
n	number of states, i.e., dimension of the state vector x
m	number of inputs, i.e., dimension of the input vector u
p	number of nodes in the network
t	time
$\triangle t$	sampling time window
u	system input vector
u_i	input vector of node i
w	eigenvector of L associated with the zero eigenvalue
x_0	leader's state vector
x	system state vector
x_i	state vector of node i
y	system output or state vector, depending on the context
y_i	output vector of node i
z	system state vector
z_i	state vector of node i

Uppercase Greek letters

Γ	adaptation gain matrix
Θ	positive diagonal matrix
Ξ_i	covariance matrix of measurement noise associated with node i

Ψ	process noise input matrix
Ω	covariance matrix of process noise

Lowercase Greek letters

α	positive constant
β_i	design parameter of node i
γ	design parameter
δ	synchronization error vector or a positive scalar, depending on the context
δ_i	synchronization error vector of node i
ϵ	positive constant
ϵ_i	local neighborhood error vector of node i
η	estimation error
$\lambda_i(M)$	the ith eigenvalue of matrix M; sorted in an ascending order
$\lambda_{\max}(M)$	the largest eigenvalue of matrix M
$\lambda_{\min}(M)$	the smallest eigenvalue of matrix M
ξ_i	measurement noise of node (sensor) i
κ_i	coupling gain reference associated with node i
ω	process noise

Contents

1

Introduction

The observed occurrence of cooperative behaviors in nature, exemplified by schools of fish, flocks of birds, swarms of insects and herds of quadrupeds, motivates their emulation and implementation of distributed cooperation in the technical world as well. This has attracted attention of many researchers from a variety of disciplines. Hence, in the past few decades, a significant progress has been made in the study of cooperative multi-agent systems [10, 53]. This together with a recent boost in computational power paved the way to decentralization, distribution and development of networked systems. Networking allowed creation of the Internet, which laid the foundation to a new phenomenon of smart networks called Internet of Things, interconnecting smart devices and building smart ecosystems in public and private sphere, e.g., intelligent buildings, smart cities, smart power grids, etc.

Networked systems hence also attract considerable research attention in control theory, where they give rise to networked control system (NCS) [49, 6, 72] and their synonymous cyber-physical systems, in which cyber-networks intensely interact with physical plants and humans [40, 31, 4]. This integrates two complementary fields, the control theory [66, 32, 2] considering the single-agent dynamics and the algebraic graph theory [21], into an emerging field of distributed systems. Distributed NCS have a wide range of application in formation control of mobile robots, satellites, and vehicles [53], heating, ventilation, and air conditioning in buildings [24], energy generation in micro-grids [7], estimation with the use of sensor networks [1], synchronization of coupled oscillators [13], reaching the agreement in human social networks [73], to name only a few. See the books [61, 43] for a comprehensive treatment.

These systems are composed of autonomous agents networked by a communication topology. Every agent uses its own information and information from its neighbors in the network to reach an agreement on states with all

other agents, called *consensus*. Over time consensus and *synchronization* of agents crystallized in this context as two canonical control problems. Those are here referred to as the *cooperative regulator problem*, in which the consensus is reached among agents, all being of equal standing, and the *cooperative tracker problem*, in which all agents synchronize to a single distinct leader. In literature, these two canonical control problems are sometimes refered to as *relative-state consensus* (*leaderless consensus*) and *leader-following consensus*.

The first developed consensus protocols solving the canonical cooperative control problems are the so-called local voting protocols [16, 58, 57, 64]. All other consensus protocols are their simpler or more complex modifications as, e.g., passivity-based design of cooperative controllers for multi-agent systems [12, 3], which was introduced later. The local voting protocols are used for synchronization of agents with a general linear time-invariant (LTI) dynamics that is stable or on the stability boundary. They do not require any centralized information to be known by each agent to reach consensus; hence they can be implemented on agents fully separately. Unfortunately, they do not allow for an implementation on agents with unstable dynamics.

The static consensus protocols [45, 76, 77] offer a refinement. They gained wide popularity in the cooperative control community because of their well developed simple design and broad applicability on agents with LTI dynamics. They are based on the synchronizing region methodology, which exhibit many advantages, such as divorcing the single-agent control design from the detailed graph topology, bringing robustness to uncertainties in the graph structure, providing a unified approach to cooperative regulator and tracking problems, all while allowing for a rather simple controller design. Nevertheless, these methods generally rely on a common coupling gain, used in all the agents, that satisfies a specific lower bound. The calculation of this bound requires knowledge of the graph topology. Since this is centralized information, the static consensus protocol design via the synchronizing region methodology is not fully distributed.

Consensus protocols are broadly applied in many distributed control and estimation approaches. Since a plant is often not fully controllable (observable) by individual agents in the network, distributed design and implementation of controllers and observers is often indispensable for proper longterm functioning and safety of networked multi-agent systems. When a centralized solution is used on a network of agents, it views the network as a single complex system; therefore, the complexity of the centralized solution increases with the complexity of the network. In most applications, centralized solution cannot observe the full state information due to communication constraints between agents. Moreover, the centralized solution might fail when the network topology changes, e.g., an agent or a communication link is added or dropped. Therefore, an incentive to avoid drawbacks and limitations of centralized approaches initiated development

of decentralized and distributed approaches for networked multi-agent systems. They handle all drawbacks of centralized approaches and enjoy many advantages, such as robustness, flexibility, and scalability.

Very early results in the centralized estimation bring the Wiener filter in continuous [71] and discrete-time [41], for estimating the target of a stochastic process. For estimation of non-stationary processes, the Kalman filter [30] was developed. The Luenberger observer [48] brings a simple design without considering models for measurement and process noises. To improve upon drawbacks of the centralized observers, their decentralized alternatives [68, 62, 63] were first developed. The decentralized observers offer fast parallel processing and increased robustness to failures. However, they require an all-to-all coupling of nodes, which leads to increased communication load, computational complexity and thereby to scaling problems on large-scale networks. The problems of decentralized observers motivated their further enhancement, which led to the birth of distributed observers. This brought the distributed estimators of a time-varying signal [59, 67, 80]. The distributed Kalman filtes (DKFs) [54, 55, 56] ensure estimation of a target system dynamics with process noise acting on the plant state and measurement noise corrupting the sensors' measurements. The DKF approaches ensure optimality of the resulting state estimates however they suffer from large communication burden, due to communication of covariances, especially for large-scale network. Different from DKFs, the distributed Luenberger observers (DLOs) [34, 79] introduce a simpler design which do not consider process and measurement noises, hence they do not suffer from large communication load. However neither they aim for the information weighted sensor fusion. A novel distributed estimation approach, presented in Chapter 3, combines the best of both approaches on DKFs and DLOs. It aims to achieve a rather simple observer design achieving reasonable sensor fusion of measurements with varying reliability by maintaining relatively small communication burden.

To allow for a fully distributed implementation of cooperative laws, consensus protocols started to incorporate adaptation of coupling gains. This gave birth to the first distributed adaptive consensus protocols (DACPs) [69, 75, 46, 47]. These consensus protocols implement an adaptive law which adapts one or more coupling gain values. Thereby, in contrast to static consensus protocols, they avoid the requirement of any centralized information about the network communication topology. Thus, they can be implemented by each agent separately without using any global information. These DACPs guarantee cooperative stability. However, benefits from adaptability suffer from possibly large control effort and lack of robustness to noise. A solution to these problems is offered by more advanced DACPs, [50] and [11], which introduce modified adaptive laws allowing all coupling gains to decay to a single static value. These protocols guarantee uniform ultimate boundedness of the synchronization error.

However the upper bound on this error depends on the network properties. This is primary caused by the static reference value to which all the coupling gains decay. Our DACPs approach presented in Chapter 4 aims to avoid this drawback by estimating the coupling gains' references from the network trajectories individually by each agent. Moreover, it also addresses the problems of existing DACPs with unbounded coupling gain values and lack of robustness to noise.

1.1 What the thesis brings

In this thesis, we first introduce basics from the graph theory and cooperative control theory. Then, we describe the above-mentioned consensus protocols in the order they were developed and discuss their benefits and drawbacks.

Later, we present a novel distributed estimation approach, [39], for large-scale sensor networks, that uses sensor fusion to merge measurements of varying reliability with locally available measurements. The proposed distributed observer addresses primarily state estimation of plants represented by flexible structures. It is based on the DLO designs; however, it shares some desirable properties with the DKF. For instance, it considers process and measurements noises as DKFs, but it does not communicate covariance matrices, as DLOs, to reduce the communication burden especially for large network. The observer design allows existence of nodes that do not measure anything but contribute to the information exchange among nodes in the network. This, in hand with a possible incorporation of redundant nodes into the network, increases robustness to node or communication link failure.

Last but not least, we present a novel DACP, [38], that addresses the cooperative regulator and tracker problems on directed graphs with a relatively simple and unified design. It is based on our recent results, [35, 36, 37], which were motivated by the previously developed DACPs, [46, 47]. The proposed DACP design introduces a novel adaptive law that allows coupling gains to decay to their reference values. Thereby it solves the problems of existing DACPs, [69, 75, 46, 47], with overly large or even unbounded coupling gains. For estimation of proper coupling gains' reference values, each agent in the network implements one of the two proposed on-line estimation algorithms based either on interval-halving method or on estimation of Laplacian eigenvalues [17, 18]. The estimation algorithm estimates the coupling gains' references from the network trajectories. This is found to improves robustness of the proposed design to noise and disturbances.

1.2 Goals of the thesis

This thesis is dedicated to development of a novel distributed cooperative estimator and a distributed adaptive consensus protocol for multi-agent systems on general directed communication graphs. Those represent two primary goals, specified by additional requirements, which are supposed to provide improvements upon the existing results in the literature. Namely, the goals of this thesis are given as follows.

1 Develop a distributed estimator for large-scale sensor networks that satisfies the following requirements.

   (a) It considers process and measurement noises.

   (b) It provides robustness to node and communication link failures.

   (c) It maintains small communication burden.

2 Develop a distributed adaptive consensus protocol satisfying the following requirements.

   (a) It is fully distributed, in a sense, not requiring any centralized information for the design and implementation.

   (b) It solves both the cooperative regulator and tracker problems.

   (c) The coupling gains are allowed not only to rise but also to decay.

Common tasks concerning both primary goals 1 and 2 aim to analyze stability and prove convergence of the network of agents implementing the corresponding approach and also to validate the results numerically by simulations.

1.3 Structure of the thesis

The thesis is structured as follows. Chapter 2 brings basic notation, mathematical preliminaries, and theoretical results from algebraic graph theory, which are used throughout this thesis. Furthermore, it introduces general consensus protocols from cooperative control theory; namely, the local voting protocol and the celebrated static consensus protocol.

Chapter 3 presents a distributed estimation approach for large-scale sensor networks. At the beginning, it brings the state of the art in distributed estimation with detailed design of the related distributed estimation approaches. It defines the problem that is being solved, presents the distributed observer, and proves its convergence. Then, it provides a detailed analysis of estimation error covariances. The observer design is summarized and it properties are further discussed. Last but not least, numerical simulations validate the proposed approach.

Chapter 4 introduces a distributed adaptive consensus protocol on general directed graphs. First, it brings the state of the art in distributed adaptive control with detailed design of the related adaptive consensus protocols. Then, it states the considered cooperative control problems, presents the adaptive consensus protocol, and concludes on its stability using Lyapunov function technique. At the end, numerical simulations demonstrate functionality of the proposed adaptive approach and provide a comparison with existing distributed adaptive protocols.

Chapter 5 concludes this thesis. It summarizes the main results and discusses possible future extensions of the presented work.

2

Theoretical preliminaries

This chapter brings basic notation and mathematical preliminaries used throughout the thesis. It introduces consensus and synchronization in distributed conrol and states the general consensus protocols applied in cooperative control. A more detailed overview of the graph theory can be found in many books, for instance, [8, 21]. Consensus and synchronization in multi-agent systems is comprehensively described in [61, 43].

2.1 Notation

In the thesis, following notation and definitions are used. Matrices are usually denoted with capital letters and vectors with lower case letters. The constants are usually denoted by small Greek letters. An element of a matrix A is denoted as a_{ij} while an element of a column or row vector v is denoted as v_i.

The sets of positive and non-negative real numbers are denoted as $\mathbb{R}^+$ and $\mathbb{R}_0^+$, respectively. $\mathbb{R}^{m\times n}$ denotes the set of $m \times n$ real matrices. The set of m-dimensional real vectors is denoted by $\mathbb{R}^m$. The orthogonal complement of a subspace $\mathcal{T}$ is denoted by $\mathcal{T}^\perp$. The $\mathbf{1}_p$ denotes a column vector with p entries, all equal to one. For a vector $v \in \mathbb{R}^p$ with elements $v_l \in \mathbb{R}$, $V = \mathrm{diag}(v_l), l \in \{1, 2, \ldots, p\}$, denotes a diagonal matrix with elements of vector v on the diagonal. A matrix $M = \mathrm{diag}(M_i)$ for $M_i \in \mathbb{R}^{n_i\times n_i}$, $i = 1, 2, \ldots, k$, denotes a block-diagonal matrix with k blocks $M_1, M_2, \ldots, M_k$ on the block-diagonal. $I_p \in \mathbb{R}^{p\times p}$ is the identity matrix. Operation $A \otimes B$ denotes the Kronecker product of matrices A and B, [9]. The symmetric part of a matrix M is denoted by $(M)_\mathrm{S}$. Eigenvalues of M are denoted by $\lambda_i(M)$. The smallest and the largest eigenvalue of M are denoted by $\lambda_{\min}(M)$ and $\lambda_{\max}(M)$. The smallest and the largest element of a vector w are denoted by $w_{\min}$ and $w_{\max}$. Positive (semi)-definite symmetric matrix is denoted by $M \succ (\succeq)\ 0$. The sum over all

agents $\sum_{i=1}^{p}$ is denoted by $\sum_i$ for $i = 1, 2, \ldots, p$, when not stated explicitly. An expected value of a wide sense stationary stochastic process $\nu(t) \in \mathbb{R}^n$ is denoted by $\mathbb{E}[\nu] \in \mathbb{R}^n$. For a zero-mean process, its covariance is $\mathbb{E}[vv^T] \in \mathbb{R}^{n \times n}$. Whenever the notation is cumbersome we discard the explicit mention of the time dependence.

2.2 Graph theory

An information exchange among agents is given by a network. It is modeled by a directed graph $\mathcal{G} = (\mathcal{V}, \mathcal{E})$, where $\mathcal{V} = \{1, 2, \ldots, p\}$ is a nonempty finite set of nodes (agents) and $\mathcal{E} \subseteq \mathcal{V} \times \mathcal{V}$ is a set of arcs (communication links). An arc is an ordered pair of nodes (i, j), $i \neq j$, where i is the parent node and j is the child node, that is, the information flows from node i to node j. The arc (i, j) is depicted by an arrow with a tail node i and a head node j. The graph $\mathcal{G}$ is *undirected* if $(i, j) \in \mathcal{E}$ implies $(j, i) \in \mathcal{E}$, otherwise the graph is *directed*. In following, it is assumed that the graph $\mathcal{G}$ is simple, that is, it has no repeated edges nor self-loops $(i, i) \notin \mathcal{E}, \forall i$.

Remark 1. Throughout the thesis, the terms "agents" and "nodes" are used interchangeably, as are the terms "network" and "communication graph". The same holds also for the terms "arcs" and "edges".

A directed path of length p from node 1 to node p is an ordered set of distinct nodes $\{1, 2, \ldots, p\}$ such that $(l, l+1) \in \mathcal{E}$ for all $l \in \{1, 2, \ldots, p-1\}$. An undirected path is defined analogously with $(l, l+1) \in \mathcal{E} \Leftrightarrow (l+1, l) \in \mathcal{E}$ for all $l \in \{1, 2, \ldots, r-1\}$. A directed graph is *strongly connected* if there exist a directed path from every node to every other node. Similarly, an undirected graph is *connected* if there is an undirected path between any two nodes. A node is termed *isolated* if it has no parent node. Hence, in strongly connected graphs there are no isolated nodes. Directed tree is a directed graph with every node having only one parent except one isolated node called a *root*. An undirected tree is an undirected graph in witch every pair of nodes is connected by exactly one path. A directed graph contains a directed *spanning tree* if there exists a subgraph which is a directed tree containing all nodes in $\mathcal{V}$; hence, by the definition, every strongly connected graph has a spanning tree. An undirected spanning tree of an undirected graph $\mathcal{G}$ is defined analogously. An undirected graph has an undirected spanning tree if and only if it is connected; therefore, the term spanning tree is used only for directed graphs and undirected graphs are said to be connected. An example of a directed graph having a spanning tree is depicted in Figure 2.1. A spanning forest is a set of directed trees such that a set of all nodes of these trees equals $\mathcal{V}$.

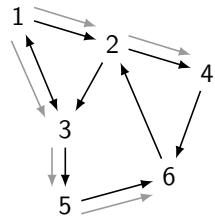

Figure 2.1: A directed graph containing a spanning tree has 6 nodes. A single spanning tree having node 1 as the root node is depicted by grey arcs.

2.2.1 Graph matrices

Properties of a graph $\mathcal{G}$ can be studied through properties of certain matrices. The adjacency matrix $E = [e_{ij}] \in \mathbb{R}^{p\times p}$ associated with the graph $\mathcal{G}$ is defined by $e_{ij} = 1$ if and only if $(j, i) \in \mathcal{E}$, otherwise $e_{ij} = 0$. By the definition, the diagonal elements of E satisfy $e_{ii} = 0$, $\forall i$. Denote $\mathcal{V}_i = \{i \in \mathcal{V} | e_{ij} \neq 0\}$ as the set of (in-)neighbors of node i, that is, the set of nodes with arcs incoming to i. Let the (in-)degree matrix $D = \mathrm{diag}(d_i) \in \mathbb{R}^{p\times p}$ be a diagonal matrix given by $d_i = \sum_j e_{ij}$. Then the graph Laplacian matrix is defined by $L = D - E$.

For instance, the adjacency matrix and the degree matrix corresponding to the directed graph in Figure 2.1 have the form

$$E = \begin{bmatrix} 0 & 0 & 1 & 0 & 0 & 0 \\ 1 & 0 & 0 & 0 & 0 & 1 \\ 1 & 1 & 0 & 0 & 0 & 0 \\ 0 & 1 & 0 & 0 & 0 & 0 \\ 0 & 0 & 1 & 0 & 0 & 0 \\ 0 & 0 & 0 & 1 & 1 & 0 \end{bmatrix}, \quad D = \begin{bmatrix} 1 & 0 & 0 & 0 & 0 & 0 \\ 0 & 2 & 0 & 0 & 0 & 0 \\ 0 & 0 & 2 & 0 & 0 & 0 \\ 0 & 0 & 0 & 1 & 0 & 0 \\ 0 & 0 & 0 & 0 & 1 & 0 \\ 0 & 0 & 0 & 0 & 0 & 2 \end{bmatrix}, \tag{2.1}$$

and the Laplacian matrix is

$$L = \begin{bmatrix} 1 & 0 & -1 & 0 & 0 & 0 \\ -1 & 2 & 0 & 0 & 0 & -1 \\ -1 & -1 & 2 & 0 & 0 & 0 \\ 0 & -1 & 0 & 1 & 0 & 0 \\ 0 & 0 & -1 & 0 & 1 & 0 \\ 0 & 0 & 0 & -1 & -1 & 2 \end{bmatrix}. \tag{2.2}$$

Remark 2. If the graph is weighted, that is, arcs have weights, elements of the adjacency matrix, E, are given by $e_{ij} > 0$ if and only if $(j, i) \in \mathcal{E}$, otherwise $e_{ij} = 0$. In other words, the weight of an arc (j, i) is given by the element e_{ij}.

In this thesis, we consider unweighted graphs, however all results generally apply to weighted graphs; therefore, by introducing various approaches from the literature we usually do not state details about the considered graph weighting.

Lemma 1. *The Laplacian matrix, L, has following properties:*

1. *It is a singular M-matrix, [26].*
2. *All its eigenvalues $\lambda_i(L)$ have non-negative real part, that is, $\Re\big(\lambda_i(L)\big) \geq 0, \forall i$.*
3. *All its eigenvalues are located in a disc centered at $\max_i\{d_i\}$, with a radius of $\max_i\{d_i\}$. This follows from the Geršgorin disc theorem, [25].*
4. *It has a zero eigenvalue with the corresponding right eigenvector $\mathbf{1}_p$. This follows from the fact that L has all row sums equal to zero.*

Lemma 2 ([43], Thm 2.1)**.** *The Laplacian matrix L has a simple zero eigenvalue if and only if its directed graph contains a spanning tree.*

From the definition of L, Lemma 1 and Lemma 2, it follows that the Laplacian matrix L of an undirected graph $\mathcal{G}$ has following properties.

1. It is a symmetric matrix, i.e., $L = L^\mathsf{T}$.
2. It has non-negative real eigenvalues. We order them as
$$0 = \lambda_1(L) \leq \lambda_2(L) \leq \ldots \leq \lambda_p(L). \tag{2.3}$$
3. The second smallest eigenvalues is positive, i.e., $\lambda_2(L) > 0$, if and only if the undirected graph is connected. This follows from Lemma 2.

Denote by $w \in \mathbb{R}^p$ the left eigenvector associated with the simple zero eigenvalue of L, i.e., $w^\mathsf{T} L = 0$. The pinning matrix $G = \mathrm{diag}(g_i) \in \mathbb{R}^{p\times p}$ associated with the graph $\mathcal{G}$ is a diagonal matrix of pinning gains $g_i \geq 0$ such that $g_i > 0$ if the ith node is pinned, otherwise $g_i = 0$, [43].

The following two lemmas are useful in constructing Lyapunov functions for cooperative control [77].

Lemma 3 ([77], Lemma 6)**.** *Let L be the Laplacian matrix associated with a directed, strongly connected graph $\mathcal{G}$. Then L has a simple zero eigenvalue and its left eigenvector w, $w^\mathsf{T} L = 0$, has all positive entries, i.e., $w_i \succ 0, \forall i$.*

Lemma 4 ([78], Proposition 1 and Corollary 3)**.** *For every strongly connected, irreducible, graph $\mathcal{G}$ with Laplacian matrix L, there exists a positive diagonal matrix $W = diag(w_i)$ satisfying*
$$L^\mathsf{T} W + W L \succeq 0. \tag{2.4}$$

Let graph $\tilde{\mathcal{G}}$ with Laplacian matrix $\tilde{L}$ contain a spanning forest with $g_i > 0$ for a root node of each tree, then the positive diagonal matrix $\Theta = diag(\theta_i)$, with $\theta = [\theta_1, \theta_2, \dots, \theta_p]^\mathsf{T} = (\tilde{L} + \tilde{G})^{-\mathsf{T}} \mathbf{1}_p$, satisfies

$$(\tilde{L} + \tilde{G})^\mathsf{T}\Theta + \Theta(\tilde{L} + \tilde{G}) \succ 0. \tag{2.5}$$

2.2.2 Irreducible matrices and Frobenius form

A graph $\mathcal{G}$ is reducible if there exists a permutation matrix T, that transforms its Laplacian L to a block triangular form

$$T^\mathsf{T} L T = \begin{bmatrix} L_{1,1} & L_{1,2} \\ 0 & L_{2,2} \end{bmatrix}. \tag{2.6}$$

If the graph is not reducible it is said to be irreducible.

Lemma 5. *A directed graph is irreducible if and only if it is strongly connected.*

Let the directed graph be reducible and let it contain a spanning forest. Then the Laplacian of the graph can be reduced by a node permutation to the Frobenius normal form [43]. If the graph contains a single spanning tree then its Frobenius normal form equals

$$T^\mathsf{T} L T = \left[\begin{array}{ccc|c} \overbrace{L_{1,1}}^{\tilde{L}+\tilde{G}} & \overbrace{\dots}^{\tilde{L}+\tilde{G}} & \overbrace{L_{1,c}}^{\tilde{L}+\tilde{G}} & L_{1,c+1} \\ & \ddots & \vdots & \vdots \\ 0 & & L_{c,c} & L_{c,c+1} \\ \hline \multicolumn{3}{c|}{0} & L_{c+1,c+1} \end{array}\right], \tag{2.7}$$

where all $L_{\kappa,\kappa}, \kappa \in \{1, 2, \dots, c\}$ blocks are irreducible. This thesis addresses graphs having a single spanning tree. Such graphs are either irreducible (strongly connected) or reducible and contain at most one irreducible leader group $L_{c+1,c+1}$. A special case of the irreducible leader group is a single isolated leader. The results presented for irreducible graphs naturally specialize to connected undirected graphs.

Remark 3. For the theoretical development in Chapters 3 and 4 we do not consider edge weights; hence we restrict elements of the adjacency matrix, E, to $e_{ij} = 1$ if and only if $(j, i) \in \mathcal{E}$ and $e_{ij} = 0$ otherwise.

2.3 Cooperative control

This section gives a short introduction to cooperative control. First, it explains two generally known consensus problems; namely, cooperative regulator and

tracker problems. Then, as a solution to these problems, it introduces the so-called local voting protocol and the static consensus protocol. Each consensus protocol is shortly described and its benefits and drawback are summarized. A more general overview of the recent progress in various fields of cooperative control can be found in [10]. A detailed introduction to cooperative control and basic consensus protocols for formation control in networked multi-agent systems is given in [57], [64], [16], [27]. Theory dedicated to cooperative control can be found in books, such as [43], [61].

Various approaches for the design of distributed cooperative controllers (including static and adaptive approach) on directed communication graphs are summarized in [77]. The passivity based design of distributed controllers is introduces in [12], [3]. A unified viewpoint on design of consensus regulators on directed graph topologies using the synchronizing region is provided in [45]. The design of distributed controllers and observers using state or output-feedback in continuous and discrete-time is considered by [76], [77], [22]. An extension to the communication graphs with switching topologies and time delays is proposed in [58], [52].

A stability of a distributed control protocol is proved mostly by the Lypaunov's direct method. To use this method on multi-agent systems, it requires a special construction of Lyapunov functions. The construction of these Lyapunov functions is described in [78] and [23].

2.3.1 Leaderless consensus

The main objective of the relative state consensus or so-called cooperative regulator problem is to reach an agreement on some information among agents. These information are usually states of agents that are being synchronized to a one common value. To present a general relative state consensus algorithm solving the cooperative regulator problem, first, consider a network of p agents, each with an identical single-integrator dynamics

$$\dot{x}_i(t) = u_i(t) \quad x_i, u_i \in \mathbb{R}. \tag{2.8}$$

Let the network be given by a directed, strongly connected graph $\mathcal{G} = (\mathcal{V}, \mathcal{E})$. The general consensus algorithm also known as the local voting protocol has the form

$$u_i(t) = \epsilon_i(t), \tag{2.9}$$

$$\epsilon_i(t) = \textstyle\sum_{j \in \mathcal{V}} e_{ij} \left(x_j(t) - x_i(t) \right), \tag{2.10}$$

where ϵ_i represents the local neighborhood error term. Using this algorithm each agent sums up the errors between its state and states of its neighbors to obtain the local neighborhood error (2.10), which is then used as the input of

agent i. This creates a negative feedback in the system having stabilizing effect on the network dynamics

$$\dot{x}(t) = -Lx(t), \tag{2.11}$$

where $x = (x_1, x_2, \dots, x_p)^\mathsf{T}$ is the vector of states of agents. By Lemma 1, the eigenvalues of L are non-negative, that is, L has one zero eigenvalue and $p-1$ negative eigenvalues; thus, the network dynamics (2.11) is stable with respect to collective dynamics of agents. From the definition of L in Section 2.2.1 follows that $\mathbf{1}_p$ is the right eigenvector corresponding to the zero eigenvalue; hence the equilibrium of the network dynamics (2.11) is given by $x = \text{span}(\mathbf{1}_p) = \alpha\mathbf{1}_p, \alpha \in \mathbb{R}$, that is, $x_1 = x_2 = \cdots = x_p = \alpha$. Moreover, by Lemma 3, it holds that

$$w^\mathsf{T}\dot{x}(t) = -w^\mathsf{T}Lx(t) = 0 \quad \Rightarrow \quad w^\mathsf{T}x(t) = w^\mathsf{T}x(0) = \alpha, \tag{2.12}$$

where w is the left eigenvector of L corresponding to zero eigenvalue. As $t \to \infty$, $x(t) \to \alpha\mathbf{1}_p$ so, using (2.12), $w^\mathsf{T}\alpha\mathbf{1}_p = w^\mathsf{T}x(0)$, which yields that the agents' states converge to a value given by

$$\alpha = \frac{w^\mathsf{T}x(0)}{\sum_{i\in\mathcal{V}} w_i}. \tag{2.13}$$

Thereby, we showed that, under the control protocol (2.9, 2.10), agents in the network reach consensus on states in the sense of

$$\lim_{t\to\infty} \|x_j(t) - x_i(t)\| = 0, \quad \forall i, j = 1, 2, \dots, p. \tag{2.14}$$

Note that for undirected and balanced graphs $L = L^\mathsf{T}$; hence $w = \mathbf{1}_p$. If $x \in \mathbb{R}^n$, the same methodology applies using the Kronecker product, [9].

2.3.2 Leader-following consensus

The goal of the leader-following consensus or so-called cooperative tracker problem is to reach an agreement of agents on leaders information. In other words, the agents have to track (follow) some reference that is usually considered as the leader and synchronize their states with leaders. The network has to contain a single leader, pinning into the root of a spanning tree or into roots of all trees in a spanning forest.

Consider a network of p agents having identical single-integrator dynamics (2.8). The network is given by a directed graph $\mathcal{G}$ having a spanning tree with a leader as the root node. The leader, labeled by 0, is represented by an uncontrolled single-agent dynamics (2.8), that is, $u_0 = 0$; in this case $\dot{x}_0 = 0$. The local voting protocol for the leader-following consensus has the form (2.9) with the local neighborhood error

$$\epsilon_i(t) = \textstyle\sum_{j\in\mathcal{V}} e_{ij}(x_j(t) - x_i(t)) + g_i(x_0(t) - x_i(t)). \tag{2.15}$$

The first term on the right-hand side of (2.15) is the local neighborhood error (2.10) stemming from the relative state consensus. It synchronizes the state of the ith agent with states of its neighbors. The second term on the right-hand side of (2.15) synchronizes the ith agent's state with the leader's. If the leader can send information directly to the ith agent, that is, there is an arc $(0, i) \in \mathcal{E}$, then $g_i > 0$ and the state of the ith agent synchronizes with the leaders. Define the synchronization error of agent i as $\delta_i = x_0 - x_i$, then the overall network error dynamics is

$$\dot{\delta} = -(L + G)\delta, \tag{2.16}$$

where $\delta = (x - \bar{x}_0) \in \mathbb{R}^p$ with $\bar{x}_0 \in \mathbb{R}^p$ representing the column vector of leader's states, $\bar{x}_0 = (x_0, x_0, \ldots, x_0)^\mathsf{T}$. Since the pined Laplacian matrix $(L + G)$ is a nonsingular M-matrix, it has all eigenvalues positive; hence the network error dynamics (2.16) is stable and the agents follow the leader. The leader-following consensus synchronizes the states of agents with the leaders in the sense of

$$\lim_{t\to\infty} \|x_i(t) - x_0(t)\| = 0, \quad \forall i, j = 1, 2, \ldots, p. \tag{2.17}$$

Note that the local neighborhood error for the leader-following consensus (2.15) is in the sense same as for the relative state consensus (2.10). The difference is only in the used representation. Considering the leader as an agent the local neighborhood error (2.10) can be used. However, considering the leader and agents separately a more straightforward representation for the local neighbor error (2.15) is used. The same holds for the network dynamics (2.11) and (2.16).

Because an agent does not distinguish a leader among all its neighboring agents — it considers all its neighbors as identical agents — it always implements the local neighborhood error (2.10). The representation (2.15) is generally used, only for mathematical purposes because it considers synchronization among agents and synchronization with the leader separately in two independent terms. Note that, similarly as by the Leaderless consensus, if $x \in \mathbb{R}^n$, the Kronecker product, [9], is used to describe the network dynamics (2.16).

2.3.3 Synchronizing region approach

To demonstrate properties of a static consensus protocol, also known as synchronizing region approach, we describe the static consensus protocol based on the state feedback. Other static consensus protocols are its more complex modifications. For more information about the static consensus protocols based on state feedback, observer and output feedback the reader is referred to [45], [77].

Consider a network consisting of p agents. The static consensus protocols are implemented on agents with an identical general LTI dynamics in the form

$$x_i(t) = Ax_i(t) + Bu_i(t), \quad i = 1, 2, \ldots, p, \tag{2.18}$$

where $x_i \in \mathbb{R}^n$ is the state vector, $u_i \in \mathbb{R}^m$ is the input vector, and $A \in \mathbb{R}^{n\times n}$ and $B \in \mathbb{R}^{n\times m}$ are constant matrices. The matrix A is not necessarily stable but the pair of matrices (A, B) is assumed to be stabilizable. In the case of the leader-following consensus, the leader node is described by the same dynamics without an input

$$\dot{x}_0(t) = Ax_0(t), \tag{2.19}$$

where $x_0 \in \mathbb{R}^n$ is the leader's state vector.

The static consensus protocol defines a control input in the form

$$u_i = cK\left(\sum_j e_{ij}(x_j - x_i) + g_i(x_0 - x_i)\right), \tag{2.20}$$

where $c > 0$ is a scalar coupling gain and $K \in \mathbb{R}^{m\times n}$ is the feedback gain matrix determined by the linear-quadratic regulator (LQR) design technique. Let $Q \in \mathbb{R}^{n\times n}$ and $R \in \mathbb{R}^{m\times m}$ be positive definite symmetric matrices, then

$$K = R^{-1}B^{\mathsf{T}}P, \tag{2.21}$$

where the positive definite symmetric matrix $P \in \mathbb{R}^{n\times n}$ is the unique solution of the algebraic Riccati equation (ARE)

$$A^{\mathsf{T}}P + PA + Q - PBR^{-1}B^{\mathsf{T}}P = 0. \tag{2.22}$$

The overall closed-loop dynamics is

$$\dot{x} = (I_N \otimes A - c(L + G) \otimes BK)x + c((L + G) \otimes BK)\bar{x}_0, \tag{2.23}$$

and the error dynamics is

$$\dot{\delta} = (I_N \otimes A - c(L + G) \otimes BK)\delta. \tag{2.24}$$

Note that for the relative state consensus $g_i = 0$, $\forall i$; thus, the control input (2.20) is

$$u_i = cK\sum_j e_{ij}(x_j - x_i), \tag{2.25}$$

and the overall closed-loop dynamics is

$$\dot{x} = (I_N \otimes A - cL \otimes BK)x. \tag{2.26}$$

Lemma 6. *Consider a communication graph $\mathcal{G}$ having a spanning tree (possibly with the leader described by (2.19)). Then the N agents described by (2.18) reach consensus under protocol (2.20) with the control gain (2.21) if the coupling gain satisfies the following condition*

$$c \geq \frac{1}{2\min_{i\in p}\Re(\lambda_i)}, \tag{2.27}$$

where λ_i is the non-zero eigenvalue of L $(L + G)$.

In comparison to the local voting protocol, the static consensus protocol can be implemented on agents with higher order LTI dynamics that can be unstable. The feedback gain matrix K stabilizes the agent dynamics and the coupling gain c stabilizes the network to reach consensus among agents. The LQR based design of the feedback gain matrix K is beneficial, since it makes the synchronizing region unbounded, that is, the network is stable for any coupling gain c higher than the lower bound (2.27). Different designs of the feedback gain matrix K might lead to a bounded synchronizing region, that is, the network is stable just for some lower and upper bounded coupling gain c.

A drawback of static consensus protocols is that the choice of c always depends on the eigenvalues of L ($L+G$). Namely, to design the scalar coupling gain c, and reach consensus, the smallest real part of the non-zero Laplacian eigenvalues, $\min_{i\in\mathcal{V}} \Re(\lambda_i)$, has to be known. However, it can be determined only from the communication graph which is considered as centralized information. Therefore each agent needs to know the graph topology to set its coupling gain. For this reason the protocol cannot be implemented on agents in a fully distributed fashion, different to the local voting protocol. A solution to this problem is proposed by adaptive approaches, which use an adaptive law to find the stabilizing coupling gain value.

2.4 Summary

This chapter brought the notation and definitions, which are used throughout the thesis. Also, it introduced the basics of the graph theory and the cooperative control theory. In particular, the general (un)directed graphs were introduced and their properties were described as, e.g., (strong) connectedness, spanning tree, etc. The mathematical description of a graph by the adjacency matrix, degree matrix, and Laplacian matrix was stated. Properties of the Laplacian matrix were discussed and related to properties of the corresponding graph. The irreducibility of the Laplacian matrix was defined and the transformation of the Laplacian matrix to the Frobenius form was show.

Last but not least, this chapter gave a brief introduction to the state of the art in cooperative control. Namely, it presented the first developed consensus protocols, the local voting protocol and the static consensus protocol, for leaderless and leader-following consensus.

3

Distributed estimation on sensor networks

In this chapter, we present a novel distributed design for sensor networks that uses sensor fusion to estimate states of a plant under process disturbance and measurement uncertainties. The introduced distributed observer addresses primarily state-estimation of large-scale flexible structures such as aircraft fuselages, truss bridges, lattice towers, etc. Structural vibration suppression is indispensable for proper longterm functioning and safety of such plants. For the design of active dampers for flexible structures, the state of the plant first has to be know, which is the task of an observer. However, implementations of centralized solutions are often expensive and prohibitively complex on the larger scale. A solution is offered by the nascent networked/distributed systems. First of all, they reduce the implementation costs and complexity of the entire design and application. Secondly, communication via network provides a potential for improvement of overall system performance, in contrast to centralized solutions. Moreover, node redundancy provides additional fault tolerance or allows for graceful degradation in the case of node failures. Thus, the networked/distributed architectures handle the drawbacks of (de)centralized approaches and enjoy many advantages, such as robustness, flexibility and scalability.

This chapter is structured as follows. Section 3.1 introduces current state of the art in distributed estimation. Section 3.2 brings our contribution in this field. The main problem that is being solved is stated in Section 3.3. Section 3.4 presents the distributed observer, proves its convergence and analyzes

The work presented in this chapter and its further extension are accepted for a publication to IEEE Transactions on Control Systems Technology [39].

estimation error covariances. Final distributed observer design is summarized and its properties are further discussed in Section 3.5. Numerical simulations are given in Section 3.6. Section 3.7 concludes this chapter.

3.1 State of the art

First designs of distributed observers are motivated by previous developments in centralized estimation. Early results in centralized estimation bring the Wiener filter in continuous [71] and discrete time [41], for estimating the target of a stochastic process. Later, the Kalman filter [30] was developed extending the Wiener filter to non-stationary processes. In contrast to the Kalman filter, the Luenberger observer [48] does not incorporate statistical models for measurement uncertainties and process noise. Albeit, the Kalman Filter and the Luenberger observer share the same structure, their designs differ in the choice of their design parameters. The design parameters of the Kalman filter are determined by the statistical properties of noises, [42], while the Luenberg observer derives the appropriate design parameters using the pole-placement method, [2].

Limitations of the centralized approach prompted a demand for data fusion over sensor networks [19, 5, 70]. This led to the birth of first decentralized Kalman filters presented in [68, 62, 63], offering fast parallel processing and increased robustness to failures. A drawback of these approaches is that they require an all-to-all coupling of nodes, i.e., their network topology is a complete graph, which leads to increased communication load, computational complexity and thereby to scaling problems on large-scale networks. For example, in [68] every agent serves as a sensor and an actuator, and for control purposes it uses pure measurements of all nodes in the network, without any sensor fusion. This approach is not robust to changes of the network topology due to agent failures, because the controller design is centralized; requiring recalculation of the controller following any network change. In contrast to [68], each node in [62] computes its own local estimate of an unknown state vector and then assimilates all the local estimates into a single final estimate of the plant state to accomplish globally optimal performance.

The computational complexity and scaling issues of the decentralized Kalman filter are improved by the DKF. DKF relaxes the requirements on the communication topology such that each node exchanges information only with its neighbors and it also offers possible redundancy in case of node failures. One of the first scalable DKF, providing data fusion over a sensor network to estimate a process modeled by a general LTI dynamics, is introduced in [54]. It is based on consensus filters [59], and dynamic average consensus [67], which solve the distributed estimation of a time-varying signal with and without measurement noise, respectively. In particular, a distributed filtering algorithm presented in [59] consists of a network of micro-Kalman filters, each embedded

with a low-pass and band-pass consensus filter. On the other hand, a recent work on distributed filtering of noisy measurements of a time-varying signal [80] proposes three algorithms loosely based on Bayesian sensor fusion. It considers two types of nodes: sensing nodes which perform the measuring task and non-sensing nodes which mediate between sensing nodes. Extension of the DKF algorithm from [54] for application to heterogeneous sensor models with different outputs can be found in [55], which offers a popular and efficient consensus-based framework for distributed state estimation. Stability and performance of this DKF algorithm are thoroughly investigated and a new optimal solution of DKF is developed in [56].

An extension of the discrete-time DKF [55] to continuous-time with embedded communication of measurement noise covariances is provided in [33]. The most recent work in this field, [29], presents an optimal information-weighted DKF, which implements a novel measurement model considering noise in communication channels. The network topology in [29] is assumed directed having a spanning tree with a target node observable by at least one root node. Note, that [68, 62, 63, 54, 59, 67, 55, 56, 33] consider undirected communication graphs, while the approaches in [80, 29] apply to general directed graphs.

A distributed estimation and control approach on directed sensor networks, [60], proposes an optimal scheme without a statistical framework; however, it suffers from a centralized design. It considers nodes which may be sensing, acting, or both. In contrast to [60], a DLO, [34], allows for a completely single-agent based design and implementation, albeit only on undirected sensor networks. A recently introduced distributed observer and controller design [79] combines appealing properties of both [60] and [34]. It applies to general directed graphs and adopts the node classification of sensing, acting, or both as in [60], while it allows for a single-agent based design as in [34] sacrificing optimality of [60]. Moreover, it also allows insertion of redundant sensor nodes into the network to increase robustness to node or communication link failures. However, in contrast to the DKF, the estimation and control approaches in [34, 60, 79] do not consider process or measurement noises.

To introduce the existing results on distributed estimation in more details, in following, we review several estimation approaches from the literature. First, in Section 3.1.1, we describe two estimation approaches using DKF [55, 33]. Then, in Section 3.1.2, we bring two DLO designs [34, 79].

3.1.1 Distributed Kalman filter

The DKF, [55], also referred to as distributed Kalman-Bucy filter, [33], is a distributed estimator incorporating statistical description of process and measurement noises. It estimates the state vector of a target system usually

represented by the LTI dynamics

$$\dot{x}(t) = Ax(t) + \Psi\omega(t), \tag{3.1}$$

where $x(t) \in \mathbb{R}^n$ is the state vector, $\omega(t) \in \mathbb{R}^m$ is the process noise, $A \in \mathbb{R}^{n\times n}$ is the system matrix and $\Psi \in \mathbb{R}^{n\times m}$ is the process noise input matrix.

The distributed estimator is given by a sensor network, which is described by a communication graph, $\mathcal{G} = (\mathcal{V}, \mathcal{E})$. It consists of p nodes (local observers), each endowed with the linear sensing model

$$y_i(t) = C_i x(t) + \xi_i(t), \quad i \in \mathcal{V}, \tag{3.2}$$

where $y_i(t) \in \mathbb{R}^{p_i}$ is the ith node measurement corrupted by the measurement noise $\xi_i(t) \in \mathbb{R}^{p_i}$ and $C_i \in \mathbb{R}^{p_i\times n}$ is the ith node observation matrix. Both $\omega(t)$ and $\xi_i(t)$ are independent zero-mean white Gaussian noises (WGNs) with

$$\mathbb{E}[\omega(t)\omega^{\mathsf{T}}(t)] = Q\delta(t-\tau), \quad \mathbb{E}[\xi_i(t)\xi_i^{\mathsf{T}}(t)] = R_i\delta(t-\tau), \quad \forall i \in \mathcal{V}, \tag{3.3}$$

where $\delta(t-\tau) = 1$ if $t = \tau$ and $\delta(t-\tau) = 0$ otherwise.

First, we briefly introduce the celebrated centralized Kalman filter, [42]. Define a global output vector $y(t) = Cx(t)$, where $C = [C_1^{\mathsf{T}}, C_2^{\mathsf{T}}, \ldots, C_p^{\mathsf{T}}]^{\mathsf{T}}$. Assume that the pair (A, C) is detectable, i.e., there is no unstable unobservable invariant subspace in the model; then the classical centralized Kalman filter is given by

$$\dot{\hat{x}}(t) = A\hat{x}(t) + K(t)\left(y(t) - C\hat{x}(t)\right), \tag{3.4a}$$

$$K(t) = P(t)C^{\mathsf{T}}R^{-1}, \tag{3.4b}$$

$$\dot{P}(t) = AP(t) + P(t)A^{\mathsf{T}} + \Psi Q\Psi^{\mathsf{T}} - P(t)C^{\mathsf{T}}R^{-1}CP(t), \tag{3.4c}$$

with $P(t) \succ 0$ and $P(0) = P_0 \succ 0$, where $R = \mathrm{diag}(R_i) \succ 0, i \in \mathcal{V}$. The centralized Kalman filter (3.4) is optimal in the sense of minimizing the limit $\lim_{t\to\infty} J(t)$ with the cost function

$$\begin{aligned} J(t) = \textstyle\sum_{j=1}^{n} \mathbb{E}[\eta_j^2(t)] = \mathbb{E}\left[\eta^{\mathsf{T}}(t)\eta(t)\right] = \\ \mathrm{trace}\left(\mathbb{E}\left[\eta(t)\eta^{\mathsf{T}}(t)\right]\right) = \mathrm{trace}(P(t)). \end{aligned} \tag{3.5}$$

where $\eta(t) = x(t) - \hat{x}(t)$ is the estimation error and $P(t)$ is its covariance matrix.

Next, we bring two distributed estimation approaches [55, 33] proposing a DKF design, which are motivated by the centralized Kalman filter (3.4), [42]. In both approaches [55, 33], the following two assumptions are required to hold.

Assumption 1. The communication graph $\mathcal{G}$ is undirected and connected.

Assumption 2. The covariance matrices $R_i \succ 0, \forall i \in \mathcal{V}$ and $Q \succeq 0$. The pair $(A, \Psi Q^{\frac{1}{2}})$ is controllable and the pair (A, C) is observable.

Note that, by Assumption 2, the pairs (A, C_i) are not necessarily observable.

DKF design proposed by Olfati-Saber et al. [55]

The distributed estimation approach in [55] proposes the DKF in the form

$$\dot{\hat{x}}_i = A\hat{x}_i + K_i(y_i - C_i\hat{x}_i) + \gamma P_i \sum_{j\in\mathcal{V}_i}(\hat{x}_j - \hat{x}_i), \tag{3.6a}$$

$$K_i = P_i C_i^{\mathsf{T}} R_i^{-1}, \quad \gamma > 0, \tag{3.6b}$$

$$\dot{P}_i = AP_i + P_iA^{\mathsf{T}} + \Psi Q \Psi^{\mathsf{T}} - P_i C_i^{\mathsf{T}} R_i^{-1} C_i P_i, \tag{3.6c}$$

with the initial conditions: $P_i(0) = P_0 \succ 0$ and $\hat{x}_i(0) = x(0)$ for all i in $\mathcal{V}$.

Theorem 1 ([55], Prop. 2)**.** *Under Assumptions 1 and 2, the DKF design (3.6) by [55], with the sensor model (3.2) and target dynamics (3.1), guarantees asymptotic stability of the distributed estimator (without noise) for γ sufficiently large, i.e., each node's estimate $\hat{x}_i(t)$ converges to the target state $x(t)$ asymptotically as $t \to \infty$.*

It is important to point out that, by [33], the boundedness of the covariance matrix $P_i(t)$ in (3.6) is guaranteed only if (A, C_i) is observable $\forall i \in \mathcal{V}$.

Remark 4. Let $J_i = \mathcal{V}_i \cup \{i\}$ denotes the inclusive set of neighbors of the ith sensor. Then all C_is are, in fact, C_{il}s (l meaning local) and $C_{il} = \mathrm{col}(H_j)_{j\in J_i}$, yielding that the observation of the ith sensor, y_i, is given by an aggregate observation of all sensors in J_i. This clearly follows from Algorithm 3.1.

Algorithm 3.1 states the iterative procedure for implementation of the DKF design (3.6) introduced in [55]. According to this algorithm, each sensor i communicates to all its neighbors $j \in \mathcal{V}_i$ its predictions $\bar{x}_i$ as well as its u_i and U_i which contain the aggregate observations, as mentioned in Remark 4, together with other covariance-related information. This brings a drawback in increased communication load especially for large sensor networks. The initialization requirements $\hat{x}_i(0) = x(0)$ for the DKF design (3.6) and $\bar{x}_i(0) = x(0)$ for Algorithm 3.1 are unrealistic to be met for the most estimation problems, which bring another difficulty. These difficulties are further addressed in [56] by new optimal and suboptimal scalable solutions for discreet-time DKF.

DKF design proposed by Kim et al. [33]

A distributed estimation approach in [33], motivated by [55], addresses some of the above mentioned drawbacks of the DKF design (3.6) with a slightly different DKF in the form

$$\dot{\hat{x}}_i = A\hat{x}_i + K_i(y_i - C_i\hat{x}_i) + \gamma P_i \sum_{j\in\mathcal{V}_i}(\hat{x}_j - \hat{x}_i), \tag{3.7a}$$

$$K_i = P_i C_i^{\mathsf{T}} R^{-1}, \quad \gamma > 0, \tag{3.7b}$$

$$\dot{P}_i = AP_i + P_iA^{\mathsf{T}} + \Psi Q \Psi^{\mathsf{T}} - P_i C_i^{\mathsf{T}} R_i^{-1} C_i P_i + k \sum_{j\in\mathcal{V}_i}(P_j - P_i). \tag{3.7c}$$

Algorithm 3.1 Iterative Kalman-Consensus Filter

1: **Initialization:** Set $P_i = P_0, \bar{x}_i = x(0), \forall i \in \mathcal{V}$.
2: **while** new data exists **do**
3: Locally aggregate data and covariance matrices:

$$J_i = \mathcal{V}_i \cup \{i\}$$
$$u_j = C_j^\mathsf{T} R_j^{-1} y_j, \forall j \in J_i, z_i = \sum_{j \in J_i} u_j$$
$$U_j = C_j^\mathsf{T} R_j^{-1} C_j, \forall j \in J_i, S_i = \sum_{j \in J_i} U_j$$

4: Compute Kalman-Consensus estimate:

$$M_i = (P_i^{-1} + S_i)^{-1}$$
$$\hat{x}_i = \bar{x}_i + M_i(z_i - S_i \bar{x}_i) + \epsilon M_i \sum_{j \in \mathcal{V}_i} (\bar{x}_j - \bar{x}_i)$$

5: Update the state of the Kalman-Consensus filter:

$$P_i =\leftarrow A M_i A^\mathsf{T} + \Psi Q \Psi^\mathsf{T}$$
$$\bar{x}_i = A \hat{x}_i$$

6: **end while**

Theorem 2 ([33], Thm. 1)**.** *Under Assumptions 1 and 2, the DKF design (3.7) by [33], with the sensor model (3.2) and target dynamics (3.1), guarantees asymptotic stability of the distributed estimator (without noise) for γ sufficiently large and $P_i(0)$ satisfying certain condition (see [33, Lemma 3]).*

Different from (3.6), all the covariance matrices $P_i(t)$ in (3.7) are bounded, hence the pairs (A, C_i) can be truly unobservable, as long as Assumption 2 remains satisfied. Note that by the asymptotic stability of the estimator we mean asymptotic convergence of all estimates $\hat{x}_i(t), i \in \mathcal{V}$ to $x(t)$ as $t \to \infty$.

For the DKF design (3.7), the initial estimates $\hat{x}_i(0)$ and covariances $P_i(0) \succ 0$ of sensors can be different, which relaxes the requirements on initial conditions from [55]. Similar to [55], each node i uses its own estimate $\bar{x}_i$ and estimates of its neighbors $\bar{x}_j, j \in \mathcal{V}_i$; however, different from [55], each node i uses purely its own observation y_i. Nevertheless all the nodes rely on communication of covariance matrices P_i with their neighbors. Thereby this approach inherits the problem of [55] with larger communication load for large sensor networks.

3.1.2 Distributed Luenberger observer

The DLO designs, as opposed to DKF, consider a target system with the LTI dynamics (3.1) and sensors with the linear model (3.2) without noises, i.e., $\omega = 0$ and $\xi_i = 0, \forall i \in \mathcal{V}$, as follows

$$\dot{x}(t) = Ax(t), \quad y_i(t) = C_i x(t). \tag{3.8}$$

Note, that by taking all the sensors' measurements together we can define a single global output vector $y(t) = Cx(t)$, with $C = [C_1^\mathsf{T}, C_2^\mathsf{T}, \ldots, C_p^\mathsf{T}]^\mathsf{T}$.

DLO design proposed by Kim et al. [34]

The DLO, presented in [34], consists of p local observers (nodes), each implementing the estimation dynamics in the form

$$\dot{\hat{x}}_i = A\hat{x}_i + L_i(y_i - C_i\hat{x}_i) + \gamma M_i^{-1}(k_i)\textstyle\sum_{j\in\mathcal{V}_i}(\hat{x}_j - \hat{x}_i), \tag{3.9}$$

where $\gamma > 0$ is a scalar coupling gain, L_i is the injection gain matrix, and $M_i(k_i)$ is the weighting matrix. The design matrices L_i and $M_i(k_i)$ are proposed as

$$L_i = T_i \begin{bmatrix} L_{i\mathrm{o}} \\ 0 \end{bmatrix}, \quad M_i(k_i) = T_i \begin{bmatrix} k_i M_{i\mathrm{o}} & 0 \\ 0 & I_{v_i} \end{bmatrix} T_i^\mathsf{T}, \tag{3.10}$$

where $k_i \geq 0$ is the weighting gain, I_{v_i} is the identity matrix of size v_i, and v_i is the dimension of the unobservable subspace of the pair (A, C_i). The matrix T_i is an orthonormal coordinate transformation matrix satisfying

$$T_i^\mathsf{T} A T_i = \begin{bmatrix} A_{i\mathrm{o}} & 0 \\ A_{i\mathrm{r}} & A_{i\bar{\mathrm{o}}} \end{bmatrix}, \quad C_i T_i = \begin{bmatrix} C_{i\mathrm{o}} & 0 \end{bmatrix}, \tag{3.11}$$

where the pair $(A_{i\mathrm{o}}, C_{i\mathrm{o}})$ is observable. The transformation (3.11) accomplishes the observability decomposition of the pair (A, C_i).

The following assumptions are required to hold by [34].

Assumption 3. The communication graph $\mathcal{G}$ is undirected and connected.

Assumption 4. The pair (A, C) is detectable.

Note that, by Assumption 4, the detectability is required for all the measurements of nodes together; hence, the individual pairs (A, C_i) are not necessarily detectable. The following theorem brings the main result of [34].

Theorem 3 ([34], Thm. 1)**.** *Consider that Assumptions 3 and 4 hold. Let the following apply:*

1. *Each $L_{i\mathrm{o}}, i \in \mathcal{V}$ is chosen such that the matrix $A_{i\mathrm{o}} - L_{i\mathrm{o}}C_{i\mathrm{o}}$ in Hurwitz.*

2. *Each $M_{io}, i \in \mathcal{V}$ is the unique positive definite solution of the following algebraic Lyapunov equation*

$$(A_{io} - L_{io}C_{io})^{\mathsf{T}} M_{io} + M_{io}(A_{io} - L_{io}C_{io}) = -I_{n-v_i}. \tag{3.12}$$

3. *Let $\gamma > 0$ and each $k_i > 0, i \in \mathcal{V}$ are sufficiently large.*

Then, by [34] ,with the dynamics (3.8) and (3.9), the observers' estimates $\hat{x}_i(t)$ asymptotically converge to the target state $x(t)$ as $t \to \infty$.

The novelty of this estimation method, [34], is in the design of the two observer gains; the injection gain, L_i, for the local measurements and the weighting matrix, $M_i(k_i)$, for the information exchange. In the local observer dynamics, (3.9), the output injection through L_i applies only to observable part, while the error between the observer i and its neighbors affects the observable part and the unobservable part differently by M_i. This separate weighting of the detectable and undetectable part follows from the block-diagonal structure of the gain matrices, (3.10), which is the main feature of the proposed approach.

The exact lower bounds on the design parameters k_i and γ are given in [34]. Although the operation of the proposed observer is a distributed one, its design is not decentralized because each observer can not choose suitable gains k_i and γ without global information. However, if the maximum number of nodes p and all possible network structures are known, then k_i and γ can be chosen sufficiently large, according to these bounds, [34].

DLO design proposed by Zhang et al. [79]

The DLO design, proposed by [79], addresses the distributed observer design problem on directed sensor network for spatially interconnected systems. This approach allows existence of nodes that do not measure anything but contribute to the sensor fusion via consensus. Moreover, it also allows incorporation or redundant sensing nodes into the sensor networks to increase robustness to communication link and sensor failures.

Assume that the target dynamics and the sensor model (3.8) are already in Jordan canonical form (JCF) with a block diagonal structure of the system matrix $A = \text{diag}(A_j)$, $A_j \in \mathbb{R}^{n_j \times n_j}$, and the observation matrix $C_i = [C_{i1}, C_{i2}, \ldots, C_{il}]$, $C_{ij} \in \mathbb{R}^{p_i \times n_j}$. The state vector $x \in \mathbb{R}^n$ is then partitioned into l state-groups $x = [x_1^{\mathsf{T}}, x_2^{\mathsf{T}}, \ldots, x_l^{\mathsf{T}}]^{\mathsf{T}}$, with $x_j \in \mathbb{R}^{n_j}$, $\sum_{j=1}^{l} n_j = n$.

Remark 5. If (3.8) is not in a block diagonal form, there always exists a nonsingular real transformation matrix $\Pi = [\Pi_1, \Pi_2, \ldots, \Pi_l] \in \mathbb{R}^{n \times n}$, with $\Pi_j \in \mathbb{R}^{n \times n_j}$, such that $A\Pi_j = \Pi_j A_j$, and $A\Pi = \Pi\tilde{A}$, were $\tilde{A} = \text{diag}(A_j) \in \mathbb{R}^{n \times n}$. The matrix Π transforms (3.8) to JCF, [2]. Note that by plants representing flexible structures modal canonical form (MCF), [20], is more appropriate to obtain a block diagonal structure of (3.8).

The DLO, presented in [79], consists of p local observers in the sensor network, each implementing the estimation dynamics

$$\dot{\hat{x}}_i = A\hat{x}_i + L_i(y_i - C_i\hat{x}_i) + \mathcal{F}_i\textstyle\sum_{k\in\mathcal{V}_i}(\hat{x}_k - \hat{x}_i), \tag{3.13}$$

where $L_i \in \mathbb{R}^{n\times p_i}$ is the Luenberger-like observer gain, [48], and $\mathcal{F}_i \in \mathbb{R}^{n\times n}$ is the communication gain matrix. The design matrices L_i and $\mathcal{F}_i$ have the form

$$L_i := T_i^{\mathsf{T}} \begin{bmatrix} L_{io} \\ 0 \end{bmatrix}, \quad \mathcal{F}_i := T_i^{\mathsf{T}} \begin{bmatrix} 0 & 0 \\ 0 & \operatorname{diag}(c_j F_j) \end{bmatrix} T_i, \tag{3.14}$$

where $c_j > 0, j \in \{1, 2, \ldots, l\}$ is the scalar coupling gain. The matrix $T_i \in \mathbb{R}^{n\times n}$ is an orthonormal coordinate transformation matrix satisfying

$$T_i A T_i^{\mathsf{T}} = \begin{bmatrix} A_{io} & 0 \\ 0 & A_{i\bar{o}} \end{bmatrix}, \quad C_i^{\mathsf{T}} = \begin{bmatrix} C_{io} & 0 \end{bmatrix}, \tag{3.15}$$

where the pair (A_{io}, C_{io}) is observable. The transformation (3.15) achieves the observability decomposition of the pair (A, C_i), i.e., it transforms the pair (A, C_i) to Kalman decomposed form, [2].

Remark 6. The block diagonal structure of the Kalman decomposed form (3.15) is more restrictive than (3.11) because [79] addressees particularly LTI spatially interconnected plants like, e.g., large-scale flexible structures, while [34] assumes plants having the general LTI dynamics. A more detailed comparison of both approaches is given in Remark 12.

In our work introduced later in this chapter, we follow a very similar development as [79]; hence, more information about the transformations to JCF, MCF, and Kalman decomposed form can be found in Section 3.3 and 3.4, directly in the paper [79], or alternatively in the appropriate literature [2, 20].

Now, let us introduce all the necessary definitions and assumptions needed by the DLO design, [79].

Definition 1. $\mathcal{S} = \{1, 2, \ldots, l\}$ defines a set of state-groups.

Assumption 5. $C_{ij} \neq 0$, where $i \in \mathcal{V}$, $j \in \mathcal{S}$, if and only if the state-group x_j is observable from the measurement y_i.

Definition 2. The observable set of agent $i \in \mathcal{V}$, is defined as $\mathcal{O}_i = \{j \in \mathcal{S} | C_{ij} \neq 0\}$; the unobservable set of agent $i \in \mathcal{V}$ is defined as $\bar{\mathcal{O}}_i = \mathcal{S}\backslash\mathcal{O}_i$.

Definition 3. The converse observable set of x_j, $j \in \mathcal{S}$, is defined as $\mathcal{D}_j = \{i \in \mathcal{V} | C_{ij} \neq 0\}$; the converse unobservable set of x_j, $j \in \mathcal{S}$ is defined as $\bar{\mathcal{D}}_j = \mathcal{V}\backslash\mathcal{D}_j$.

Assumption 6. The system is globally observable, i.e., $\mathcal{O}_1 \cup \mathcal{O}_2 \cup \cdots \cup \mathcal{O}_p = \mathcal{S}$.

Assumption 7. The directed communication graph $\mathcal{G}$. given a priori, satisfies the following condition: for any $j \in \mathcal{S}$, the subgraph $\mathcal{G}_j$ formed by the nodes belonging to $\mathcal{D}_j$, has outgoing edges pinning into all the roots of a spanning forest of the subgraph $\bar{\mathcal{G}}_j$, formed by the nodes belonging to $\bar{\mathcal{G}}_j$.

Note that the reduced Lalpacian matrix $\mathcal{L}_j$ of the graph $\mathcal{G}_j$ is obtained via deleting the kth row and column form the original Laplacian matrix L of the graph $\mathcal{G}$, for all $k \in \mathcal{D}_j$.

The following theorem brings the main result on this DLO design, [79].

Theorem 4 ([79], Thm. 1)**.** *Consider that Assumptions 5, 6, and 7 hold. Let the following apply:*

1. *Each $L_{io}, i \in \mathcal{V}$ is chosen such that the matrix $A_{io} - L_{io}C_{io}$ in Hurwitz.*
2. *Each $F_j = \hat{R}_j^{-1}\hat{P}_j, j \in \mathcal{S}$, where $\hat{P}_j = \hat{P}_j^{\mathsf{T}} \succ 0 \in \mathbb{R}^{n_j \times n_j}$ is the unique positive definite solution of the ARE*

$$A_j^{\mathsf{T}}\hat{P}_j + \hat{P}_j A_j - \hat{P}_j \hat{R}_j^{-1}\hat{P}_j + \hat{Q}_j = 0, \tag{3.16}$$

   with given $\hat{Q}_j \succeq 0 \in \mathbb{R}^{n_j \times n_j}$ and $\hat{R}_j \succ 0 \in \mathbb{R}^{n_j \times n_j}$.

3. *$c_j > 0, j \in \mathcal{S}$ is sufficiently large.*

Then, by [79], with the dynamics (3.8) and (3.13), $\lim_{t\to\infty}(\hat{x}_i(t) - x(t)) = 0, \forall i \in \mathcal{V}$.

The node dynamics (3.13) contains two type of gains; the Luenberger-like observer gain L_i, which ensures estimation of the observable subsystem from the ith node measurements, and the communication gain matrix F_i, which synchronizes the unobservable subsystem of the ith node with its neighbors. This follows from the block-diagonal structure (3.14). Note that this differs from the distributed estimation approach in [34], which applies the synchronization to both the observable and the unobservable subsystem, see (3.9) and (3.10). Note also that this approach addresses directed graphs while [34] applies only to undirected sensor networks.

The exact lower bound on c_i is derived in [79]. Albeit this observer implementation is fully distributed, the design is centralized because the lower bound on c_i depends on the graph topology, which is a centralized information. However, by knowing the maximal number of nodes, p, in the network, the lower bound on c_i can be evaluated for the worst case scenario and the gains can be set sufficiently large, similarly as in [34].

The work in [79] introduces also an appropriate distributed controller design, however we do not state it here. For more information about the controller design, an interested reader is pointed to [79].

3.2 Our contribution

In the following, we bring a judicious DLO design, [39], similar to [79], which takes into account the precision of the available measurements, similar to a general Kalman filter [42] and the DKF in [55, 33]. Note that we do not aim here for an optimal Kalman filter design but rather a generally suboptimal, albeit easier to implement, consensus-based distributed Luenberger estimator that nevertheless shares some desirable properties of the Kalman filter. The proposed approach extends the DLO designs [34, 79] by considering multiple information sources of varying reliability, similarly as in [80], to achieve reasonable sensor fusion while retaining a relatively simple distributed design. Thereby it inherits flexibility of single-agent based design, scalability on large-scale sensor networks and robustness to node or communication link failures.

This work differs from the existing results by:

- Assuming only partial pining and observability, from each single-agent perspective, as opposed to the conventional pinning control in [43] and the DKF in [54].
- We consider general directed communication graphs while many existing results, [54, 55, 56, 60, 34, 33], focus on undirected graphs. Moreover, we relax the requirements on the network topology in [80] to directed graphs having a spanning tree with all sensing nodes in one strongly connected component as in [79, 29].
- In contrast to [79], we consider disturbances corrupting the sensors' measurements, as in [80], and process noises acting on plant states as the DKF in [54, 55, 56, 33].
- As compared to [80], here we aim for state estimation of a plant modeled by a general LTI dynamics, in line with the developments in [79].
- To minimize the communication burden, we do not communicate covariances or other covariance-related matrices as the discrete-time DKF with embedded consensus filters in [54, 55, 56] and the continuous-time DKF in [33]. Neither do we assume communication channel noise as in [29], but rather rely on digital communication channels with data validation.

The main contributions of our results are:

- We consider a more general communication topology than the previously proposed distributed observers.
- Nodes implement a local micro-Kalman filter to estimate the observable fraction of the plant state.

- Nodes use information on process and measurement noises and apply information-weighted fusion to reach an agreement on the estimate of a plant state.
- Both the design and implementation of the proposed observer is fully distributed in the sense that each node designs and implements its local observer based on its own information and information from its neighbors.
- The proposed design allows incorporation of redundant nodes or insertion of new communication links in the network to improve robustness to node or communication link failures.

The convergence of the presented distributed observer is rigorously proven by structured Lyapunov functions introduced in [78, 23]. Evolution of expected values and estimation error covariances are further analyzed. Our distributed estimators lend themselves to control applications along the lines of [79], though this development is not pursued here.

3.3 Problem statement and motivation

Consider a plant with a continuous LTI dynamics

$$\dot{x}(t) = Ax(t) + \Psi\omega(t), \tag{3.17}$$

where $x(t) \in \mathbb{R}^n$ is the plant state, $\omega(t) \in \mathbb{R}^m$ is the process noise acting on states, $A \in \mathbb{R}^{n\times n}$ is the system matrix and $\Psi \in \mathbb{R}^{n\times m}$ is the process noise input matrix. Each node in a sensor network has a linear sensing model

$$y_i(t) = C_i x(t) + \xi_i(t), \quad i \in \mathcal{V}, \tag{3.18}$$

where $y_i(t) \in \mathbb{R}^{p_i}$ is the ith node measurement corrupted by the measurement noise $\xi_i(t) \in \mathbb{R}^{p_i}$ and $C_i \in \mathbb{R}^{p_i\times n}$ is the ith node observation matrix. Both $\omega(t)$ and $\xi_i(t)$ are WGN, [33], uncorrelated in the sense that $\mathbb{E}[\xi_i\omega^\mathsf{T}] = 0, \forall i$ and $\mathbb{E}[\xi_i\xi_j^\mathsf{T}] = 0, \forall(i,j), i \neq j$. Note that unlike [34], some nodes in the network may be allowed not to measure anything, similarly as in [60, 79]; for such a node i, y_i is not considered. Note also that [60, 34, 79] does not consider noises while (3.18) does.

To implement estimation of the plant's state vector x in a distributed fashion, it is convenient to transform the system matrix A to a block diagonal form, $\tilde{A} = \text{diag}(A_j) \in \mathbb{R}^{n\times n}, A_j \in \mathbb{R}^{n_j\times n_j}, j = \{1, 2, \ldots, l\}$, where l represents the number of dynamically independent state-groups. There are two generally known representations offering block diagonal system matrix. They are the JCF and the MCF. A transformation to MCF is more common for models describing flexible structures [20], while JCF is used for other general systems

[2]. In case of MCF for flexible structures, each block A_j corresponds to one eigenmode of a flexible structure and the blocks are of the same dimension, i.e., $n_i = n_j, \forall(i,j)$. On the other hand, blocks of the system matrix in JCF correspond to eigenvalues of the system and the dimension of each block is given by the algebraic multiplicity of the pertaining eigenvalue.

Hence, define a linear transformation $x = \Pi z = \sum_{j=1}^{l} \Pi_j z_j$ with a new state vector $z = [z_1^\mathsf{T}, z_2^\mathsf{T}, \ldots, z_l^\mathsf{T}]^\mathsf{T} \in \mathbb{R}^n$ composed of state-groups, $z_j \in \mathbb{R}^{n_j}$, and a nonsingular transformation matrix $\Pi = [\Pi_1, \Pi_2, \ldots, \Pi_l] \in \mathbb{R}^{n \times n}$, such that Π transforms the system matrix A to a block diagonal form. This transformation leads to a block-diagonal representation of the plant dynamics and the transformed sensing model

$$\dot{z}(t) = \tilde{A}z(t) + \tilde{\omega}(t), \tag{3.19}$$

$$y_i(t) = \tilde{C}_i z(t) + \xi_i(t), \quad i \in \mathcal{V}, \tag{3.20}$$

where $\tilde{A} = \Pi^{-1}A\Pi$, $\tilde{C}_i = C_i\Pi$ and $\tilde{\omega}(t) = \Pi^{-1}\Psi\omega(t)$. Note, that there always exists a matrix Π, such that $\tilde{A} = \Pi^{-1}A\Pi$ and $\Pi_j A_j = A\Pi_j$, [25]. Let $\mathbb{E}[\tilde{\omega}\tilde{\omega}^\mathsf{T}] = \Omega$ and $\mathbb{E}[\xi_i\xi_i^\mathsf{T}] = \Xi_i$ denote covariance matrices of process noise $\tilde{\omega}(t)$ and measurement noise $\xi_i(t)$, where Ω and Ξ_i are assumed real, symmetric and positive definite.

Before proceeding further, we introduce several important definitions and assumptions adopted from [79].

Definition 4. $\mathcal{S} = \{1, 2, \ldots, l\}$ defines a set of state-groups.

Assumption 8. $C_{ij} = C_i\Pi_j \neq 0$, where $i \in \mathcal{V}$ and $j \in \mathcal{S}$, iff the state-group z_j is observable from measurement y_i.

This assumption tells that pairs $(\tilde{A}, \tilde{C}_i), i \in \mathcal{V}$ can be transformed to a Kalman Decomposed Form, [2], by a permutation of state-groups. In general it holds that if the state-group z_j is observable from the output y_i then $C_{ij} \neq 0$ but the converse is not necessarily true. However, the systems we address in this work satisfy Assumption 8 either completely or approximately, [79].

Remark 7. Note, that Assumption 8 is trivially satisfied if blocks A_j are of dimension 1. For blocks A_j of dimension greater than one, $n_j > 1, j \in \mathcal{S}$, it can be approximately satisfied under both following conditions:

- if the plant is a flexible structure with independent eigenmodes corresponding to blocks A_j, it naturally leads to a decomposition of C_i into C_{ij};
- if $C_{ij} \neq 0$ but is small in magnitude, then the jth state-group can be considered as unobservable from ith node output y_i and C_{ij} can be set to zero $C_{ij} = 0$ for the purposes of the design. The distributed observer

design proposed in Section 3.5 is robust to such a change as long as Assumption 9 below remains satisfied.

Definition 5. The observable and unobservable sets of state-groups from ith node's perspective, $i \in \mathcal{V}$, are defined as $\mathcal{O}_i = \{j \in \mathcal{S} | C_{ij} \neq 0\}$ and $\bar{\mathcal{O}}_i = \mathcal{S} \backslash \mathcal{O}_i$, respectively.

Definition 6. The converse observable and unobservable sets of nodes for jth state-group, $j \in \mathcal{S}$, are defined as $\mathcal{D}_j = \{i \in \mathcal{V} | C_{ij} \neq 0\}$ and $\bar{\mathcal{D}}_j = \mathcal{V} \backslash \mathcal{D}_j$, respectively.

Note, that Definition 5 and Definition 6 are complementary, i.e., $j \in \mathcal{O}_i \iff i \in \mathcal{D}_j$ and $j \in \bar{\mathcal{O}}_i \iff i \in \bar{\mathcal{D}}_j$.

Assumption 9. The plant state z is globally observable, i.e.,

$$\mathcal{O}_1 \cup \mathcal{O}_2 \cup \cdots \cup \mathcal{O}_p = \mathcal{S}. \tag{3.21}$$

This means that the LTI dynamics of the plant (3.17) is observable from measurements of all nodes (3.18) taken together. In other words, every state-group z_j is observable at least by one node, (from one output y_i), in the network, similarly as in [79]. Ideally, however, different from [79], we want each state-group to be observable by several nodes so to affect sensor fusion while facing process and measurement noises. Let us point out that all this still allows existence of nodes that do not measure anything. The main contribution of such nodes is in maintaining network connectivity. These nodes can be also used for actuation purposes, along the lines of the distributed controller design in [79]. We refer to them as to non-sensing nodes. To all the other nodes in the network we refer to as the sensing nodes.

Assumption 10. The communication topology is given by a directed graph having a spanning tree with all the sensing nodes contained in the irreducible leader group.

Remark 8. The irreducible leader group is a strongly connected component of the graph given by its Laplacian $L_{c+1,c+1}$ in the Frobenius normal form (2.7). Here the leaders are themselves connected to allow for sensor fusion, as needed with multiple measurements of differing reliability, in contrast to [79] where measurements are assumed perfect. It is important to point out, that the irreducible leader group can additionally contain also some non-sensing nodes.

Remark 9. This approach utilizes directed graphs, unlike some existing results [54, 55, 56, 60, 34, 33], which consider undirected graphs. In comparison to these results the requirements on the communication topology, given by Assumption 10, are more relaxed.

Let each node in the network be endowed with the following LTI dynamics

$$\dot{\hat{z}}_i = \tilde{A}\hat{z}_i + G_i(y_i - \hat{y}_i) + F_i \sum_{j\in\mathcal{V}} e_{ij}(\hat{z}_j - \hat{z}_i), \tag{3.22}$$

where $G_i \in \mathbb{R}^{n\times p_i}$ is the *local observer gain* and $F_i \in \mathbb{R}^{n\times n}$ is the *distributed observer gain*. The ith observer state vector, $\hat{z}_i = [\hat{z}_{i1}^\mathsf{T}, \hat{z}_{i2}^\mathsf{T}, \dots, \hat{z}_{il}^\mathsf{T}]^\mathsf{T} \in \mathbb{R}^n$, is, similarly as the plant's state vector z, partitioned into state-groups $\hat{z}_{ij}$. Note that all nodes (3.22) share the same drift dynamics $\tilde{A}$, which equals the dynamics of the plant.

The node estimation dynamics (3.22) has a similar structure to those presented in [34, 33, 79]. It uses two information sources necessary for proper estimation of the plant state. The first is the measurement y_i, contained in the estimation term $G_i(y_i - \hat{y}_i)$, motivated by the Luenberger observer design [48]. It ensures estimation of observable state-groups $j \in \mathcal{O}_i$ by the ith node from its local measurements. The second information source is given by the state estimates of neighboring nodes contained in the local neighborhood error term $F_i \sum_{j\in\mathcal{V}} e_{ij}(\hat{z}_j - \hat{z}_i)$. Its purpose is to synchronize the unobservable state-groups $j \in \bar{\mathcal{O}}_i$ of the ith node with those of its neighboring nodes and effect sensor fusion for the observable state-groups using information from the network.

Define an observation error as a difference between the estimated state (3.22) and the true state of the plant (3.19)

$$\eta_i(t) = \hat{z}_i(t) - z(t), \tag{3.23}$$

then the observation error dynamics reads

$$\dot{\eta}_i = (\tilde{A} - G_i\tilde{C}_i)\eta_i + F_i \sum_{j\in\mathcal{V}} e_{ij}(\eta_j - \eta_i) + G_i\xi_i - \tilde{\omega}. \tag{3.24}$$

The goal is to design matrices G_i and F_i so that the observation errors (3.23) are asymptotically stable in expectation and their covariances remain finite for all times with their upper bounds depending on the noises, appropriately taking into account the reliability of individual measurements.

3.4 Observer convergence

For the convergence analysis of proposed estimation dynamics (3.22), in this section we first consider the plant dynamics (3.19) and sensor model (3.20) without noises, i.e., $\tilde{\omega} = 0$ and $\xi_i = 0, \forall i$. Our goal is then to design the local observer gains G_i and the distributed observer gains F_i so that the observation error (3.23) in noise-free settings asymptotically converges to zero

$$\lim_{t\to\infty} \eta_i(t) = 0, \quad \forall i \in \mathcal{V}. \tag{3.25}$$

For each node i we can reorder the state-groups $\hat{z}_{ij}$ in the state vector $\hat{z}_i$, such that the new state vector $\hat{z}_i^{\text{new}}$ is a tandem of observable $\hat{z}_{i_o} \in \mathbb{R}^{n_{i_o}}$, containing observable state-groups $\hat{z}_{ij}$ for $j \in \mathcal{O}_i$, and unobservable $\hat{z}_{i_{\bar{o}}} \in \mathbb{R}^{n_{i_{\bar{o}}}}$, containing unobservable state-groups $\hat{z}_{ij}$ for $j \in \bar{\mathcal{O}}_i$. Hence, for every node i there exists a permutation matrix T_i, $T_i^{-1} = T_i^{\mathsf{T}}$, such that

$$\hat{z}_i^{\text{new}} = \begin{bmatrix} \hat{z}_{i_o} \\ \hat{z}_{i_{\bar{o}}} \end{bmatrix} = T_i \hat{z}_i. \tag{3.26}$$

Correspondingly, in the new coordinates, the system matrices are in the Kalman decomposed form

$$\hat{A}_i = T_i \tilde{A} T_i^{\mathsf{T}} = \begin{bmatrix} A_{i_o} & 0 \\ 0 & A_{i_{\bar{o}}} \end{bmatrix}, \quad \hat{C}_i = \tilde{C}_i T_i^{\mathsf{T}} = \begin{bmatrix} C_{i_o} & 0 \end{bmatrix}, \tag{3.27}$$

where $A_{i_o} = \text{diag}(A_j)$, $j \in \mathcal{O}_i$ and $A_{i_{\bar{o}}} = \text{diag}(A_j)$, $j \in \bar{\mathcal{O}}_i$ are block diagonal matrices with $|\mathcal{O}_i|$ and $|\bar{\mathcal{O}}_i|$ blocks on their diagonal. Matrix C_{i_o} can be interpreted as a row vector consisting of $|\mathcal{O}_i|$ elements (matrices) C_{ij}, $j \in \mathcal{O}_i$. Note that the transformed system matrix $\hat{A}_i$ in (3.27) has zero matrices on the off-diagonal blocks because of the Assumption 8 considering observability of a state-group.

Remark 10. The state vector of a non-sensing node is composed completely of unobservable state-groups, $\hat{z}_i^{\text{new}} = \hat{z}_i = \hat{z}_{i_{\bar{o}}}$, hence no permutation of state-groups is needed. The matrices ($\hat{A}_i \equiv A_{i_{\bar{o}}} \equiv \tilde{A}$, $\hat{C}_i \equiv \tilde{C}_i \equiv 0$) are then already in the Kalman decomposed form. The same would hold for a sensing node observing all the state-groups, except that ($\hat{C}_i \equiv C_{i_o} \equiv \tilde{C}_i$), because its state vector would be composed completely of observable state-groups, $\hat{z}_i^{\text{new}} = \hat{z}_i = \hat{z}_{i_o}$.

Remark 11. The permutation of state-groups achieving (3.27) is made possible by Assumption 8. It allows each node to transform the drift dynamics $\tilde{A}$ to the Kalman decomposed form with respect to its sensing model $\tilde{C}_i$. Each node can then in principle estimate its observable state vector $\hat{z}_{i_o}$ using only its local measurements y_i, by designing a Luenberger-like local observer. For those states, the distributed gain is used to improve the nodes' local estimates for the observable state vector $\hat{z}_{i_o}$. To estimate the unobservable state vector $\hat{z}_{i_{\bar{o}}}$, local measurements are to no avail. Therefore a node uses communication with its neighbors to gather estimates on $\hat{z}_{i_{\bar{o}}}$. For this purpose every node designs its distributed observer for unobservable state vector.

Remark 12. The block diagonal structure of the Kalman decomposed form (3.27), adopted from (3.15), [79], is more specific that (3.11) presented in [34]. It requires clear separation into dynamically independent observable and unobservable state-groups from each single-agent perspective. These more

specific assumptions are found to be fulfilled to an acceptable degree of certainty in flexible structures. Robustness of the proposed distributed observer design can, in fact, handle small off-diagonal terms. Furthermore, similarly as in [79], the assumptions made here lead to developments which rely on more relaxed (global) conditions than those in [34] like, e.g., directed graphs, existence of nodes that do not measure, robustness to node or link failures.

In order to show observer convergence on the considered network topology, as detailed in Assumption 10, we proceed first by proving the convergence for strongly connected graphs representing, in general, the irreducible leader group. Then we show convergence of the remainder of the network, considered as pinned. Ultimately using those two results we conclude convergence on the entire graph satisfying Assumption 10.

The following theorem brings the design of local observer gains G_i and distributed observer gains F_i together with conclusion on convergence of the observer dynamics (3.22) in the noise-free case on strongly connected graphs.

Theorem 5. *Consider a network of nodes given by a directed strongly-connected graph $\mathcal{G}$. Let each node with the sensor model (3.20) implement the estimation dynamics (3.22) to estimate states of the plant dynamics (3.19) in noise-free settings; $\tilde{\omega} = 0$ and $\xi_i = 0, \forall i$. Suppose that Assumptions 8 and 9 hold.*

Let Q_i and U_i be symmetric positive definite matrices. Choose the local observer gain as

$$G_i = T_i^{\mathsf{T}} \begin{bmatrix} \bar{M}_i^{-1} C_{i_o}^{\mathsf{T}} U_i^{-1} \\ 0 \end{bmatrix}, \tag{3.28}$$

where $T_i \in \mathbb{R}^{n \times n}$ is the permutation matrix bringing the pair $(\tilde{A}, \tilde{C}_i)$ to the Kalman decomposed form (3.27) and $\bar{M}_i^{-1}$ is the solution of the observer ARE

$$\bar{M}_i^{-1} A_{i_o}^{\mathsf{T}} + A_{i_o} \bar{M}_i^{-1} + Q_i - \bar{M}_i^{-1} C_{i_o}^{\mathsf{T}} U_i^{-1} C_{i_o} \bar{M}_i^{-1} = 0. \tag{3.29}$$

Furthermore, define $N_j := \alpha_j I_{n_j}$ such that

$$0 < \alpha_j < \frac{w_{min} \sum_{i \in \mathcal{D}_j} \lambda_{\min}(\bar{M}_i Q_i \bar{M}_i)}{w_{max}(p - |\mathcal{D}_j|) \lambda_{max}\left(A_j + A_j^{\mathsf{T}}\right)}, \tag{3.30}$$

and choose the distributed observer gain as

$$F_i = \gamma T_i^{\mathsf{T}} \begin{bmatrix} \bar{M}_i^{-1} & 0 \\ 0 & diag(N_j^{-1}) \end{bmatrix} T_i, \quad j \in \bar{\mathcal{O}}_i, \tag{3.31}$$

with $\gamma > 0$. Then each observer state $\hat{z}_i(t)$ asymptotically converges to the plant state $z(t)$, in the sense of (3.25) for γ sufficiently large.

Proof. Define a Lyapunov function candidate in the quadratic form

$$V = \sum_{i\in\mathcal{V}} w_i \eta_i^{\mathsf{T}} M_i \eta_i, \tag{3.32}$$

where $w_i > 0$ is the element of the left eigenvector corresponding to zero eigenvalue of the Laplacian matrix L as in Lemma 3 and $M_i \in \mathbb{R}^{n\times n}$ is a positive definite symmetric matrix to be specified later in the proof. The time-derivative of this Lyapunov function candidate is

$$\dot{V} = \sum_{i\in\mathcal{V}} w_i (\dot{\eta}_i^{\mathsf{T}} M_i \eta_i + \eta_i^{\mathsf{T}} M_i \dot{\eta}_i), \tag{3.33}$$

$$\begin{aligned}\dot{V} = &\sum_{i\in\mathcal{V}} w_i \eta_i^{\mathsf{T}} \left(M_i(\tilde{A} - G_i\tilde{C}_i) + (\tilde{A} - G_i\tilde{C}_i)^{\mathsf{T}} M_i\right) \eta_i \\ &+ 2\sum_{i\in\mathcal{V}} w_i \eta_i^{\mathsf{T}} M_i F_i \sum_{j\in\mathcal{V}} e_{ij}(\eta_j - \eta_i).\end{aligned} \tag{3.34}$$

Let $M_i F_i = \gamma I_n$ with $\gamma \in \mathbb{R}^+$. As the graph is strongly connected, the second term can be rewritten to a quadratic form according to [77] as follows

$$2\sum_{i\in\mathcal{V}} w_i \eta_i^{\mathsf{T}} M_i F_i \sum_{j\in\mathcal{V}} e_{ij}(\eta_j - \eta_i) \tag{3.35}$$

$$= 2\gamma \sum_{i,j} w_i e_{ij} \eta_i^{\mathsf{T}} (\eta_j - \eta_i) \tag{3.36}$$

$$= \gamma \sum_{i,j} w_i e_{ij} \eta_i^{\mathsf{T}} (\eta_j - \eta_i) + \gamma \sum_{i,j} w_i e_{ij} \eta_j^{\mathsf{T}} (\eta_i - \eta_j) \tag{3.37}$$

$$= -\gamma \sum_{i,j} w_i e_{ij} (\eta_j - \eta_i)^{\mathsf{T}} (\eta_j - \eta_i), \tag{3.38}$$

yielding the derivative of the Lyapunov function in the form

$$\begin{aligned}\dot{V} = &\sum_{i\in\mathcal{V}} w_i \eta_i^{\mathsf{T}} \left(M_i(\tilde{A} - G_i\tilde{C}_i) + (\tilde{A} - G_i\tilde{C}_i)^{\mathsf{T}} M_i\right) \eta_i \\ &- \gamma \sum_{i,j\in\mathcal{V}} w_i e_{ij} (\eta_j - \eta_i)^{\mathsf{T}} (\eta_j - \eta_i).\end{aligned} \tag{3.39}$$

Note that the second term in (3.39) is negative semi-definite. It is zero only for the case $\eta_i = \eta_j, \forall (j,i) \in \mathcal{E}$. To show $\dot{V} < 0$ we investigate two cases; first, for $\eta_i = \eta_j, \forall (j,i) \in \mathcal{E}$, the second term vanishes and we show that the first term is negative definite. Then, for $\exists (j,i) \in \mathcal{E}, \eta_i \neq \eta_j$, we show that the second negative definite term dominates the first indefinite one.

1) Let $\eta_i = \eta_j, \forall (j,i) \in \mathcal{E}$. The time-derivative of the Lyapunov function then retains only the first term

$$\dot{V} = \sum_{i\in\mathcal{V}} w_i \eta_i^{\mathsf{T}} \left(M_i(\tilde{A} - G_i\tilde{C}_i) + (\tilde{A} - G_i\tilde{C}_i)^{\mathsf{T}} M_i\right) \eta_i. \tag{3.40}$$

Applying the state transformation (3.67), the time-derivative of the Lyapunov function can be written as

$$\dot{V} = \sum_{i\in\mathcal{V}} w_i \hat{\eta}_i^{\mathsf{T}} T_i \left(M_i(\tilde{A} - G_i\tilde{C}_i) + (\tilde{A} - G_i\tilde{C}_i)^{\mathsf{T}} M_i\right) T_i^{\mathsf{T}} \hat{\eta}_i, \tag{3.41}$$

$$\begin{aligned}\dot{V} = &\sum_i w_i \hat{\eta}_i^{\mathsf{T}} \left(T_i M_i T_i^{\mathsf{T}} (T_i \tilde{A} T_i^{\mathsf{T}} - T_i G_i \tilde{C}_i T_i^{\mathsf{T}})\right. \\ &\left. + (T_i \tilde{A} T_i^{\mathsf{T}} - T_i G_i \tilde{C}_i T_i^{\mathsf{T}})^{\mathsf{T}} T_i M_i T_i^{\mathsf{T}}\right) \hat{\eta}_i^{\mathsf{T}},\end{aligned} \tag{3.42}$$

$$\dot{V} = \sum_i w_i \hat{\eta}_i^\mathsf{T} \left(\hat{M}_i (\hat{A}_i - \hat{G}_i \hat{C}_i) + (\hat{A}_i - \hat{G}_i \hat{C}_i)^\mathsf{T} \hat{M}_i \right) \hat{\eta}_i, \tag{3.43}$$

with the system matrices $(\hat{A}_i, \hat{C}_i)$ in the Kalman decomposed form (3.27), the local observer gain $\hat{G}_i$ given by (3.69), and the matrix $\hat{M}_i$ in the form

$$\hat{M}_i = T_i M_i T_i^\mathsf{T} = \begin{bmatrix} \bar{M}_i & 0 \\ 0 & \bar{N}_i \end{bmatrix}, \tag{3.44}$$

where $\bar{N}_i = \mathrm{diag}(N_j), N_j \in \mathbb{R}^{n_j \times n_j}, j \in \bar{\mathcal{O}}_i$.

This allows to write the time-derivative of the Lyapunov function as $\dot{V} = \sum_i w_i \hat{\eta}_i^\mathsf{T} (J_i + J_i^\mathsf{T}) \hat{\eta}_i$ with

$$J_i = \begin{bmatrix} \bar{M}_i & 0 \\ 0 & \bar{N}_i \end{bmatrix} \left(\begin{bmatrix} A_{i_o} & 0 \\ 0 & A_{i_{\bar{o}}} \end{bmatrix} - \begin{bmatrix} G_{i_o} \\ 0 \end{bmatrix} \begin{bmatrix} C_{i_o} & 0 \end{bmatrix} \right), \tag{3.45}$$

which yields the kernel

$$J_i + J_i^\mathsf{T} = \begin{bmatrix} \bar{M}_i (A_{i_o} - G_{i_o} C_{i_o}) + (A_{i_o} - G_{i_o} C_{i_o})^\mathsf{T} \bar{M}_i & 0 \\ 0 & \bar{N}_i A_{i_{\bar{o}}} + A_{i_{\bar{o}}}^\mathsf{T} \bar{N}_i \end{bmatrix}. \tag{3.46}$$

This transformation allows us to split the time-derivative of the Lyapunov function into two terms representing the contributions of observable and unobservable state-groups separately

$$\begin{aligned} \dot{V} = & \sum_i w_i \eta_{i_o}^\mathsf{T} \left(\bar{M}_i (A_{i_o} - G_{i_o} C_{i_o}) + (A_{i_o} - G_{i_o} C_{i_o})^\mathsf{T} \bar{M}_i \right) \eta_{i_o} \\ & + \sum_i w_i \eta_{i_{\bar{o}}}^\mathsf{T} \left(\bar{N}_i A_{i_{\bar{o}}} + A_{i_{\bar{o}}}^\mathsf{T} \bar{N}_i \right) \eta_{i_{\bar{o}}}. \end{aligned} \tag{3.47}$$

Referring to Theorem 5, let $Q_i \succ 0$ and $U_i \succ 0$ are chosen matrices and the local observer gain is given by $G_{i_o} = \bar{M}_i^{-1} C_{i_o}^\mathsf{T} U_i^{-1}$, where $\bar{M}_i^{-1}$ is the solution of the ARE (3.29). Then by using ARE (3.29), the first term of the time-derivative of the Lyapunnov function can be simplified to

$$\begin{aligned} & \bar{M}_i (A_{i_o} - G_{i_o} C_{i_o}) + (A_{i_o} - G_{i_o} C_{i_o})^\mathsf{T} \bar{M}_i \\ = & \bar{M}_i \left((A_{i_o} - G_{i_o} C_{i_o}) \bar{M}_i^{-1} + \bar{M}_i^{-1} (A_{i_o} - G_{i_o} C_{i_o})^\mathsf{T} \right) \bar{M}_i \\ = & \bar{M}_i (\bar{M}_i^{-1} A_{i_o}^\mathsf{T} + A_{i_o} \bar{M}_i^{-1} - 2 \bar{M}_i^{-1} C_{i_o}^\mathsf{T} U_i^{-1} C_{i_o} \bar{M}_i^{-1}) \bar{M}_i \\ = & \bar{M}_i (-Q_i - \bar{M}_i^{-1} C_{i_o}^\mathsf{T} U_i^{-1} C_{i_o} \bar{M}_i^{-1}) \bar{M}_i. \end{aligned}$$

Then the time-derivative of the Lyapunov function equals

$$\begin{aligned} \dot{V} = & \sum_i w_i \eta_{i_o}^\mathsf{T} \bar{M}_i (-Q_i - \bar{M}_i^{-1} C_{i_o}^\mathsf{T} U_i^{-1} C_{i_o} \bar{M}_i^{-1}) \bar{M}_i \eta_{i_o} \\ & + \sum_i w_i \eta_{i_{\bar{o}}}^\mathsf{T} \left(\bar{N}_i A_{i_{\bar{o}}} + A_{i_{\bar{o}}}^\mathsf{T} \bar{N}_i \right) \eta_{i_{\bar{o}}}. \end{aligned} \tag{3.48}$$

By neglecting the negative semi-definite term with $(-\bar{M}_i^{-1}C_{i_o}^{\mathsf{T}}U_i^{-1}C_{i_o}\bar{M}_i^{-1})$ we find an upper bound on the time-derivative of the Lyapunov function as

$$\dot{V} < -\sum_i w_i \eta_{i_o}^{\mathsf{T}} \bar{M}_i Q_i \bar{M}_i \eta_{i_o} + \sum_i w_i \eta_{i_{\bar{o}}}^{\mathsf{T}} \left(\bar{N}_i A_{i_{\bar{o}}} + A_{i_{\bar{o}}}^{\mathsf{T}} \bar{N}_i\right) \eta_{i_{\bar{o}}}. \tag{3.49}$$

A lower bound on the first term gives

$$\sum_i w_i \lambda_{\min}(\bar{M}_i Q_i \bar{M}_i) \eta_{i_o}^{\mathsf{T}} \eta_{i_o} \leq \sum_i w_i \eta_{i_o}^{\mathsf{T}} \bar{M}_i Q_i \bar{M}_i \eta_{i_o}. \tag{3.50}$$

Let $R_j = N_j A_j + A_j^{\mathsf{T}} N_j$; then, with $\bar{N}_i = \text{diag}(N_j), j \in \bar{\mathcal{O}}_i$, the time-derivative of the Lyapunov function is

$$\begin{aligned} \dot{V} < &-\sum_{i\in\mathcal{V}} w_i \left(\sum_{j\in\mathcal{O}_i} \lambda_{\min}(\bar{M}_i Q_i \bar{M}_i) \eta_{ij}^{\mathsf{T}} I_{n_j} \eta_{ij}\right) \\ &+ \sum_{i\in\mathcal{V}} w_i \left(\sum_{j\in\bar{\mathcal{O}}_i} \eta_{ij}^{\mathsf{T}} R_j \eta_{ij}\right). \end{aligned} \tag{3.51}$$

Let us recall that here $\eta_i = \eta_j, \forall (j,i) \in \mathcal{E}$, which implies that all corresponding state-groups of all nodes are equal, i.e., $\eta_j^* := \eta_{1j} = \eta_{2j} = \cdots = \eta_{pj}, \forall j \in \mathcal{S}$. This allows us to rewrite the time-derivative of the Lyapunov function into the form $\dot{V} = \sum_{j\in\mathcal{S}} \eta_j^{*T} E_j \eta_j^*$, where

$$E_j \prec -\sum_{i\in\mathcal{D}_j} w_i \lambda_{\min}(\bar{M}_i Q_i \bar{M}_i) I_{n_j} + \sum_{i\in\bar{\mathcal{D}}_j} w_i R_j, \tag{3.52}$$

with sum over state-groups instead of sum over agents and vice versa. For $\dot{V} < 0$, as state-groups are dynamically independent, $E_j \prec 0$ has to be satisfied by each state-group j. The second sum in (3.52) is indefinite while the first sum is negative definite. To allow $\dot{V} < 0$, every state-group has to be observable by at least one agent to have at least one negative definite term in E_j. Note that this property is guaranteed by Assumption 9.

Using the definition $N_j = \alpha_j I_{n_j}$ from Theorem 5, we derive an upper bound on matrix E_j as follows

$$\begin{aligned} E_j \preceq &-w_{min} \sum_{i\in\mathcal{D}_j} \lambda_{\min}(\bar{M}_i Q_i \bar{M}_i) I_{n_j} \\ &+ (p - |\mathcal{D}_j|)\alpha_j w_{max} \lambda_{max}\left(A_j + A_j^{\mathsf{T}}\right) I_{n_j}. \end{aligned} \tag{3.53}$$

Choosing α_j as in (3.30), $E_j \prec 0$, thus $\dot{V} < 0$ for the investigated case, $\eta_i = \eta_j, \forall (j,i) \in \mathcal{E}$.

2) Let now $\exists (j,i) \in \mathcal{E}, \eta_i \neq \eta_j$. Define a matrix $\mathbf{W} = W \otimes I_n$, $W = \text{diag}(w_i)$ and a block diagonal matrix $H = \text{diag}(M_i(\tilde{A} - G_i\tilde{C}_i))$, $i \in \mathcal{V}$. Rewriting the derivative of the Lyapunov function (3.39) to the matrix form gives

$$\dot{V} = \eta^{\mathsf{T}} \left(\mathbf{W}\left(H + H^{\mathsf{T}}\right)\right) \eta - \gamma \eta^{\mathsf{T}} \left((WL + L^{\mathsf{T}}W) \otimes I_n\right) \eta. \tag{3.54}$$

The first term of (3.54) is generally indefinite while the second term is negative definite. Finding upper and lower bounds on these two terms we get

$$\dot{V} \leq w_{max}\lambda_{max}\big(H + H^{\mathsf{T}}\big)\|\eta\|^2 - \gamma\lambda_{min>0}(WL + L^{\mathsf{T}}W)\|\eta\|^2. \tag{3.55}$$

Hence the time-derivative of the Lyapunov function is negative definite for

$$\gamma > w_{max}\frac{\lambda_{max}\big(H + H^{\mathsf{T}}\big)}{\lambda_{min>0}(WL + L^{\mathsf{T}}W)}. \tag{3.56}$$

In other words, for sufficiently large γ, $\dot{V} < 0$ for the second investigated case, $\exists(j,i) \in \mathcal{E}, \eta_i \neq \eta_j$.

Hereby we showed that the time-derivative of the Lyapunov function (3.32) is negative definite for α_j in (3.30) and γ sufficiently large, satisfying (3.56), in all cases. Hence nodes' estimation dynamics (3.22) is stable in the sense that nodes' states always converge to the plant state. This concludes the proof. □

Theorem 5 brings general methodology for the design of local observer gains G_i and distributed observer gains F_i for the strongly connected leader group without explicitly considering noises. The implication of this design to observation error covariance, when measurement and process noises are acting, is given in Section 3.4.1.

Remark 13. From Theorem 5 it follows that both sensing and non-sensing nodes, in the irreducible leader group at least, share the same design of G_i and F_i. Moreover, all the non-sensing nodes have the same distributed observer gain $F_i = F_{\bar{o}} := \mathrm{diag}(N_j^{-1})$ and also, trivially, the local observer gain, as it is identically zero, i.e., $G_i = G_{\bar{o}} := 0$.

Now consider the remainder of the network. It is given by a graph generally having a spanning forest with root nodes of all trees pinned by the outgoing edges of the irreducible leader group from Theorem 5, (due to the assumed existence of a spanning tree). According to Assumption 10, the nodes in the remainder of the graph are all necessarily non-sensing. The node dynamics (3.22), for such nodes, can be written in the form containing two local neighborhood error terms

$$\dot{\hat{z}}_k = \tilde{A}\hat{z}_k + F_{\bar{o}}\textstyle\sum_r e_{kr}(\hat{z}_r - \hat{z}_k) + F_{\bar{o}}\sum_i e_{ki}(\hat{z}_i - \hat{z}_k), \tag{3.57}$$

The first term $F_{\bar{o}}\sum_r e_{kr}(\hat{z}_r - \hat{z}_k)$ serves to synchronize the non-sensing nodes with their peers from the remainder of the network and the second term $F_{\bar{o}}\sum_i e_{ki}(\hat{z}_i - \hat{z}_k)$ serves to synchronize these nodes with the irreducible leader group. Because the remainder of the network contains only non-sensing nodes, the dynamics (3.57) has no estimation term. Let $g_k = \sum_i e_{ki}$ represent the overall pinning gain from the irreducible leader group to the kth node in the

remainder of the graph. In terms of the observation error dynamics (3.23), the node dynamics (3.57) is then given by

$$\dot{\eta}_k = \tilde{A}\eta_k + F_{\bar{o}}\left(\sum_r e_{kr}(\eta_r - \eta_k) - g_k\eta_k\right) + F_{\bar{o}}\sum_i e_{ki}\eta_i, \tag{3.58}$$

which is considered as composed of the nominal dynamics

$$\dot{\eta}_k = \tilde{A}\eta_k + F_{\bar{o}}\left(\sum_r e_{kr}(\eta_r - \eta_k) - g_k\eta_k\right), \tag{3.59}$$

and the interconnection term $F_{\bar{o}}\sum_i e_{ki}\eta_i$. Note that the nominal dynamics (3.59) is a special case of conventional leader following consensus, also known as the *cooperative tracking problem*, [43], with a static leader node representing a zero reference.

The following result proves convergence of the nominal dynamics (3.59) for nodes in the remainder of the network.

Proposition 1. *Consider a graph with a spanning forest having root nodes of all trees pinned. Let each node in this graph implement the nominal dynamics (3.59) with $F_{\bar{o}} = \gamma diag(N_j^{-1})$ with N_j as in Theorem 5. Then the nominal dynamics (3.59) is asymptotically stable, i.e., the observation error $\eta_k(t)$ converges to 0 as $t \to \infty$, for γ sufficiently large.*

Proof. By use of the Kronecker product, the nominal dynamics (3.59) can be written in the form

$$\dot{\eta} = (I_n \otimes \tilde{A})\eta - ((\tilde{L} + \tilde{G}) \otimes F_{\bar{o}})\eta, \tag{3.60}$$

where $\tilde{L}$ is the Laplacian matrix of the spanning forest and $\tilde{G} = \text{diag}(\tilde{g}_k)$ is the pinning matrix.

Define a Lyapunov function candidate in the quadratic form

$$V = \eta^{\mathsf{T}}(\Theta \otimes M)\eta > 0, \tag{3.61}$$

where $\Theta = \text{diag}(\theta_i) > 0$ is selected based on Lemma 4 for $\tilde{L} + \tilde{G}$ and M is positive definite symmetric such that $MF_{\bar{o}} = \gamma I_n$. Then the time-derivative of the Lyapunov function candidate (3.61) equals

$$\dot{V} = \eta^{\mathsf{T}}\left(\Theta \otimes (M\tilde{A} + \tilde{A}^{\mathsf{T}}M) - \gamma\left(\Theta(\tilde{L} + \tilde{G}) + (\tilde{L} + \tilde{G})^{\mathsf{T}}\Theta\right) \otimes I_n\right)\eta, \tag{3.62}$$

with $M = \text{diag}(N_j) = \text{diag}(\alpha_j I_{n_j})$.

An upper bound on the time-derivative of the Lyapunov function (3.62) is

$$\begin{aligned}\dot{V} < {} & \alpha_{\max}\theta_{\max}\lambda_{\max}\left(\tilde{A} + \tilde{A}^{\mathsf{T}}\right)\|\eta\|^2 \\ & - \gamma\lambda_{\min}\left(\Theta(\tilde{L} + \tilde{G})^{\mathsf{T}} + (\tilde{L} + \tilde{G})\Theta\right)\|\eta\|^2,\end{aligned} \tag{3.63}$$

which is negative if

$$\gamma > \frac{\alpha_{\max}\theta_{\max}\lambda_{\max}\left(\tilde{A}+\tilde{A}^{\mathsf{T}}\right)}{\lambda_{\min}\left(\Theta(\tilde{L}+\tilde{G})+(\tilde{L}+\tilde{G})^{\mathsf{T}}\Theta\right)}. \tag{3.64}$$

As the time-derivative of the Lyapunov function (3.62) is negative for γ sufficiently large, satisfying (3.64), this implies asymptotic stability of the nominal dynamics (3.59), and concludes the proof. □

Remark 14. Design details for G_i and F_i coincide in Theorem 5 and Proposition 1 as they should for a practical design. Namely, a node need not know if it is in the irreducible leader group or in the remainder of the graph.

The entire network is thus a hierarchically coupled system given by the observation error dynamics for the irreducible leader group and the remainder of the network

$$\dot{\eta}_i = (\tilde{A} - G_i\tilde{C}_i)\eta_i + F_i\textstyle\sum_j e_{ij}(\eta_j - \eta_i), \tag{3.65}$$

$$\dot{\eta}_k = \tilde{A}\eta_k + F_{\bar{o}}\left(\textstyle\sum_r e_{kr}(\eta_l - \eta_k) - g_k\eta_k\right) + F_{\bar{o}}\textstyle\sum_i e_{ki}\eta_i, \tag{3.66}$$

which are coupled through the interconnection term $F_{\bar{o}}\sum_i e_{ki}\eta_i$. We use results of Theorem 5, Proposition 1, and the well known results on hierarchically interconnected systems to show the convergence of the entire network satisfying Assumption 10. The following theorem constitutes the main result of this section.

Theorem 6. *Consider a network of nodes with the sensor model (3.20) implementing estimation dynamics (3.22) to estimate states of the plant dynamics (3.19) in noise-free settings; $\tilde{\omega} = 0$ and $\xi_i = 0, \forall i$. Suppose that Assumptions 8, 9 and 10 hold. Let conditions of both Theorem 5 and Proposition 1 apply respectively to the irreducible leader group and the remainder of the graph, considered as pinned. Then each estimate $\hat{z}_i(t)$ asymptotically converges to the plant state $z(t)$, in the sense of (3.25) for γ sufficiently large.*

Proof. The entire network is a hierarchically coupled LTI system of the irreducible leader group (3.65) and the remainder of the graph (3.66). The eigenvalues of hierarchically interconnected LTI systems are given by the eigenvalues of their autonomous subsystem blocks on the system matrix block-diagonal, (which is a generally known result in linear systems). Theorem 5 shows the asymptotic stability of (3.65) and Proposition 1 shows the asymptotic stability of the autonomous subsystem (nominal dynamics) in (3.66), hence implying stability of the hierarchically coupled system. □

Alternatively, to show stability of the entire network, a composite Lyapunov function could be constructed as in [23]. Since this work deals with LTI systems, asymptotic stability is exponential. Note that Theorem 6 shows stability of the entire network but the convergence rate of each estimator depends on all initial conditions and the graph topology. Nevertheless, it is bounded from below by the slowest eigenvalue of the total system.

The following subsection analyses the effect of the process and measurement noises on the estimation error η_i, building on the results of Theorem 5, Proposition 1, and Theorem 6.

3.4.1 Estimation error covariance

If the process and measurement noises are acting, it will be shown that the covariance of observation error (3.23) is finite for all times, with an upper bound depending on the noises.

Assume that the process and measurement noises are nonzero, i.e., $\tilde{\omega}(t) \neq 0$ and $\xi_i(t) \neq 0, \forall i$, then the local observation error η_i has the dynamics (3.24). Applying the transformation

$$\hat{\eta}_i = \begin{bmatrix} \hat{\eta}_{i_o} \\ \hat{\eta}_{i_{\bar{o}}} \end{bmatrix} = T_i \eta_i, \tag{3.67}$$

with the permutation matrix T_i that rearranges the state-groups η_{ij} of the ith observer node into observable, $\hat{\eta}_{i_o}$, and unobservable ones, $\hat{\eta}_{i_{\bar{o}}}$, as in (3.26), the observation error dynamics reads

$$\dot{\hat{\eta}}_i = (\hat{A} - \hat{G}_i \hat{C}_i)\hat{\eta}_i + \hat{F}_i \textstyle\sum_{j \in \mathcal{V}} e_{ij}(\hat{\eta}_j - \hat{\eta}_i) + \hat{G}_i \xi_i - \hat{\omega}_i, \tag{3.68}$$

where the state-space matrices $(\hat{A}, \hat{C}_i)$ are in the Kalman decomposed form (3.27), the observer gain matrices are

$$\hat{G}_i = T_i G_i = \begin{bmatrix} G_{i_o} \\ 0 \end{bmatrix}, \quad \hat{F}_i = T_i F_i T_i^{\mathsf{T}} = \begin{bmatrix} F_{i_o} & 0 \\ 0 & F_{i_{\bar{o}}} \end{bmatrix}, \tag{3.69}$$

and the transformed process noise is $\hat{\omega}_i = T_i \tilde{\omega}$.

The global observation error dynamics has the form

$$\dot{\hat{\eta}} = A_{tot}\eta + \hat{G}\xi - \hat{\omega}, \tag{3.70}$$

with $\hat{\omega} = [\hat{\omega}_1^{\mathsf{T}}, \hat{\omega}_2^{\mathsf{T}}, \ldots, \hat{\omega}_p^{\mathsf{T}}]^{\mathsf{T}}$, $\hat{G} = \operatorname{diag}(\hat{G}_i)$, and

$$A_{tot} = \operatorname{diag}(\hat{A} - \hat{G}_i \hat{C}_i) - \operatorname{diag}(\hat{F}_i)(L \otimes I_n). \tag{3.71}$$

Define the observation error covariance $P(t) \in \mathbb{R}^{np \times np}$ as

$$P(t) = \mathbb{E}\left[(\eta(t) - \mathbb{E}[\eta(t)]) \, (\eta(t) - \mathbb{E}[\eta(t)])^{\mathsf{T}} \right], \tag{3.72}$$

then its time evolution is governed by

$$\dot{P} = A_{tot}P + PA_{tot}^{\mathsf{T}} + \hat{\Omega} + \hat{G}\Xi\hat{G}^{\mathsf{T}}, \tag{3.73}$$

where $\hat{\Omega}$ has blocks $\hat{\Omega}_{ij} = T_i\Omega T_j^{\mathsf{T}}$ and $\Xi = \mathrm{diag}(\Xi_i)$.

Since, by Theorem 6, the system matrix A_{tot} is asymptotically stable, $P(t)$, the covariance matrix of the estimation error $\hat{\eta}$, is finite for all times, with an upper bound depending on the noises. Moreover, this estimation error covariance P is naturally partitioned into blocks

$$P_{ij} = \begin{bmatrix} P_{ij_{oo}} & P_{ij_{o\bar{o}}} \\ P_{ij_{\bar{o}o}} & P_{ij_{\bar{o}\bar{o}}} \end{bmatrix} \in \mathbb{R}^{n\times n}, \tag{3.74}$$

which allows one to write (3.73) in the block form

$$\begin{aligned} \dot{P}_{ij} = {} & (\hat{A} - \hat{G}_i\hat{C}_i)P_{ij} + P_{ij}(\hat{A} - \hat{G}_j\hat{C}_j)^{\mathsf{T}} \\ & - \hat{F}_i \textstyle\sum_{k\in\mathcal{V}} e_{ik}(P_{ij} - P_{kj}) - \sum_{k\in\mathcal{V}} e_{jk}(P_{ij} - P_{ik})\hat{F}_j^{\mathsf{T}} \\ & + \hat{\Omega}_{ij} + \hat{G}_i\Xi_i\hat{G}_i^{\mathsf{T}}\delta_{ij}, \end{aligned} \tag{3.75}$$

with $\delta_{ij} = 1$ iff $i = j$ and $\delta_{ij} = 0$ otherwise.

For minimizing the cost

$$\begin{aligned} J(t) = \mathrm{trace}(P(t)) &= \textstyle\sum_i \mathrm{trace}(P_{ii}(t)) \\ &= \textstyle\sum_i \left(\mathrm{trace}(P_{ii_{oo}}(t)) + \mathrm{trace}(P_{ii_{\bar{o}\bar{o}}}(t))\right), \end{aligned} \tag{3.76}$$

one could consider two differential equations for $P_{ii_{oo}}$ and $P_{ii_{\bar{o}\bar{o}}}$, corresponding to observable and unobservable state-groups of the ith node as follows

$$\begin{aligned} \dot{P}_{ii_{oo}} = {} & (A_{i_o} - G_{i_o}C_{i_o})P_{ii_{oo}} + P_{ii_{oo}}(A_{i_o} - G_{i_o}C_{i_o})^{\mathsf{T}} \\ & - F_{i_o} \textstyle\sum_{k\in\mathcal{V}} e_{ik}(P_{ii_{oo}} - P_{ki_{oo}}) - \sum_{k\in\mathcal{V}} e_{ik}(P_{ii_{oo}} - P_{ik_{oo}})F_{i_o}^{\mathsf{T}} \\ & + \Omega_{i_o} + G_{i_o}\Xi_i G_{i_o}^{\mathsf{T}}, \end{aligned} \tag{3.77}$$

$$\begin{aligned} \dot{P}_{ii_{\bar{o}\bar{o}}} = {} & A_{i_{\bar{o}}}P_{ii_{\bar{o}\bar{o}}} + P_{ii_{\bar{o}\bar{o}}}A_{i_{\bar{o}}}^{\mathsf{T}} \\ & - F_{i_{\bar{o}}} \textstyle\sum_{k\in\mathcal{V}} e_{ik}(P_{ii_{\bar{o}\bar{o}}} - P_{ki_{\bar{o}\bar{o}}}) - \sum_{k\in\mathcal{V}} e_{ik}(P_{ii_{\bar{o}\bar{o}}} - P_{ik_{\bar{o}\bar{o}}})F_{i_{\bar{o}}}^{\mathsf{T}} \\ & + \Omega_{i_{\bar{o}}}, \end{aligned} \tag{3.78}$$

where Ω_{i_o} and $\Omega_{i_{\bar{o}}}$ are found from

$$\hat{\Omega}_{ii} = T_i\Omega T_i^{\mathsf{T}} = \begin{bmatrix} \Omega_{i_o} & \Omega_{i_{12}} \\ \Omega_{i_{21}} & \Omega_{i_{\bar{o}}} \end{bmatrix}. \tag{3.79}$$

Given a constant distributed observer gain $\hat{F}_i$, to derive the optimal G_i minimizing (3.76) it is sufficient to minimize $\mathrm{trace}(\dot{P}_{ii_{oo}})$ with respect to G_{i_o} as

$$\frac{\partial(\mathrm{trace}(\dot{P}_{ii_{oo}}))}{\partial G_{i_o}} = -P_{ii_{oo}}C_{i_o}^{\mathsf{T}} - P_{ii_{oo}}C_{i_o}^{\mathsf{T}} + 2G_{i_o}\Xi_i, \tag{3.80}$$

which yields

$$G_{i_o} = P_{ii_{oo}} C_{i_o} \Xi_i^{-1}. \tag{3.81}$$

Remark 15. The optimal solution for G_i, (3.69, 3.81), requires $P_{ii_{oo}}$ for its design. This can be obtained either by solving the Lyapunov equation (3.73) for P globally for all nodes, which does not allow for a fully distributed design; or by solving the Lyapunov equation (3.77) locally, which would require communicating covariances. The reason stems from the two terms

$$- F_{i_o} \textstyle\sum_{k\in\mathcal{V}} e_{ik}(P_{ii_{oo}} - P_{ki_{oo}}) - \sum_{k\in\mathcal{V}} e_{ik}(P_{ii_{oo}} - P_{ik_{oo}})F_{i_o}^{\mathsf{T}} \tag{3.82}$$

in (3.77) representing network interconnections.

Note that, here we do not aim for optimality but rather for an effective sensor fusion and reduced communication load. The distributed observer design proposed by Theorem 5 introduces G_i, (3.28), having the same structure as the optimal one (3.69, 3.81). It requires solving the ARE (3.29) for $\bar{M}_i^{-1}$ which, in comparison to the Lyapunov equation (3.77), does not include the interconnection terms (3.82). The similarity of the proposed design with the celebrated Kalman Filter is further analyzed in Section 3.5.1 after introducing the design steps.

Remark 16. Results of this section extend [80] by considering a general plant dynamics, while considering process and measurement noises, unlike [79], which assumes perfect measurements. Moreover, different from [79], all nodes in the irreducible leader group and the remainder of the network implement the same observer dynamics (3.22) and design their local observer gains G_i and distributed observer gains F_i in the same way, independently of each other. In particular, a given non-sensing node need not know if it is in the irreducible leader group or in the remainder of the network. Theorem 5 and Proposition 1 imply different lower bounds on γ hence, for the design, a more conservative one should be chosen by all nodes to guarantee stability of the entire network.

The general conclusions of this section provide a basis for the specific design detailed in the following section. Theorem 5, Proposition 1 and Theorem 6 require several design parameters, Q_i, U_i, α_j, and γ, which are not specified yet, giving a family of DLOs. Their specific choice influences the performance of the proposed distributed observer dynamics. In the following section, we detail the design procedure and address the specific choice of these design parameters. Those pertain to distributed observers, nevertheless they will be chosen, in fact, to emulate certain desirable properties of the Kalman filter.

3.5 Design procedure

This section proposes the distributed observer design, satisfying conditions of Theorem 6, for an individual node under the original plant dynamics with process noise (3.19) and sensor model with measurement noise (3.20).

Algorithm 3.2 DKF design procedure

Preliminary steps:

1: Choose $\gamma > 0$ satisfying both following conditions

$$\gamma > w_{max} \frac{\lambda_{max}\left(\tilde{A} + \tilde{A}^{\mathsf{T}}\right)}{\lambda_{min>0}(WL_{c+1,c+1} + L_{c+1,c+1}^{\mathsf{T}}W)}, \tag{3.83}$$

$$\gamma > \theta_{\max} \frac{\lambda_{\max}\left(\tilde{A} + \tilde{A}^{\mathsf{T}}\right)}{\lambda_{\min}\left(\Theta(\tilde{L} + \tilde{G}) + (\tilde{L} + \tilde{G})^{\mathsf{T}}\Theta\right)}. \tag{3.84}$$

2: Choose β, such that $0 < \beta \leq 1$.

3: Let every node i know the values of Ω, γ, and β.

Design steps:

1: Every node $i, \mathcal{O}_i \neq \emptyset$, sets its $U_i = \Xi_i$ and $Q_i = \Omega_{i_o}$, with Ω_{i_o} from (3.79).

2: Every node $i, \mathcal{O}_i \neq \emptyset$, calculates M_i^{-1} as the solution of the ARE (3.29).

3: Every node $i, \mathcal{O}_i \neq \emptyset$, also calculates

$$\alpha_{ij_{\max}} = \frac{w_{\min}\lambda_{\min}\left(\bar{M}_i Q_i \bar{M}_i\right)}{w_{\max}(p-1)\lambda_{\max}\left(A_j + A_j^{\mathsf{T}}\right)}, j \in \mathcal{O}_i, \tag{3.85}$$

and communicates the value of $\alpha_{ij_{\max}}$ to all other nodes in the network.

4: Every node $k \in \bar{\mathcal{D}}_j, \forall j$, chooses its α_j as

$$\alpha_j = \min\{1, \beta\alpha_{*j_{\max}}\}, \tag{3.86}$$

where $\alpha_{*j_{\max}} = \min\{\alpha_{ij_{max}} | i \in \mathcal{D}_j\}$.

5: All nodes design their G_i and F_i according to Theorem 5.

The preliminary steps in Algorithm 3.2 are the only centralized elements of the design. Note that, in contrast to [54, 55, 56, 33], our communication scheme does not require communicating the covariance-related matrices. Neither do we consider channel noise as [29]. This reduces the communication burden.

Remark 17. The design procedure outlined in Algorithm 3.2 relies on having $Q_i \succ 0$ as this is needed in Theorem 5. If, however, there is no disturbance acting on the plant, $\Omega = 0$, we propose a slight modification of the design by

choosing the design parameter Q_i as $Q_i = \epsilon I_{n_{i_o}}$, where ϵ is a small positive scalar chosen considering magnitudes of the noise covariances Ξ_i.

Furthermore, for purposes of the design, the assigned covariance matrices Q_i and U_i can be scaled equally by an arbitrary constant, at least for asymptotically stable plants or unstable plants with $\alpha_{*j_{\max}} > 1, \forall j \in \bigcup_{i=1}^{p} \bar{\mathcal{O}}_i$. This scaling brings an additional degree of freedom offered by the design.

Note, that the choice of α_j in (3.86) is conservative to satisfy the upper bound on α_j in (3.30). This conservativeness comes from the choice of $\alpha_{ij_{\max}}$ in (3.85). If $|\mathcal{D}_j| = 1$, i.e., only one node observes the jth state-group, then (3.85) is the same as (3.30). On the other hand, if $|\mathcal{D}_j| > 1$, i.e., more than one node observes the jth state-group, then (3.85) is more conservative that (3.30).

According to (3.86), if the upper bound on α_j is greater than 1, i.e., $\alpha_{*j_{max}} > 1$, then $\alpha_j = 1$. Otherwise α_j is chosen such that $0 < \alpha_j \leq 1$. There is no reason for α_j to be chosen greater than 1, since the greater the α_j the smaller the stability margin guaranteed by the Lyapunov function in the proof of Theorem 5. The exact value of α_j is in this case determined by the auxiliary design parameter β.

The lower bounds on γ in (3.83) and (3.84) imply (3.56) and (3.64). The lower bound (3.56), following from Proof of Theorem 5, is primarily determined by the indefinite term $\lambda_{max}(H + H^{\mathsf{T}})$. The block diagonal matrix $(H + H^{\mathsf{T}})$ is composed of two types of blocks $(H_{i_o} + H_{i_o}^{\mathsf{T}})$ and $(H_{i_{\bar{o}}} + H_{i_{\bar{o}}}^{\mathsf{T}})$. The first type, given by $H_{i_o} = \bar{M}_{i_o}(A_{i_o} - G_{i_o}C_{i_o}), i \in \mathcal{V}, j \in \mathcal{O}_i$, corresponds to the observable state-groups of the ith node and the eigenvalues of such a block are negative. Hence those do not affect the lower bound on γ in (3.56) and can be disregarded. The second type $(H_{i_{\bar{o}}} + H_{i_{\bar{o}}}^{\mathsf{T}})$ is also a block diagonal matrix but with indefinite blocks $(H_{ij} + H_{ij}^{\mathsf{T}}) = \alpha_{\max}(A_j^{\mathsf{T}} + A_j), i \in \mathcal{V}, j \in \mathcal{O}_i$, where $\alpha_{\max}$ is an upper bound on all α_j. It yields a new numerator of the lower bound (3.56) in the form

$$\lambda_{max}(H + H^{\mathsf{T}}) \leq \alpha_{\max}\lambda_{max}(A_j + A_j^{\mathsf{T}}). \tag{3.87}$$

Taking into consideration an upper bound on α_j, (3.86), one can put $\alpha_{\max} = 1$. Then the new numerator (3.87) of (3.56) and also the second lower bound (3.84), yield simplified lower bounds (3.83) and (3.84).

Hereby we showed that the outlined design indeed satisfies conditions of Theorem 5 and Proposition 1, guaranteeing observer convergence as per Theorem 6.

Remark 18. The conservative choice of α_js brings robustness to sensor failures. If one node stops measuring and its previously measured state-groups are still measured by other nodes in the network, the observation error dynamics remains stable according to Theorem 6. This property allows incorporation of redundant nodes in the network to increase robustness of the distributed

observer. Moreover, fixing of the upper bound on α_j, (3.86), brings an additional benefit; it establishes definite lower bounds on γ, which are independent of α_j.

3.5.1 Theoretical analysis

This subsection provides further discussion on the properties of the presented distributed observer, in particular reflecting on the similarities with the celebrated Kalman filter.

Remark 19. Design parameters Q_i and U_i are chosen as covariance matrices of the process and measurement noise to emulate the Kalman filter design. Hence every sensing node implements its local Kalman filter to estimate observable state-groups of the plant given only its local measurements and noises. This brings local sensor fusion.

To elucidate this further, we analyze the behavior of the local observer gain G_i in dependence of the design matrices Q_i and U_i given by noise covariances. Following the properties of the Kalman filter, which are well documented, [42, 65, 28], if for the ith node G_i is chosen according to the solution $\bar{M}_i^{-1}$ of the ARE (3.29), then if U_i increases while Q_i is fixed G_{i_o} decreases in magnitude and if Q_i increases while U_i is fixed G_{i_o}, defined in (3.69), increases in magnitude. In other words, the more uncertain the plant state, the greater the weight given to the measurements and vice versa; the more uncertain the measurements, the less the weight given to them, or rather greater weight is given to the plant state. This describes the local sensor fusion that fuses the already known state estimate with newly incoming measurement, akin to that of the Kalman filter.

Let us recall properties of the ARE in the following result.

Lemma 7. *By scaling both design matrices Q_i and U_i by some positive scalar $\delta > 0$, for all i, $\mathcal{O}_i \neq \emptyset$, the local observer gain G_i does not change but the distributed observer gain F_i scales with δ for γ fixed.*

Proof. Multiplying the ARE (3.29) by the scaling gain δ yields

$$\delta\bar{M}_i^{-1}A_{i_o}^{\mathsf{T}} + A_{i_o}\delta\bar{M}_i^{-1} + \delta Q_i - 2\delta\bar{M}_i^{-1}C_{i_o}^{\mathsf{T}}U_i^{-1}C_{i_o}\bar{M}_i^{-1} = 0, \tag{3.88}$$

$$(\delta\bar{M}_i^{-1})A_{i_o}^{\mathsf{T}} + A_{i_o}(\delta\bar{M}_i^{-1}) + \delta Q_i - 2(\delta\bar{M}_i^{-1})C_{i_o}^{\mathsf{T}}(\frac{1}{\delta}U_i^{-1})C_{i_o}(\delta\bar{M}_i^{-1}) = 0. \tag{3.89}$$

Hence, by multiplying both Q_i and U_i by δ the solution $\bar{M}_i^{-1}$ of the ARE (3.29) scales as δ. Inserting the scaled terms into (3.30) we get

$$0 < \alpha_j < \frac{1}{\delta}\frac{w_{min}\lambda_{min}\left(\sum_{i\in\mathcal{D}_j}\bar{M}_iQ_i\bar{M}_i\right)}{w_{max}(p-|\mathcal{D}_j|)\lambda_{max}\left(A_j+A_j^{\mathsf{T}}\right)}, \tag{3.90}$$

which yields that the upper bound on α_j scales as $1/\delta$ and thereby $\bar{N}_j^{-1}$ scales as δ. Inserting this scaling into (3.31) we obtain

$$F_i = \gamma T_i^{\mathsf{T}} \begin{bmatrix} \delta \bar{M}_i^{-1} & 0 \\ 0 & \operatorname{diag}(\delta \bar{N}_j^{-1}) \end{bmatrix} T_i, \quad j \in \bar{\mathcal{O}}_i. \tag{3.91}$$

This shows, that by scaling Q_i and U_i by δ, $\forall i \in \mathcal{V}$ the distributed observer gain F_i scales as δ.

In contrast, this scaling does not affect the local observer gain G_i because the contributions of M_i^{-1} and U_i^{-1} cancel each other

$$G_i = T_i^{\mathsf{T}} \begin{bmatrix} (\delta \bar{M}_i^{-1}) C_{i_o} (\frac{1}{\delta} U_i^{-1}) \\ 0 \end{bmatrix}. \tag{3.92}$$

□

Remark 20. This has a clear interpretation in the context of our design. The local observer gain G_i effects the local Kalman filter from the history of local measurements and state estimate. If both the process noise Ω and local measurement noise Ξ_i scale equally, the local observer gain G_i will not change but the distributed observer gain F_i will increase, if γ is kept the same. Simply, the more uncertain the measurements for the state-group j the greater weight will be given to the information coming from the network.

Moreover, the restriction of the upper bound on all α_j to 1 brings an additional degree of freedom in the observer design as it was already mentioned in Remark 17. It separates scaling of the observable and unobservable parts of F_i. From the proof of Lemma 7 it follows that scaling of Ω and Ξ_i by some δ scales only the block of F_i corresponding to the observable subsystem, as long as all $\alpha_j = 1$. This additional functionality can improve overall performance of the estimator, however it applies only to stable systems or unstable systems with $\alpha_{*j_{\max}} > 1, \forall j \in \bigcup_{i=1}^{p} \bar{\mathcal{O}}_i$.

Remark 21. The value of α_j is chosen the same for all nodes not measuring the jth state-group directly to design their F_i. But in fact, α_j is determined by the nodes that do measure this state-group directly, by (3.30). To be more precise, α_j is determined by the worst sensor sensing state-group j. This means, if we have a faulty measurement somewhere in the network, in average we have more corrupt sources of information, the more the non-sensing nodes will listen to the network. This increases network cohesion and ultimately reduces the steady state error covariances.

Remark 22. The solution $\bar{M}_i^{-1}$ of the ARE (3.29) gives the optimal estimation error covariance, that would be obtained by using the Kalman filter on locally available measurements. This would be the best that a sensing node can achieve, without any information from the network. Our design however, via

the Lyapunov equation (3.77), leads to $P_{ii_{oo}}$ which is the actual estimation error covariance found in the system. Hence, due to network interconnections, the final error covariances may be less than that obtainable by using purely local measurements, which is also confirmed numerically, (see Section 3.6.3).

Moreover, we can state the following conclusion.

Proposition 2. *If trace*$(P_{ii_{oo}})$ $>$ *trace*$(P_{ik_{oo}})$, $\forall\ k \in \mathcal{V}_i$, *then the distributed estimator can not be absolutely worse than the purely local Kalman filter. Furthermore, if* $\bar{M}_i^{\frac{1}{2}} P_{ii_{oo}} \bar{M}_i^{-\frac{1}{2}} \succ \bar{M}_i^{\frac{1}{2}} P_{ik_{oo}} \bar{M}_i^{-\frac{1}{2}}$ *and* $\bar{M}_i^{-\frac{1}{2}} P_{ii_{oo}} \bar{M}_i^{\frac{1}{2}} \succ \bar{M}_i^{-\frac{1}{2}} P_{ki_{oo}} \bar{M}_i^{\frac{1}{2}}$, $\forall\ k \in \mathcal{V}_i$, *in the sense of quadratic forms, then the distributed observer certainly outperforms the purely local Kalman filter, in the sense* $P_{ii_{oo}} \prec \bar{M}_i^{-1}$.

Proof. The stationary solution of $P_{ii_{oo}}$ can be obtained by solving (3.77) with zero left-hand side, i.e., $dP_{ii_{oo}}/dt = 0$. The ARE (3.29) giving $\bar{M}_i^{-1}$, with $Q_i = \Omega_{i_o}$ and $U_i = \Xi_i$, can be written in the closed-loop form

$$(A_{i_o} - G_{i_o} C_{i_o})\bar{M}_i^{-1} + \bar{M}_i^{-1}(A_{i_o} - G_{i_o} C_{i_o})^{\mathsf{T}} + \Omega_{i_o} + G_{i_o} \Xi_i G_{i_o}^{\mathsf{T}} = 0, \tag{3.93}$$

Note, that $F_{i_o} = \gamma \bar{M}_i^{-1}$. Subtracting (3.93) from (3.77) with the zero left-hand side leads to

$$\begin{aligned} &(A_{i_o} - G_{i_o} C_{i_o})(P_{ii_{oo}} - \bar{M}_i^{-1}) + (P_{ii_{oo}} - \bar{M}_i^{-1})(A_{i_o} - G_{i_o} C_{i_o})^{\mathsf{T}} \\ &-\gamma \bar{M}_i^{-1} \textstyle\sum_{k \in \mathcal{V}} e_{ik}(P_{ii_{oo}} - P_{ki_{oo}}) - \gamma \sum_{k \in \mathcal{V}} e_{ik}(P_{ii_{oo}} - P_{ik_{oo}})\bar{M}_i^{-1} = 0. \end{aligned} \tag{3.94}$$

Multiplying both sides of (3.94) with $\bar{M}_i^{\frac{1}{2}} = \bar{M}_i^{\frac{T}{2}} \succ 0$ gives

$$\begin{aligned} 0 = &(\bar{A}_{i_o} - \bar{G}_{i_o} \bar{C}_{i_o})(\bar{M}_i^{\frac{1}{2}} P_{ii_{oo}} \bar{M}_i^{\frac{1}{2}} - I_{n_{i_o}}) \\ &+ (\bar{M}_i^{\frac{1}{2}} P_{ii_{oo}} \bar{M}_i^{\frac{1}{2}} - I_{n_{i_o}})(\bar{A}_{i_o} - \bar{G}_{i_o} \bar{C}_{i_o})^{\mathsf{T}} \\ &- \gamma \bar{M}_i^{-\frac{1}{2}} \textstyle\sum_{k \in \mathcal{V}} e_{ik}(P_{ii_{oo}} - P_{ki_{oo}})\bar{M}_i^{\frac{1}{2}} \\ &- \gamma \bar{M}_i^{\frac{1}{2}} \textstyle\sum_{k \in \mathcal{V}} e_{ik}(P_{ii_{oo}} - P_{ik_{oo}})\bar{M}_i^{-\frac{1}{2}}, \end{aligned} \tag{3.95}$$

with $\bar{A}_{i_o} - \bar{G}_{i_o} \bar{C}_{i_o} = \bar{M}_i^{\frac{1}{2}} (A_{i_o} - G_{i_o} C_{i_o}) \bar{M}_i^{-\frac{1}{2}}$. Note, that

$$\begin{aligned} 2(\bar{A}_{i_o} - \bar{G}_{i_o} \bar{C}_{i_o})_{\mathrm{S}} = &\bar{M}_i^{\frac{1}{2}} (A_{i_o} - G_{i_o} C_{i_o}) \bar{M}_i^{-\frac{1}{2}} \\ &+ \bar{M}_i^{-\frac{1}{2}} (A_{i_o} - G_{i_o} C_{i_o})^{\mathsf{T}} \bar{M}_i^{\frac{1}{2}} \prec 0, \end{aligned} \tag{3.96}$$

which follows from (3.93). Applying traces to (3.95) gives

$$\begin{aligned} 2 \text{ trace} \left((\bar{A}_{i_o} - \bar{G}_{i_o} \bar{C}_{i_o})_{\mathrm{S}} (\bar{M}_i^{\frac{1}{2}} P_{ii_{oo}} \bar{M}_i^{\frac{1}{2}} - I_{n_{i_o}}) \right) = \\ 2\gamma \text{ trace} \left(\bar{M}_i^{-\frac{1}{2}} \textstyle\sum_{k \in \mathcal{V}} e_{ik}(P_{ii_{oo}} - P_{ki_{oo}}) \bar{M}_i^{\frac{1}{2}} \right), \end{aligned} \tag{3.97}$$

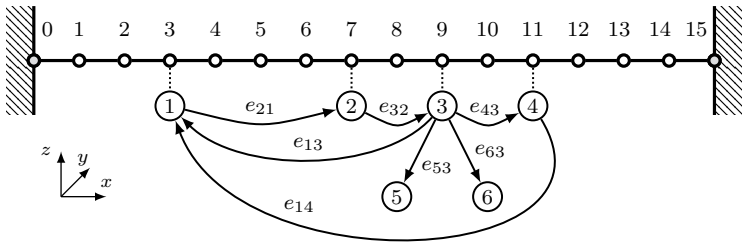

Figure 3.1: A beam divided into 15 finite elements with a sensor network consisting of 4 sensing nodes, $\{1, 2, 3, 4\}$, and 2 non-sensing nodes, $\{5, 6\}$.

Let $\text{trace}(P_{ii_{oo}}) > \text{trace}(P_{ik_{oo}})$, $\forall\ k\ \in\ \mathcal{V}_i$, then the right-hand side of (3.97) is positive, which implies

$$2\ \text{trace}\left((\bar{A}_{i_o} - \bar{G}_{i_o}\bar{C}_{i_o})_{\text{S}}(\bar{M}_i^{\frac{1}{2}} P_{ii_{oo}} \bar{M}_i^{\frac{1}{2}} - I_{n_{i_o}})\right) > 0. \tag{3.98}$$

Since, by (3.96), $(\bar{A}_{i_o} - \bar{G}_{i_o}\bar{C}_{i_o})_{\text{S}}$ is symmetric and negative definite, $(\bar{M}_i^{\frac{1}{2}} P_{ii_{oo}} \bar{M}_i^{\frac{1}{2}} - I_{n_{i_o}})$ can not be a positive-semidefinite matrix, which implies $P_{ii_{oo}} \not\succeq \bar{M}_i^{-1}$. Hence the distributed estimator can not be absolutely worse than the purely local Kalman filter; this proves the first part of Proposition 2.

To prove the second part of Proposition 2 we proceed as follows. Let $\bar{M}_i^{\frac{1}{2}} P_{ii_{oo}} \bar{M}_i^{-\frac{1}{2}} \succ \bar{M}_i^{\frac{1}{2}} P_{ik_{oo}} \bar{M}_i^{-\frac{1}{2}}$ and $\bar{M}_i^{-\frac{1}{2}} P_{ii_{oo}} \bar{M}_i^{\frac{1}{2}} \succ \bar{M}_i^{-\frac{1}{2}} P_{ki_{oo}} \bar{M}_i^{\frac{1}{2}}$, $\forall\ k\ \in\ \mathcal{V}_i$, then the last two terms in (3.95) are negative definite and hence

$$\begin{aligned} 0 \prec\ & (\bar{A}_{i_o} - \bar{G}_{i_o}\bar{C}_{i_o})(\bar{M}_i^{\frac{1}{2}} P_{ii_{oo}} \bar{M}_i^{\frac{1}{2}} - I_{n_{i_o}}) \\ & + (\bar{M}_i^{\frac{1}{2}} P_{ii_{oo}} \bar{M}_i^{\frac{1}{2}} - I_{n_{i_o}})(\bar{A}_{i_o} - \bar{G}_{i_o}\bar{C}_{i_o})^{\mathsf{T}}. \end{aligned} \tag{3.99}$$

Since, by Theorem 6, $(\bar{A}_{i_o} - \bar{G}_{i_o}\bar{C}_{i_o})$ is asymptotically stable, from the Instability Theorem [32, Theorem 3.3] it follows by contradiction that $(\bar{M}_i^{\frac{1}{2}} P_{ii_{oo}} \bar{M}_i^{\frac{1}{2}} - I_{n_{i_o}})$ must be negative definite, hence $P_{ii_{oo}} \prec \bar{M}_i^{-1}$. This concludes the proof. □

3.6 Numerical simulations

The proposed distributed observer design is numerically validated on a model of a clamped beam adopted from [20, Section 1.1.4]. The beam is 150 cm long, with a cross-section of 1 cm^2. It is divided into 15 elements, i.e., 14 free and 2 clamped (fixed) nodes as depicted in Fig. 3.1. Each node has 3 degrees of freedom (displacement in x and z axis, and pitch in y axis. In general,

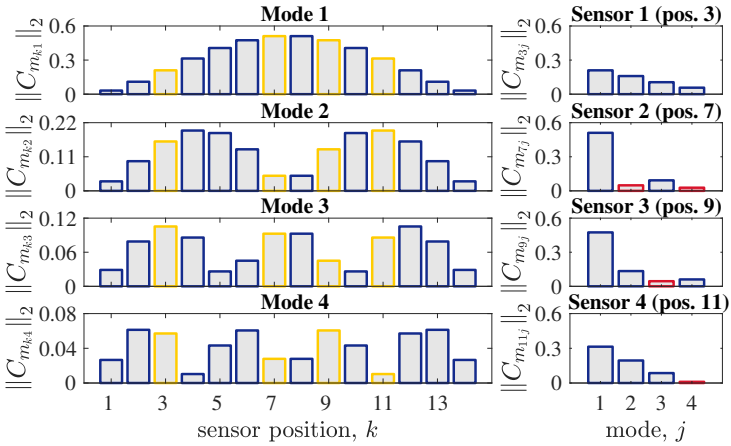

Figure 3.2: The 2-norm of the output matrices $C_{m_{kj}}$ for the first four modes j and all possible sensor positions k on the beam on the left and chosen sensor positions on the right.

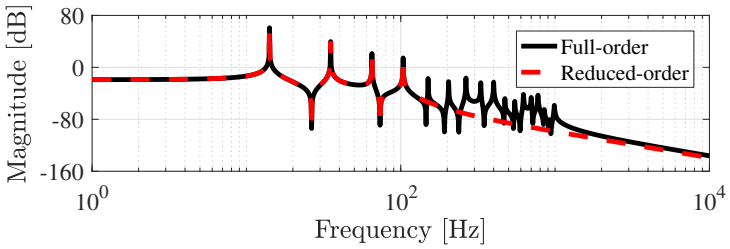

Figure 3.3: Frequency response from 6th input to 3rd output.

the clamped beam model represents a mass-spring-damper system which is described in nodal form by a second order matrix differential equation

$$M\ddot{q}(t) + D\dot{q}(t) + Kq(t) = B_o u(t), \tag{3.100}$$

$$y = C_{oq}q(t) + C_{ov}\dot{q}(t), \tag{3.101}$$

where $q, \dot{q}$, and $\ddot{q}$ are nodal displacement, velocity, and acceleration vectors in $\mathbb{R}^{42}$, M, D, and K are the mass damping, and stiffness matrices in $\mathbb{R}^{42\times 42}$, $B_o \in \mathbb{R}^{42\times 14}$ is the input matrix and C_{oq}, and C_{ov} are the output matrices in $\mathbb{R}^{14\times 42}$. The beam mass and stiffness matrices are given in [20, Appendix C.2]. The damping matrix is given by Rayleigh damping in the form $D = M \cdot 10^{-5} + K \cdot 10^{-6}$. The sensor locations are given by $C_{oq} = I_{14} \otimes c_{oq}$, where $c_{oq} = [0\ 1\ 0]$ and C_{ov} is a zero matrix. For purposes of a proper sensor placement

we first evaluate performance of all possible sensor locations. For the distributed observer design we consider zero control input, i.e., $u = 0$.

A transformation to modal form is used to obtain the block diagonal structure of the system required by the design. Following the transformation procedure, described in [20], we obtain the full modal state-space representation

$$\dot{z}(t) = A_m z(t), \tag{3.102}$$
$$y(t) = C_m z(t), \tag{3.103}$$

with $A_m = diag(A_{m_j})$ and $C_m = [C_{m_1}, C_{m_2}, \ldots, C_{m_f}]$, where $j = 1, 2, ..., f$ and f represents the number of modal pairs (state-groups) $z_j = [\bar{\omega}_j q_{m_j} \ \dot{q}_{m_j}]^\mathsf{T}$ consisting of modal displacement $z_{j_a} = \bar{\omega}_j q_{m_j}$ and modal velocity $z_{j_b} = \dot{q}_{m_j}$. The matrices A_{m_j} are in the form

$$A_{m_j} = \begin{bmatrix} 0 & \bar{\omega}_j \\ -\bar{\omega}_j & -2\zeta_j\bar{\omega}_j \end{bmatrix}, \tag{3.104}$$

where $\bar{\omega}_j$ is the jth modal frequency and ζ_j is the jth modal damping ratio. Since the plant is a flexible structure, the modal output matrix C_m satisfies Assumption 8.

The model order reduction technique, [20], is used to obtain the reduced model containing the first $l = 4$ dominant modes given by frequencies $\bar{\omega} = [89, 221, 409, 651]^\mathsf{T}$ Hz, hence the set of state-groups is $\mathcal{S} = \{1, 2, 3, 4\}$. The output matrix C_m is reduced column-wise to contain only the 4 chosen modes. The 2-norm of the output matrices $C_{m_{kj}}$ for the 4 considered modes $j \in \mathcal{S}$ and all possible sensor positions $k \in \{1, 2, \ldots, 14\}$ is depicted in Fig. 3.2 on the left. The output matrix is further reduced row-wise by choosing only the sensor locations $3, 7, 9, 11$ for good sensing performance of all 4 modes. A detailed comparison of the 2-norm of output matrices $C_{m_{kj}}$ for chosen sensor locations is shown in Fig. 3.2 on the right. As discussed in Remark 7, the magnitude of some $C_{m_{kj}}$ is very small for the distributed design, hence one can consider them to be zero as long as the Assumption 9 remains satisfied. The small magnitudes of $C_{m_{kj}}$ for chosen sensor locations appear in Fig. 3.2 in red color. Observable set for each node is allocated as follows: $\mathcal{O}_1 = \{1, 2, 3, 4\}, \mathcal{O}_2 = \{1, 3\}, \mathcal{O}_3 = \{1, 2, 4\}, \mathcal{O}_4 = \{1, 2, 3\}, \mathcal{O}_5 = \emptyset$ and $\mathcal{O}_6 = \emptyset$. The observability of modes is found to satisfy Assumption 9.

After the model order reduction and sensor placement we obtain the reduced-order model of the beam given by the plant dynamics with process noise, (3.19), and sensor model with measurement noise, (3.20). The reduced-order model has $\tilde{A} \in \mathbb{R}^{8\times8}$ and $\tilde{C} \in \mathbb{R}^{4\times8}$. Fig. 3.3 shows a comparison of the amplitude characteristic of frequency response for the nominal plant and the reduced model. The frequency response is calculated by considering an input displacement at node 6 in z direction and measuring a response of a sensor at node 4 in y

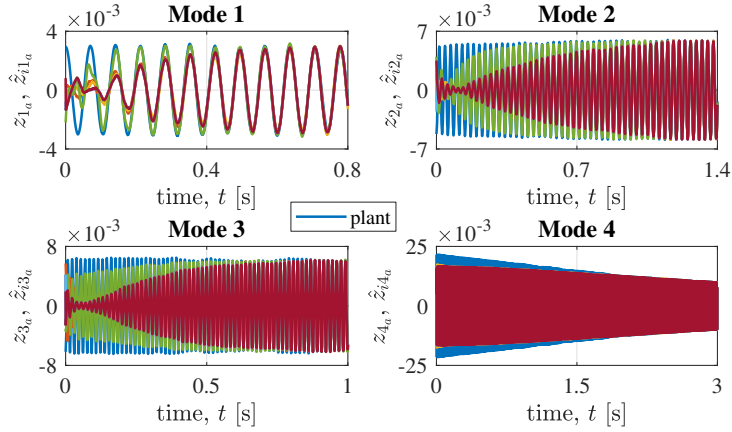

Figure 3.4: The plants modal displacements and nodes' estimates, z_{j_a} and $\hat{z}_{ij_a}$, $\forall(i,j), i \in \mathcal{V}, j \in \mathcal{S}$, in time-domain, response to initial conditions.

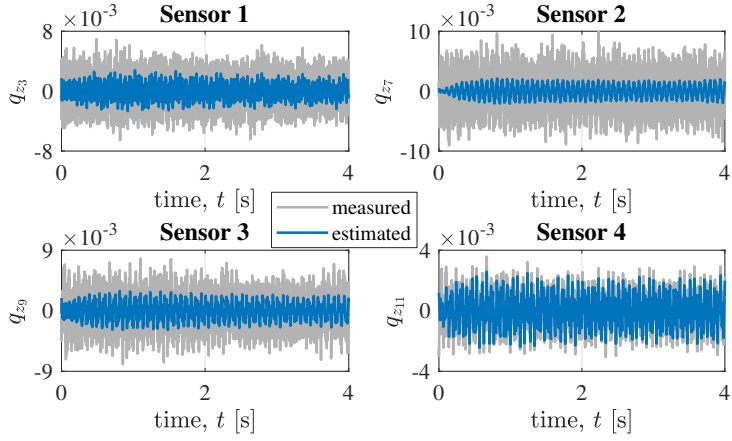

Figure 3.5: Comparison of measured and estimated nodal displacement $q_{z_k}, \forall k \in \{3, 7, 9, 11\}$ of the sensing nodes, response to initial conditions.

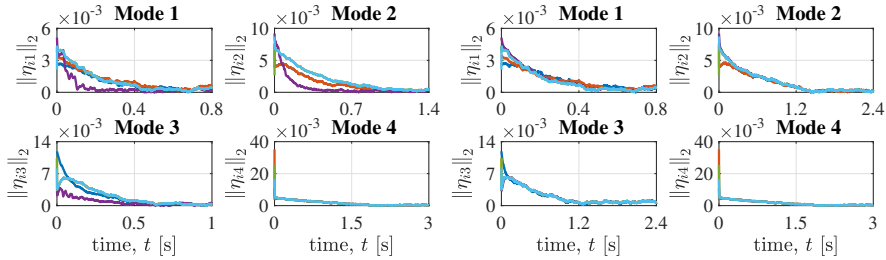

(a) $\Omega_{44} = 10^{-7}$, $e_{14} = 1$

(b) $\Omega_{44} = 10^{-2}$, $e_{14} = 1$

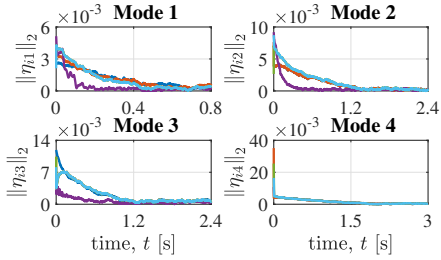

(c) $\Omega_{44} = 10^{-7}$, $e_{14} = 0$

Figure 3.6: The 2-norm of the state observation error η_{ij}, $\forall(i,j), i \in \mathcal{V}, j \in \mathcal{S}$, response to initial conditions. Simulation for three cases: a) general case for demonstration of the observer convergence; b) 4th sensor measurement degradation; c) failure of the communication link from node 4 to node 1.

direction. It is introduced for a better interpretation of the reduced model, however for purposes of this design we do not consider any input.

The communication topology of the sensor network is given in Fig. 3.1. It consists of four sensing nodes $\mathcal{V}_1 = \{1, 2, 3, 4\}$ contained in an irreducible leader group and two non-sensing nodes $\mathcal{V}_2 = \{5, 6\}$ located in the remainder of the graph, i.e., $\mathcal{V} = \mathcal{V}_1 \cup \mathcal{V}_2$. Note that the topology satisfies Assumption 10.

The beam model represents a low damped flexible structure with stable poles close to the imaginary axis. For this reason the bounds on the α_j and γ do not restrict the design, i.e., their values can be set arbitrary large. Nevertheless, following the design guidelines from Section 3.5 we set $\alpha_j = 1, \forall j$. The value of γ is chosen later such that the rate of convergence corresponds to the speed of the local observers.

3.6.1 Simulation with initial conditions

Functionality of the proposed distributed observer is demonstrated on a simulation of the clamped beam excited only by initial conditions. The plant

initial conditions in nodal coordinates are set to zero except the displacement in z direction at 7th position which is set to 0.01. The corresponding initial conditions in modal coordinates are: $z(0) = [2.9, 0, -5.2, 0, -6.2, 0, 21.5, 0]$. Initial conditions of nodes in the sensor network are chosen randomly in appropriate scales. The sensing nodes' measurement noises are WGN with covariance matrix $\Xi = \text{diag}([2, 5, 3, 0.1]) \cdot 10^{-6}$. Process noises are also WGN with randomly generated diagonal covariance matrix $\Omega = \text{diag}([6, 10, 10, 6, 18, 14, 8, 8]) \cdot 10^{-4}$. The remaining design parameters are: $\alpha = 1$, $\beta = 1$, and $\gamma = 10^4$.

Our analysis follows three simulated scenarios:

a) General simulation with introduced parameters.

b) Measurement degradation of 4th node, i.e., $\Omega_{44} = 10^{-2}$.

c) Failure of the communication link $4 \to 1$, i.e., $e_{14} = 0$.

For all the investigated cases, the state observation error η_{ij} is asymptotically stable in its expected value and has a finite covariance, which can be seen in Fig. 3.6; hence each node $i \in \mathcal{V}$ obtains a full estimate of the plant state vector. These results validate the conclusion of Theorem 6. In general, more dominant modes have better observability, therefore their convergence speed is faster, which is evident from the figures.

General simulation

This simulation shows the functionality of the proposed observer. The convergence of the ith node modal estimate $\hat{z}_{ij}$ to the plant modal vector z_j can be seen in Fig. 3.4. and also in Fig. 3.6a in form of 2-norm of the estimation error η_{ij}. The comparison of the sensing nodes' measurements with their measurement estimates is given in Fig. 3.5.

The small noise variance in the 4th node's measurement causes the 4th node to assign larger confidence to its measurements than to information from the network, therefore the 4th node's estimates of the modes 1, 2, and 3 show faster convergence than the other nodes' estimates, which can be seen in Fig. 3.6a. On the other hand, the 4th mode is unobservable from the 4th node's perspective, hence it receives information on that mode from the network. This is in line with the analysis of the observer convergence given in Section 3.4.

Measurement degradation

In case of corrupted measurements of the 4th sensing node, the convergence of the estimator is shown in Fig. 3.6b. The 4th node obtains the full estimates of the plant state together with the rest of the network in spite of its corrupted measurement. The reason is the judiciously designed distributed observer which for the 4th node takes into consideration the large noise variance of that

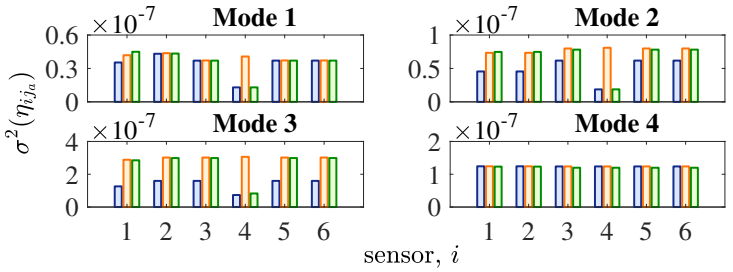

Figure 3.7: Variance of modal displacement estimation error η_{ij_a}, $\forall(i,j), i \in \mathcal{V}, j \in \mathcal{S}$, steady-state simulation for the three cases *a)*, *b)*, and *c)*.

measurement and thereby imposes small G_{4_o} and large F_{4_o}. This also follows from the 2-norms of G_{4_o} and F_{4_o} before and after the measurement degradation, which are $\|G_{4_o}\|_2 = 77$, $\|F_{4_o}\|_2 = 0.64$ and $\|G_{4_o}\|_2 = 0.11$, $\|F_{4_o}\|_2 = 33$, respectively. By its comparison to a general case from Fig. 3.6a it can be seen, that small noise variance in 4th sensing node provides slight improvement in convergence rate of the estimator.

Communication link failure

By failure of the communication link from node 4 to node 1, the redundant sensing node 4 gets disconnected from the irreducible leader group. Since the Assumption 9 remains satisfied, the nodes are still able to obtain full estimate of the plant states. In this particular case, the rest of the network is not able to obtain information from the 4th node, hence the network cannot benefit from the accurate estimates of the 4th sensing node. This causes slightly slower convergence of the nodes' estimates, which can be seen by comparing Fig. 3.6c with Fig. 3.6a. Note that, because there is no other link from the node 4 to the irreducible leader group, failure of this link is identical to the failure of the sensing node 4 from all other nodes' perspective.

3.6.2 Steady-state simulation

To provide insight into the overall deterioration of precision of nodes' estimates for all three investigated cases from Section 3.6.1, the plant and the sensor network are simulated in a steady state with zero initial conditions. Fig. 3.7 shows a comparison of the calculated variances of modal displacement observation errors z_{ij_a}. It can be seen that differences in the variances are negligible, hence the proposed design is found robust to measurement degradation and a link/node failure.

3.6.3 Evaluation of covariances

To obtain the covariance matrix P, which gives the real uncertainty in the system, the global Lyapunov equation (3.73) is solved with G_is as in Theorem 5. By comparing $\bar{M}_i^{-1}$ with $P_{ii_{oo}}$, all diagonal elements of $P_{ii_{oo}}$ are found to be smaller. For instance, the diagonal elements of $\bar{M}_1^{-1}$ are $[27, 27, 33, 33, 73, 73, 74, 74] \cdot 10^{-5}$ and for $P_{11} = P_{11_{oo}}$ are $[14, 14, 17, 17, 33, 33, 66, 66] \cdot 10^{-5}$. Evaluation of the sum of traces gives $\sum_i \text{trace}(\bar{M}_i^{-1}) = 10.5 \cdot 10^{-3}$, and $\sum_i \text{trace}(P_{ii_{oo}}) = 6.4 \cdot 10^{-3}$. This shows that the final variances are lower than the purely local design would allow, thereby clearly showing the benefit of network communication and sensor fusion. Hence, the resulting variance over the observable states of a sensing node, when it is integrated into a network, is smaller than the variance that would be optimally obtained using only a local Kalman filter.

Moreover, variances for the unobservable states $P_{ii_{\bar{o}\bar{o}}}$ are comparable to those for observable states $P_{ii_{oo}}$. For example the 5th node, which does not sense anything has $P_{55} = P_{55_{\bar{o}\bar{o}}}$ with diagonal elements $[14, 14, 24, 24, 42, 42, 67, 67] \cdot 10^{-5}$, which are similar in magnitude to those in $P_{11_{oo}}$. Hence, even nodes that do not sense certain state-groups, obtain reasonable estimates over those state-groups, comparable to those achieved by nodes which are sensing them. This is verified also by calculating $\text{trace}(P) = 16.1 \cdot 10^{-3}$.

For comparison with an optimal centralized approach, the general Kalman filter, [42], having access to measurements of all nodes taken together, achieves the following variances of its states' estimates: $[4, 4, 6, 6, 20, 20, 60, 60] \cdot 10^{-5}$.

3.7 Concluding remarks

In this chapter, we proposed a DLO design for sensor networks, which considers disturbance acting on states of the plant and noise corrupting the sensor measurements. Observer nodes in the sensor network are designed and implemented in a fully distributed manner using only their local information and information from their neighbors. The presented distributed observer design exhibits good scalability on large-scale sensor networks and flexibility to integrating new nodes into the network. Moreover, it is found to potentially improve the precision of nodes' estimates above that optimally available from purely local measurements. Additional node redundancy provides robustness to communication link or node failures. The convergence of the state estimates of networked observers to the plant (target) state are rigorously proven. The observer design is thoroughly described and its theoretical analysis is provided. Numerical simulations validate the proposed distributed observer design.

4

Distributed adaptive consensus protocol

A communication topology of real-word multi-agent systems, e.g., networks of mobile robots, satellites, and vehicles, often varies in time; therefore such spatially interconnected systems require distributed consensus protocols which can handle network changes. General distributed static consensus protocols do not satisfy this requirement, because they assume knowledge of the network topology. For this purpose DACPs were developed. DACPs use adaptive laws which allows them to adapt to network changes. Since these protocols do not require any centralized information, they are fully distributed in the sense, that each agent can implemented these protocols fully individually.

In this chapter, we develop a novel DACP that uses an adaptive law to adapt coupling weights (gains) between agents in the network. The introduced protocol solves the cooperative regulator and tracker problems on directed communication graphs, with agents described by LTI dynamics. Its novelty stems from a new coupling gain dynamics allowing coupling gains to decay to some estimated references. This tackles the problems of existing DACPs with considerable control effort and a lack of robustness to noise or disturbances.

This chapter is organized as follows. Section 4.1 describes the recent progress in development of distributed adaptive laws. The main contribution of the proposed adaptive approach is given in Section 4.2. Section 4.3 states the considered cooperative control problems and brings the relevant stability notions. Sections 4.4 and 4.5 respectively present the DACP for cooperative regulator and tracker problems. Lyapunov function candidates are introduced and their

The content of this chapter is published in International Journal of Robust and Nonlinear Control [38].

time-derivatives are elaborated, concluding on the stability of the adaptive protocol given appropriate reference values. Section 4.6 brings the methodology for distributed on-line estimation of these references. Numerical simulations are given in Section 4.7. Section 4.8 concludes the chapter.

4.1 State of the art

Some laws in distributed control and estimation incorporate adaptation to handle system and network uncertainties, unmodelled dynamics and guarantee robustness to disturbances, [15, 14, 51, 74, 77, 69, 75, 46, 47, 44, 50, 11]. Most of these adaptive laws, also known as adaptive consensus protocols (ACPs), can be broadly categorized into two general groups.

The first group of ACPs handles networks of agents with unknown dynamics and known communication topology. Few of these laws assume knowing only the agent model structure [51, 74], while others instead use a neural network (NN) to estimate it [77, 14]. In the latter case, the adaptive law is used by each agent to estimate its model parameters or its NN weights from local information and information from neighboring agents. The estimated agent model or NN weights are then used for control purposes to reach consensus among agents. Since global properties of the communication topology are required to design the appropriate coupling gain, similarly as in static consensus protocol designs, those also cannot be implemented in a fully distributed fashion.

This particular problem motivates ACPs that fit into the second general group usually referred to as distributed ACPs (DACPs); those that handle networks with known agent dynamics but unknown communication topologies. There, the agents are assumed to have identical linear [46, 47, 11] or non-linear dynamics [69, 75]. Some adaptive protocols solve only the cooperative regulator problem [69] , while others solve both cooperative regulator and tracking, but only apply to undirected connected communication graphs [46, 75, 11]. Similar noteworthy results solving output regulation introduce ACPs addressing the cooperative tracker problem for identical agents [50] and the cooperative regulator problem for heterogeneous agents having general LTI dynamics [44]. The coupling gains, which conventionally require global information on the communication graph, are there updated by an adaptive law. Namely, each agent adapts one or more feedback coupling gains individually based on its local information and information from neighboring agents. The coupling gains' values are then used for synchronization to reach the consensus among agents. The adapting coupling gains are associated with the agents themselves [75, 47, 44, 50], the network edge weights [46], or both the agents and the edge weights [69]. These protocols do not rely on any centralized information; therefore, they can be implemented by each agent separately. They guarantee cooperative stability; however, they suffer from possibly large resulting control efforts and a lack of

robustness to noise [69, 46, 75, 47]. Moreover, widely different protocols are currently proposed in the literature for very similar consensus problems that are conventionally treated quite similarly via the synchronizing region approach. Our work introduced later in this chapter tries to tackle these difficulties.

There are also woks in distributed control and estimation, which take an advantage of adaptation but they do not belong to the above-mentioned two categories of ACPs. From this field, it is worth to mention [15]. The author investigates the distributed filtering of spatially varying processes using a sensor network. The sensor network consists of interconnected filters (state estimator) each having its own group of sensors. The sensor group provides number of state measurements from sensing devices, that are not necessarily identical. Each filter is essentially a Luenberger observer. It produces its own state estimates for the local plants and additionally synchronize these estimates with other filters in the sensor network. Thereby, an agreement on state estimates is reached among filters. The adaptive law is used by each filter to estimate the proper coupling gain value for an agreement with other filters.

In following we introduce several existing results on ACPs in more details. First, from the group of ACPs adaptively estimating the agent dynamics, we briefly present two works [51, 14]. Then we thoroughly describe several DACP approaches adapting the coupling gains' values, [69, 75, 46, 47], which are more relevant to our work.

4.1.1 Adaptive estimation of agent dynamics

This section brings few of the above-mentioned ACPs, which are using an adaptive law for estimation of an unknown agent dynamics, in more details.

ACP design proposed by Min et al. [51]

An ACP for synchronization of networked Euler-Lagrange system, [51], solves the relative state consensus and the leader-following consensus on directed networks with switching topologies and communication time delays. All agents in the network share the same Lagrangian dynamics with a known structure. An adaptive law, implemented by each agent, estimates parameters of the agent's Lagrangian dynamics. These parameters are then applied in the agent's control law to reach consensus. The proposed control law uses two graphs, the communication (velocity) graph and the sensing (position) graph, that are assumed to be directed and balanced. This approach, [51], guarantees convergence of the ACP on switching topologies, if the changing communication graph is directed and balanced, and the sensing graph is static and strongly connected; however, it do not state how the communication time delays affect the overall performance and the convergence rate of the ACP. Details of this adaptive control law won't be stated here. In following, we introduce other

more general adaptive control laws that share the same goal and also capture the agents with Lagrangian dynamics.

ACP design proposed by Das et al. [14]

An neural adaptive design for synchronization of unknown non-linear networked systems, [14] presents a synchronization protocol which addresses leader-following consensus on directed strongly connected communication graphs. The agents are assumed to have different unknown non-linear dynamics with disturbances. The i-th agent dynamic is defined as

$$\dot{x}_i(t) = f_i(x_i(t)) + u_i(t) + w_i(t), \tag{4.1}$$

where $x_i \in \mathbb{R}$ is the agent state, $u_i \in \mathbb{R}$ is the control input, $w_i \in \mathbb{R}$ is the external disturbance, which is unknown but is assumed to be bounded, and $f_i(\cdot) : \mathbb{R} \to \mathbb{R}$ is the agent dynamics that is assumed to be continuously differentiable or Lipschitz. The leader's target dynamics to be tracked is also assumed to be non-linear and unknown. It is described by

$$\dot{x}_0(t) = f_0(x_0(t), t), \tag{4.2}$$

where $x_0 \in \mathbb{R}$ is the leader's state and $f_0(\cdot) : \mathbb{R} \times [0, \infty) \to \mathbb{R}$ is the leader's dynamics.

The idea of the protocol is to use the information of states from neighbours to evaluate the performance of the current control protocol along with the current estimates of the non-linear functions. The local control input for the i-th agent is given by

$$u_i = c\epsilon_i - \hat{f}_i(x_i), \tag{4.3}$$

where the coupling gain $c > 0$, the local neighbourhood error ϵ_i is defined by (2.15) and the estimates of the i-th agent nonlinearity $\hat{f}_i(x_i)$ are given by

$$\hat{f}_i(x_i) = \hat{W}_i^{\mathsf{T}} \cdot \varphi_i(x_i), \tag{4.4}$$

where $\hat{W}_i \in \mathbb{R}^{\nu_i}$ is a current estimate of NN weights for the i-th agent, ν_i is the number of neurons maintained at each agent and $\varphi_i(x_i) : \mathbb{R} \to \mathbb{R}^{\nu_i}$ is a suitable basis set of NN activation functions. A NN design technique that adapts the neuron weights is used to estimate each agent nonlinearity modeled by $f_i(x_i) = W_i^{\mathsf{T}} \cdot \varphi_i(x_i) + \varepsilon_i$. The estimation error of NN weight, W_i, is then denoted by $\tilde{W}_i = W_i - \hat{W}_i$. The local agent NN weight estimates $\hat{W}_i$ are generated by the following NN adaptive tuning law

$$\dot{\hat{W}}_i = -F_i \varphi_i \epsilon_i^{\mathsf{T}} p_i (d_i + g_i) - \kappa F_i \hat{W}_i, \tag{4.5}$$

with $F_i = \Pi_i I_{\nu_i}$, where $I_{\nu_i} \in \mathbb{R}^{\nu_i \times \nu_i}$ is the identity matrix, $\Pi_i > 0$ and $\kappa > 0$ are scalar tuning gains and $p_i > 0$ is some constant defined in [14, Lem 2].

Note that for the relative state consensus $g_i = 0$, $\forall i$, thus the local neighbourhood error (2.15) simplifies into (2.10) and the NN tuning law (4.5) changes to

$$\dot{\hat{W}}_i = -F_i \varphi_i \epsilon_i^{\mathsf{T}} p_i d_i - \kappa F_i \hat{W}_i. \tag{4.6}$$

Theorem 7 ([14], Thm. 1)**.** *Consider a directed strongly connected communication graph $\mathcal{G}$ consisting of p agents and a leader described by (4.1) and (4.2), respectively. Under the control protocol (4.3) with (4.4, 4.5) and properly chosen κ and c given in [14], there exist a number of neurons $\bar{\nu}_i, i = 1, \ldots, N$ such that $\bar{\nu}_i > \nu_i, \forall i$ and the local neighborhood error vectors ϵ_i and the NN weight estimation errors $\tilde{W}_i$ are uniform ultimate boundedness (UUB). Therefore, the control node trajectory x_0 is UUB and all agents synchronize to x_0.*

Unlike the local voting protocol and the static consensus protocol, this ACP does not require the knowledge of the agent and the leader dynamics. The agent dynamics just have to satisfy certain week conditions like continuous differentiability or Lipschitz continuity, which are fulfilled by majority of real systems. We haven't stated the design of the tuning gain κ, coupling gain c and constants p_i; however, it is important to note that they depend on the (pinned) Laplacian matrix, $L(+G)$. The knowledge of the graph topology is required at the design stage as it is by the static consensus protocol, and therefore this ACP is not fully distributed.

Other ACP designs

Alternative ACPs for synchronization of unknown nonlinear systems are proposed in [74] and [77]. The work in [74] introduces an ACP that addresses undirected graphs with jointly connected switching topologies. This approach also handles communication drop-outs in the network. On the other hand, [77] applies to directed communication graphs having a spanning tree. In contras to [14] and [74], which consider agents with first order nonlinear dynamics, [77] considers agents of higher order non-linear dynamics. Although both approaches in [74] and [77] solve the leader-following consensus, they can be applied also to relative state consensus.

4.1.2 Adaptive estimation of coupling gains

This section brings four DACPs designs from the literature [69, 75, 46, 47] in more details. The DACPs use an adaptive law to adapt the coupling gains.

DACP design proposed by Su et al. [69]

Early DACP introduced in [69] implements an adaptation of coupling gains to solve the leader-following consensus on a network of p interconnected agents

(mobile robots) following a leader in n-dimensional Euclidean space. The communication graph is assumed to be undirected, initially connected and just a small fraction of agents are informed about the leader. A connectivity preserving algorithm is introduced. Once the topology is connected, it guaranties connectedness for all future times [69]. Following from the algorithm, the communication topology is time-varying. When the consensus is reached, the agents have all-to-all coupling and all are connected to the leader. The algorithm is not related to the adaptive control law; therefore, its details are omitted.

The agents and the leader are assumed to have unknown identical second-order non-linear dynamics. The motion of each agent is governed by

$$\begin{aligned} \dot{p}_i(t) &= v_i(t), \\ \dot{v}_i(t) &= f(v_i(t)) + u_i(t), \end{aligned} \tag{4.7}$$

where $p_i \in \mathbb{R}^n$ is the position vector of agent i, $v_i \in \mathbb{R}^n$ is its velocity vector, $f(\cdot) : \mathbb{R}^n \to \mathbb{R}^n$ is its intrinsic dynamics, that is Lipschitz-like continuous [69], and $u_i \in \mathbb{R}^n$ is its control input. The leader is specified by

$$\begin{aligned} \dot{p}_0(t) &= v_0(t), \\ \dot{v}_0(t) &= f_0(v_0(t)), \end{aligned} \tag{4.8}$$

where $p_0 \in \mathbb{R}^n$ is the leader's position vector, $v_0 \in \mathbb{R}^n$ is its velocity vector and $f_0(\cdot) : \mathbb{R}^n \times [0, \infty) \to \mathbb{R}^n$ is its intrinsic dynamics. The local control law takes the form

$$\begin{aligned} u_i = &- \underbrace{\textstyle\sum_j e_{ij} \nabla_{p_i} \psi(\|p_i - p_j\|)}_{\alpha_i} - \underbrace{\textstyle\sum_j m_{ij} e_{ij} (v_i - v_j)}_{\beta_i} \\ &- \underbrace{g_i c_s (p_i - p_0) - g_i c_i (v_i - v_0)}_{\gamma_i}, \end{aligned} \tag{4.9}$$

where the constant $c_s > 0$ is the weight on the position feedback that can take any fixed value, time-varying parameters $m_{ij} > 0$ and $c_i > 0$ represent the velocity coupling strengths and the weights on the velocity navigational feedbacks, respectively, and the function $\psi(\cdot)$ is a non-negative potential function of the displacement between agent i and agent j with given properties [69]. The local control law (4.9) is written without time labels for clarity; however, note that the elements of the adjacency matrix e_{ij} and the pinning matrix g_i are time-varying.

The term denoted by α_i is a gradient-based term, which enforces agents' positions to converge to a common value, β_i is the consensus term, which drivers the agents' velocities to a common value, and γ_i is the navigational feedback term, which forces the agents to track the leader.

The local adaptation laws for both the weights on the velocity navigational feedback and the velocity coupling strength are

$$\dot{m}_{ij} = k_{ij}(v_i - v_j)^{\mathsf{T}}(v_i - v_j), \tag{4.10}$$

$$\dot{c}_i = k_i(v_i - v_0)^{\mathsf{T}}(v_i - v_0), \tag{4.11}$$

where the constants $k_{ij} = k_{ji} > 0$ and $k_i > 0$ are the corresponding weighting factors of the adaptation laws.

Theorem 8 ([69], Thm. 1)**.** *Consider system of p mobile agents with dynamics (4.7) each steered by protocol (4.9) to follow a virtual leader with dynamics (4.8). Suppose that the initial network $\mathcal{G}(0)$ is connected, the agent intrinsic dynamics $f(\cdot)$ is Lipschitz-like continuous and that the initial network energy is finite [69]. Then the velocities and positions of all agents will converge to those of the leader asymptotically, i.e., the agents reach consensus with the leader.*

The DACP introduces the control input (4.9) that uses a constant gain c_s, two types of time-varying gains m_{ij}, c_i and a constant function $\psi(\cdot)$ that can be interpreted as a variable gain. The static gain c_s, chosen by the design, is used for synchronization of positions of agents with the leaders. The time-varying coupling gain m_{ij} is associated with each agents' interconnection e_{ij} and it takes care of the consensus in agents' velocities. A time-varying coupling gain c_i is associated with each leader-agent interconnection g_i and it is used for synchronization of agents' velocities with the leaders. The time-varying coupling gains m_{ij} and c_i are being adapted by the adaptive control laws (4.10) and (4.11), respectively. The potential function $\psi(\cdot)$ takes care of consensus in agents' positions.

The authors state that the DACP can be used on unknown connected communication graph with agents described by unknown second-order nonlinear dynamics. Nevertheless, they do not state all the details of the protocol design. Thus, it is not clear how to properly choose the coupling gain values c_s and the weighting factor values k_{ij} and k_i.

The adaptive laws (4.10) and (4.11) introduce also several drawbacks. Since the coupling gains' derivatives in (4.10) and (4.11) are monotonically increasing functions, values of the coupling gains m_{ij} and c_i rise until there is some error in positions and velocities of agents. The coupling gains might therefore attain higher value than it is necessary for the network stability. The coupling gains are also decoupled; therefore, they end up with different final values and the network gets unbalanced, i.e., the agents react differently to the input signal. Additionally, if there is some noise in position or velocity measurements, the coupling gains would rise reaching some saturation level. Therefore, instead of implementing the adaptive control laws, the coupling gains could from the outset be initialized to this saturation value. As it will be shown later in this section, this is a common problem of recent DACPs.

DACP design proposed by Yu et al. [75]

A similar DACP proposed in [75] solves the relative state consensus and the leader-following consensus on undirected and connected communication graphs. Agents have unknown second-order non-linear dynamics given by

$$\begin{aligned} \dot{p}_i(t) &= v_i(t), \\ \dot{v}_i(t) &= f(p_i(t), v_i(t)) + u_i(t), \end{aligned} \tag{4.12}$$

where $p_i \in \mathbb{R}^n$ is the position vector of agent i, $v_i \in \mathbb{R}^n$ is its velocity vector, $f(\cdot) : \mathbb{R}^n \times \mathbb{R}^n \to \mathbb{R}^n$ is its continuously differentiable vector-valued non-linear dynamics, and $u_i \in \mathbb{R}^n$ is its control input. The leader's dynamics is given by

$$\begin{aligned} \dot{p}_0(t) &= v_0(t), \\ \dot{v}_0(t) &= f_0(p_0(t), v_0(t), t), \end{aligned} \tag{4.13}$$

where $p_0 \in \mathbb{R}^n$ is the leader's position vector, $v_0 \in \mathbb{R}^n$ is its velocity vector and $f_0(\cdot) : \mathbb{R}^n \times \mathbb{R}^n \times [0, \infty) \to \mathbb{R}^n$ is its continuously differentiable vector-valued non-linear dynamics.

The local control law and the adaptive law for the relative state consensus are given by

$$u_i = \alpha c_i \textstyle\sum_j e_{ij}(p_j - p_i) + \beta c_i \sum_j e_{ij}(v_j - v_j), \tag{4.14}$$

$$\begin{aligned} \dot{c}_i = \xi_i \Big(&\alpha (\textstyle\sum_j L_{ij} p_j)^{\mathsf{T}} (\sum_j L_{ij} p_j) + \beta\gamma (\sum_j L_{ij} v_j)^{\mathsf{T}} (\sum_j L_{ij} v_j) \\ &+ (\beta + \alpha\gamma)(\textstyle\sum_j L_{ij} p_j)^{\mathsf{T}} (\sum_j L_{ij} v_j) \Big), \end{aligned} \tag{4.15}$$

and for the leader-following consensus take the form

$$u_i = \alpha c_i \textstyle\sum_j H_{ij}(p_j - p_0) + \beta c_i \sum_j H_{ij}(v_j - v_0), \tag{4.16}$$

$$\begin{aligned} \dot{c}_i = \xi_i \Big(&\alpha (\textstyle\sum_j H_{ij} p_j)^{\mathsf{T}} (\sum_j H_{ij} p_j) + \beta\gamma (\sum_j H_{ij} v_j)^{\mathsf{T}} (\sum_j H_{ij} v_j) \\ &+ (\beta + \alpha\gamma)(\textstyle\sum_j H_{ij} p_j)^{\mathsf{T}} (\sum_j H_{ij} v_j) \Big), \end{aligned} \tag{4.17}$$

where $H = L + G$ it the pinning matrix, $\alpha > 0$ and $\beta > 0$ are coupling weights, and $\xi_i > 0$ and $\gamma > 0$ are constants.

Theorem 9 ([75], Thm. 1, thm. 2)**.** *Suppose that the graph $\mathcal{G}$ is connected and for the agent intrinsic dynamics $f(\cdot)$ holds the so-called QUAD condition on vector fields [75]. Then the agents described by (4.12) reach consensus or follow the leader (4.13) under the distributed control law (4.14) or (4.16) and the coupling gain dynamic (4.15) or (4.17).*

This DACP requires the knowledge of the weighted Laplacian matrix L that has to be defined by the designer; therefore, it is not fully distributed. Since each agent has just one adapted coupling gain that is used for the velocity feedback and also the position feedback, the protocol appears to be simpler than in [69]. However, the design of this protocol appears to be incomplete. The authors do not state how to properly design the coupling strengths α, β and constants ξ_i, γ. Nonetheless, the DACP inherits the problems of previously introduced DACP with different, large, and unbounded coupling gain values.

DACP design proposed by Li et al. [46], [47]

Novel DACPs are introduced by Li et al. [46], [47] for the agents having known identical LTI, (2.18, 2.19), or Lipschitz non-linear dynamics. For simplicity, we introduce the consensus protocols just for the agents with LTI dynamics. These results can be analogously adopted to agents described by Lipschitz non-linear dynamics.

The DACP in [46] solves the relative state consensus on undirected connected communication graphs. The control input with the coupling gain dynamics for i-th agent are given by

$$u_i = K \sum_j c_{ij} e_{ij} (x_i - x_j), \tag{4.18}$$

$$\dot{c}_{ij} = \kappa_{ij} e_{ij} (x_i - x_j)^{\mathsf{T}} \Gamma (x_i - x_j), \tag{4.19}$$

where $\kappa_{ij} = \kappa_{ji} > 0$ are constants, $c_{ij} > 0$ is the time-varying coupling gain between j-th and i-th agent with $c_{ij}(0) = c_{ji}(0)$, $K = -B^{\mathsf{T}} P^{-1}$ is the feedback control gain matrix, $\Gamma = P^{-1} B B^{\mathsf{T}} P^{-1}$ is the adaptation matrix, and $P \succ 0$ is a unique solution of the linear matrix inequality (LMI)

$$AP + PA^{\mathsf{T}} - 2BB^{\mathsf{T}} < 0. \tag{4.20}$$

Note that the solution of the LMI (4.20) equals the solution of ARE (2.22) for $R = I_m$. Also note that this adaptive approach addresses unweighted undirected graphs, hence $e_{ij} = e_{ji} = 1$ if $(j, i) \in \mathcal{E}$ and $e_{ij} = e_{ji} = 0$ otherwise.

Theorem 10 ([46], Thm. 1)**.** *Suppose that the communication graph $\mathcal{G}$ is connected. Then p agents (2.18) reach consensus under the control input (4.18) and the coupling gain dynamics (4.19).*

A similar DACP proposed by the same authors in [47] solves the leader-following consensus on directed graphs containing a spanning tree with a leader as the root node. Each agent implements a control input with the coupling gain dynamics in the form

$$u_i = c_i \rho_i (\xi_i^{\mathsf{T}} P^{-1} \xi_i) K \xi_i, \tag{4.21}$$

$$\dot{c}_i = \xi_i^{\mathsf{T}} \Gamma \xi_i, \tag{4.22}$$

where $\xi_i \triangleq \sum_{j=1}^{N} e_{ij}(x_j - x_i)$, $c_i > 0$ is the time-varying coupling gain associated with the i-th follower with the initial condition $c_i(0) \geq 1$, $K = -B^{\mathsf{T}}P^{-1}$ and $\Gamma = P^{-1}BB^{\mathsf{T}}P^{-1}$ are the feedback gain matrices, ρ_i is a smooth monotonically increasing function, satisfying $\rho_i(s) \geq 0$ for $s > 0$, chosen as $\rho_i = (1 + \xi_i^{\mathsf{T}}P^{-1}\xi_i)^3$, and $P \succ 0$ is a unique solution of the LMI (4.20).

Theorem 11. *Suppose that the communication graph $\mathcal{G}$ has a spanning tree. Then p agents described by (2.18) follow the leader defined by (2.19) under the control law (4.21) with the coupling gain dynamics (4.22).*

The DACPs, [46] and [47], do not rely on any centralized information, and therefore they can be implemented on agents in a fully distributed fashion. Nevertheless, they suffer from several drawbacks. The coupling gain dynamics in both DACPs (4.19) and (4.22) contain a quadratic term leading to non-negative coupling gain derivative, $\dot{c}_i \geq 0$. Therefore, both protocols inherit the problems of already mentioned DACPs with different, large, and unbounded coupling gains.

Other DACP designs

Recently published DACPs, [50] and [11], address these problems by proposing a modified adaptive laws which allows coupling gains to decay to lover values. More precisely, these protocols add a new decay term to the coupling gain dynamics that pushes the coupling gains' values to a predefined constant: 1 in [50] or 0 in [11]. This is found to solve the problems related with unbounded coupling gain values. Nevertheless, since this reference value for the coupling gains is a constant regardless of the network configuration and protocol design, under certain conditions it might lead to large UUB bounds on the local neighbourhood errors.

4.2 Our contribution

To tackle the aforementioned drawbacks of existing DACPs, specifically the considerable control effort and a lack of robustness to noise or disturbances, a new DACP [35] was first developed. It proposes to solve the cooperative regulator problem on undirected connected communication graphs, and is subsequently extended to directed graphs having a spanning tree [36]. The protocol introduces a novel coupling gain dynamics allowing coupling gains to synchronize and decay to some estimated reference values. Thereby it solves the issues of the recent DACPs with a one static reference value [50, 11]. The on-line estimation mechanism for these reference values, based on interval-halving method, compensates for the unavailability of centralized information, [35, 36]. To handle changes in network topology, an alternative estimation

algorithm, based on a distributed estimation of Laplacian eigenvalues [17, 18], was elaborated later, [37]; however, it applies only to undirected connected graphs.

This chapter presents an improved DACP, [38], solving both the cooperative regulator and tracker problems for agents with LTI dynamics on directed communication graphs. It is based on the previous results [35, 36, 37] and it extends the earlier seminal work on undirected graphs [46] to more general directed graphs while providing a simpler control protocol, comparable to the conventional synchronizing region control design, as opposed to [47] which involves additional nonlinearities.

This work differs from the existing results by:

- We consider general directed communication graphs, similarly as in [47, 44, 50], while other existing results [69, 75, 46, 11] focus on undirected graphs.
- The adaptive law differs from the conventional adaptive approaches [69, 75, 46, 47, 44, 50] by allowing coupling gains to decay to estimated coupling gains' references, rather that to a constant [50, 11].
- The coupling gains are associated with agents, similarly as in [75, 47, 50, 44], while other adaptive approaches have coupling gains associated with edges in the network [69, 46, 11].
- The Lyapunov function used here differs from those conventionally appearing in cooperative control [77, 78, 23].

The main contributions of our results are:

- The introduced DACP is fully distributed, in the sense that each agent designs its local controller based only on its own information and information from its neighbors.
- Both the cooperative regulator and tracker problems on general directed communication graphs are treated in a similar fashion using essentially the same adaptive consensus protocol.
- The novel adaptive law avoids problems of existing adaptive consensus protocols which possibly result in large control efforts and a lack of robustness to noise and disturbances.
- References values for the coupling gains are estimated by one of the two presented estimation algorithms: the interval halving estimation algorithm and the eigenvalue estimation algorithm.

A formal proof of uniform ultimate boundedness and convergence of a network dynamics implementing the presented DACP is given using Lyapunov function techniques. A thorough stability analysis of the proposed adaptive protocol is carried out, and simulations are provided validating its performance.

4.3 Problem statement and motivation

Consider a set of p identical agents networked by a communication topology. Each agent is described by a general LTI dynamics

$$\dot{x}_i(t) = Ax_i(t) + Bu_i(t), \tag{4.23}$$

where $x_i(t) \in \mathbb{R}^n$ is the agent's state, $u_i(t) \in \mathbb{R}^m$ is the agent's input, and $A \in \mathbb{R}^{n\times n}$ and $B \in \mathbb{R}^{n\times m}$ are constant matrices. The matrix A need not be stable, but the pair (A, B) is assumed stabilizable.

Assumption 11. The communication topology of the network of agents is given by a directed strongly connected graph $\mathcal{G}_1$.

With Assumption 11, the goal is to solve the cooperative regulator problem [43] and thereby reach an agreement on states of all the agents in the sense that $\|x_i(t) - x_j(t)\| \to 0$ as $t \to \infty$, $\forall(i, j)$, without requiring any centralized information.

Additionally, consider a leader given by an autonomous LTI dynamics $\dot{x}_0(t) = Ax_0(t)$, where $x_0(t) \in \mathbb{R}^n$ is its state.

Assumption 12. If a single leader is present, the communication topology is given by a directed graph $\mathcal{G}_2$ either having a spanning tree with a root pinned by the leader or a spanning forest with roots of all trees pinned by the leader.

With Assumption 12, the goal is to solve the cooperative tracker problem [43] and thereby synchronize the states of all agents with the leader's state in the sense that $\|x_0(t) - x_i(t)\| \to 0$ as $t \to \infty$, $\forall i$, without requiring any centralized information.

A class of distributed adaptive consensus protocols [46, 47, 69, 75] proposes possible solutions to these two cooperative control problems. They do not require any global information on a communication graph, therefore they are fully distributed. Nevertheless, they generally suffer from high final coupling gain values and a lack of robustness to noise.

To solve the cooperative regulator problem on directed strongly connected graphs and address the above-mentioned issues, we previously presented a novel adaptive control protocol [35, 36, 37], that allows coupling gains to decay and synchronize. This adaptive protocol was first introduced to solve the cooperative regulator problem on undirected graphs [35] which was later extended to directed

strongly-connected graphs [36]. In both results we provided an algorithm for estimation of coupling gains' references, based on the interval-halving method. Robust, albeit more complex, estimation algorithm based on estimation of the Laplacian eigenvalues [17, 18], was later proposed [37]. Note, that stability of this adaptive protocol has not been rigorously proven yet.

This chapter builds upon our previous results [35, 36, 37] and provides an improved adaptive consensus protocol with a detailed stability analysis and rigorous proofs of the UUB and convergence. Moreover, it also extends the adaptive control law to solve the cooperative tracker problem on directed graphs under Assumption 12.

Before introducing this adaptive consensus protocol we state technical results required for the subsequent stability analysis.

Lemma 8 (Uniform Ultimate Boundedness [32])**.** *The solution of an autonomous system $\dot{x} = f(x), f(0) = 0, x \in \mathbb{R}^n$, is guaranteed to be UUB if there exists a continuously differentiable function $V : \mathcal{D} \to \mathbb{R}$, defined on a domain $0 \in \mathcal{D} \subset \mathbb{R}^n$, and a positive constant r, such that $\dot{V}(x) < 0$ outside a ball $B_r = \{x \in \mathbb{R}^n | \|x\| \leq r\} \subset \mathcal{D}$ of finite radius r. Moreover, the solution is said to be globally UUB, if $\mathcal{D} = \mathbb{R}^n$ and $V(x)$ is radially unbounded.*

Remark 23. If there exists a closed and bounded region $\mathcal{J} \subset \mathcal{D}$, such that $\dot{V}(x) < 0$ on the exterior of $\mathcal{J}$, then one can always find a ball $B_r = \{x \in \mathbb{R}^n | \|x\| \leq r\} \subset \mathcal{D}$ containing $\mathcal{J}$, such that $\dot{V}(x) < 0$ on its exterior, and hence Lemma 8 guarantees UUB. Note in fact, that the existence of a closed and bounded region $\mathcal{J}$ is equivalent to the existence of a ball B_r with a finite radius required for UUB in Lemma 8.

4.4 Adaptive leaderless consensus protocol

To solve the cooperative regulator problem and avoid the above-mentioned issues of the previously proposed adaptive consensus protocols we consider an adaptive control law in the form

$$u_i(t) = c_i(t) K \sum_j e_{ij} \left(x_j(t) - x_i(t)\right), \tag{4.24}$$

$$\dot{c}_i(t) = \sum_j e_{ij} \left(x_j(t) - x_i(t)\right)^T \Gamma \left(x_j(t) - x_i(t)\right) - \beta_i \left(c_i(t) - \kappa_i\right), \tag{4.25}$$

where $c_i(t) > 0$ is an adaptive coupling gain associated with the ith agent, $\kappa_i > 0$ is a reference value estimated by the ith agent as detailed later, and $\beta_i > 0$ is a constant design parameter associated with the ith agent. The $K \in \mathbb{R}^{n \times n}$ and $\Gamma \in \mathbb{R}^{n \times n}$ are feedback and adaptation gain matrices. Let $Q = Q^T \in \mathbb{R}^{n \times n}$ and $R = R^T \in \mathbb{R}^{m \times m}$ be given positive definite symmetric

matrices, then K and Γ are taken as

$$K = R^{-1}B^T P, \tag{4.26}$$

$$\Gamma = K^T R K = PBK = PBR^{-1}B^T P, \tag{4.27}$$

where matrix $P > 0$ is the unique stabilizing solution of the ARE

$$A^T P + PA + Q - PBR^{-1}B^T P = 0. \tag{4.28}$$

For purposes of the convergence analysis, define the synchronization error as $\delta_i = x_i - x^*$, where x^* is a *virtual leader*

$$x^* := \frac{\sum_i \frac{w_i}{c_i} x_i}{\sum_i \frac{w_i}{c_i}}. \tag{4.29}$$

Then one has the constraint

$$\textstyle\sum_i \frac{w_i}{c_i} \delta_i = 0, \tag{4.30}$$

which implies that $\delta_i = \delta_j, \forall (i,j) \Leftrightarrow \delta_i = 0, \forall i$. Expressed in terms of (δ, c), the network dynamics reads

$$\dot{\delta}_i = A\delta_i + c_i BK \textstyle\sum_j e_{ij}(\delta_j - \delta_i) - a, \tag{4.31}$$

$$\dot{c}_i = \textstyle\sum_j e_{ij}(\delta_j - \delta_i)^T \Gamma (\delta_j - \delta_i) - \beta_i (c_i - \kappa_i), \tag{4.32}$$

where $a := \dot{x}^* - Ax^*$ is the same for all agents i.

Remark 24. The adaptive consensus protocol (4.24, 4.25) is motivated by previous results [46, 47], however there are several major differences to existing work. As opposed to [46, 11], having adaptive gains corresponding to edges in the network, in (4.24, 4.25) each agent has only one adaptive gain, much along the lines of [47, 75, 50]. For comparison, note that some adaptive consensus protocols [69] use both types of adaptive gains: ones corresponding to edges and those corresponding to agents in the network.

Furthermore, the coupling gain dynamics (4.25) allows the coupling gains c_i to decay to their reference values κ_i; hence, it is not a monotonically increasing function as in most present adaptive laws [46, 47, 69, 44]. It consists of two terms. The first term $\sum_j e_{ij}(x_j - x_i)^T \Gamma (x_j - x_i)$ is the non-negative quadratic term similar as in [46, 47]. Its purpose is to push the coupling gains to higher values until the states of agents become synchronized. The second term $-\beta_i(c_i - \kappa_i)$ pushes c_is to κ_is. The value of κ_i is updated by an estimation algorithm as detailed in Section 4.6. The decay rate β_i determines the strength of the convergence of c_i to κ_i.

Also, different from previous work [35, 36, 37], the coupling gain dynamics (4.25) does not contain the coupling gain synchronization term. Omitting

synchronization of coupling gains simplifies the protocol design. Moreover, in (4.24, 4.25) each agent has its own decay rate β_i. Note however, that this does not prevent the implementation of only one decay rate $\beta = \beta_i, \forall i$ along the lines of [35, 36, 37].

To the best of our knowledge, none of the existing results on adaptive consensus protocols introduce the decay of coupling gains in the way (4.24,4.25) does. There exist proposals [50, 11] which incorporate decay of adaptive gains in the protocol design. Nevertheless, nonzero decay rate there implies nonzero consensus error, hence they involve a trade-off between the rate of decay and the bound on the resulting consensus error.

For better understanding of the following stability analysis and proofs of UUB and convergence of the network dynamics (4.31, 4.32) let us first examine a simple motivating example which exhibits a very similar development.

4.4.1 Motivating example

The introduced network dynamics (4.31, 4.32) shares some similarities with a simpler dynamical system

$$\dot{x} = (1 - y)x, \tag{4.33}$$

$$\dot{y} = x^2 + (\kappa - y), \tag{4.34}$$

in $\mathbb{R} \times \mathbb{R}_0^+$ where $x \in \mathbb{R}$, $y \in \mathbb{R}_0^+$ and $\kappa > 0$ is a parameter. The system (4.33, 4.34) can be analyzed by the Lyapunov function

$$V(x, y) = \frac{r}{y}x^2 + \alpha y, \tag{4.35}$$

with $r > 0$ and $\alpha > 0$, having the time-derivative

$$\dot{V}(x, y) = \left[\frac{3r}{y} - \frac{r\kappa}{y^2} - (2r - \alpha)\right] x^2 - r\frac{x^4}{y^2} + \alpha(\kappa - y). \tag{4.36}$$

The Lyapunov function (4.35) is defined on the domain $\{x, y | x \in \mathbb{R}, y \geq \epsilon > 0\}$, which is forward invariant for (4.33, 4.34) if $\epsilon \leq \kappa$. For definiteness, let $r = 1.75$ and $\alpha = 1/2$, then the level sets of $V(x, y)$ and $\dot{V}(x, y) = 0$ lines are depicted in Figure 4.1.

The time-derivative of the Lyapunov function, (4.36), is negative for $|x|$ or y sufficiently large and it is positive only on some closed and bounded region, which is obvious also from Figure 4.1. This region is indeed different for different values of κ, actually, it grows with κ, but it always remains closed and bounded, as shown in Figure 4.1. Hence for every value of κ there exists a closed and bounded region on which $\dot{V}(x, y) \geq 0$ and $\dot{V}(x, y) < 0$ on its exterior. Thus,

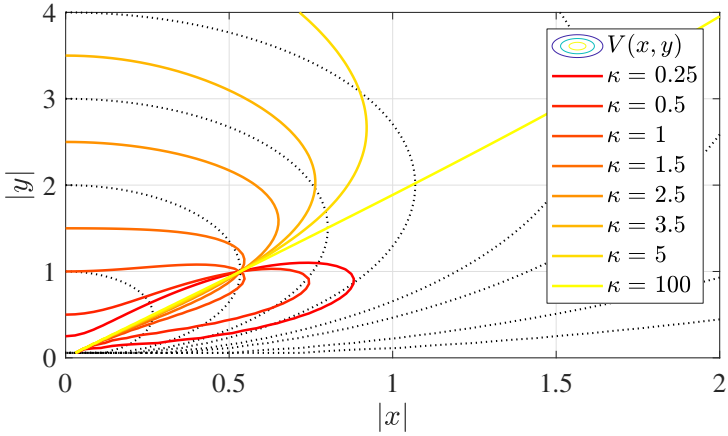

Figure 4.1: Level sets of $V(x, y)$ and lines $\dot{V}(x, y) = 0$ for different values of κ.

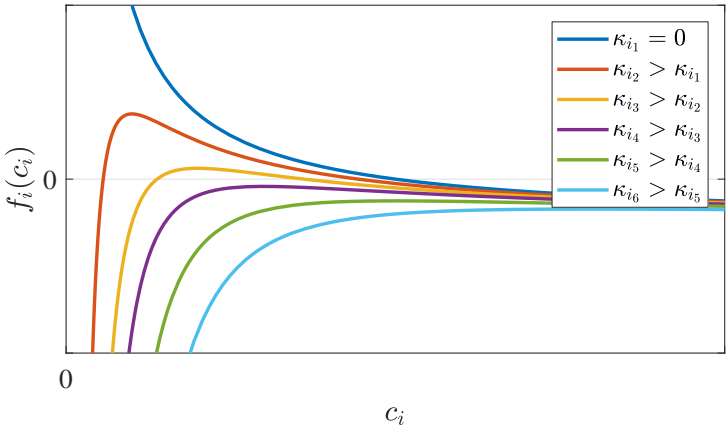

Figure 4.2: Plots of $f_i(c_i)$ for different values of κ_i.

by Lemma 8, a trajectory of the system (4.33, 4.34) is UUB for every $\kappa > 0$. Furthermore, as $\dot{y} > 0$, for $y < \kappa$, in (4.34), the trajectory of the system (4.33, 4.34) has to eventually end in a positively invariant closed and bounded region $\{x \in \mathbb{R}, y \geq \kappa\}$. Once, the trajectory enters this region, it will stay there for all future times. Note, that due to UUB and radial unboundedness of $V(x, y)$, the trajectory cannot escape to infinity in finite time before entering this region. For κ large enough, this region has $\dot{V}(x, y) \leq 0$ in its interior. Hence, the considered trajectory will be contained in the intersection of $\{x \in \mathbb{R}, y \geq \kappa\}$ with some sublevel set of $V(x, y)$, which is compact. Applying the LaSalle's invariance principle [32] to a trajectory bounded in this compact set, the trajectories of (4.33, 4.34) converge to the largest invariant set in $\{x, y | \dot{V}(x, y) = 0\}$, consisting only of the equilibrium point $\{x = 0, y = \kappa\}$. In summary, trajectories of the system (4.33, 4.34) are UUB for every $\kappa > 0$, and they converge to the equilibrium point $\{x = 0, y = \kappa\}$ for κ large enough.

Although (4.33, 4.34) does not exhibit any peculiarities of network interactions found in (4.31, 4.32), this consideration motivates the form of the Lyapunov function chosen for (4.31, 4.32) and its subsequent analysis.

4.4.2 Lyapunov function candidate

Consider a Lyapunov function candidate $V(\delta, c) : \mathcal{D} \to \mathbb{R}$ for the system (4.31, 4.32), given by

$$V(\delta, c) = \sum_i \frac{w_i}{c_i} \delta_i^T P \delta_i + \alpha \sum_i w_i c_i, \tag{4.37}$$

where $\alpha > 0$ is a parameter, defined on a domain $\mathcal{D} = \{\delta, c | \delta_i \in \mathbb{R}^n, c_i \geq \epsilon > 0, \forall i\}$. The region $\mathcal{D}$ is positively invariant with respect to (4.31, 4.32) if $0 < \epsilon \leq \min_i(\kappa_i)$.

Remark 25. Note that the Lyapunov function (4.37) is radially unbounded, i.e., if $\|\delta\| \to \infty$ or $\|c\| \to \infty$ then $V(\delta, c) \to \infty$. Moreover, for $\delta_i \neq 0$, if $c_i \to 0$ then $V(\delta, c) \to \infty$, which is the other boundary of $\mathcal{D}$. Hence, by approaching any boundary of $\mathcal{D}$, $V(\delta, c) \to \infty$ everywhere, except at $\{\delta_i = 0, c_i = 0\}$, where the Lyapunov function (4.37) looses continuity.

The time-derivative of the Lyapunov function (4.37), under dynamics (4.31, 4.32), equals

$$\dot{V}(\delta, c) = 2 \sum_i \frac{w_i}{c_i} \delta_i^T P \dot{\delta}_i - \sum_i \frac{w_i}{c_i^2} \delta_i^T P \delta_i \dot{c}_i + \alpha \sum_i w_i \dot{c}_i, \tag{4.38}$$

$$\begin{aligned} \dot{V}(\delta, c) = {} & 2 \sum_i \frac{w_i}{c_i} \delta_i^T P \left[A\delta_i + c_i B K \sum_j e_{ij}(\delta_j - \delta_i) - a \right] \\ & - \sum_i \frac{w_i}{c_i^2} (\delta_i^T P \delta_i) \left[\sum_j e_{ij}(\delta_j - \delta_i)^T \Gamma (\delta_j - \delta_i) - \beta_i (c_i - \kappa_i) \right] \\ & + \alpha \sum_i w_i \left[\sum_j e_{ij}(\delta_j - \delta_i)^T \Gamma (\delta_j - \delta_i) - \beta_i (c_i - \kappa_i) \right], \end{aligned} \tag{4.39}$$

$$\begin{aligned}\dot{V}(\delta,c) = {} & 2\textstyle\sum_i \frac{w_i}{c_i}\delta_i^T PA\delta_i + 2\sum_i w_i\delta_i^T \overbrace{PBK}^{=\Gamma}\sum_j e_{ij}(\delta_j-\delta_i) - 2\overbrace{\textstyle\sum_i \frac{w_i}{c_i}\delta_i^T}^{=0,\text{ due to (4.30)}} Pa \\ & - \textstyle\sum_i \frac{w_i}{c_i^2}(\delta_i^T P\delta_i)\sum_j e_{ij}(\delta_j-\delta_i)^T\Gamma(\delta_j-\delta_i) + \sum_i \frac{w_i}{c_i^2}(\delta_i^T P\delta_i)\beta_i(c_i-\kappa_i) \\ & + \alpha\textstyle\sum_i w_i\sum_j e_{ij}(\delta_j-\delta_i)^T\Gamma(\delta_j-\delta_i) - \alpha\sum_i w_i\beta_i(c_i-\kappa_i). \end{aligned} \tag{4.40}$$

Note, that the a term does not contribute to $\dot{V}(\delta,c)$. Due to 4.30, since $\mathcal{G}_1$ is strongly connected and Γ is symmetric, it holds that

$$\begin{gathered} 2\textstyle\sum_{i,j} w_i e_{ij}\delta_i^T\Gamma(\delta_i-\delta_j) = 2\sum_{i,j} w_i e_{ij}\delta_j^T\Gamma(\delta_j-\delta_i) = \\ \textstyle\sum_{i,j} w_i e_{ij}(\delta_j-\delta_i)^T\Gamma(\delta_j-\delta_i), [77,\ 46], \end{gathered} \tag{4.41}$$

hence

$$\begin{aligned}\dot{V} = {} & \textstyle\sum_i \frac{w_i}{c_i}\delta_i^T(PA+A^TP)\delta_i + \overbrace{2\sum_i w_i\delta_i^T\Gamma\sum_j e_{ij}(\delta_j-\delta_i)}^{=-\sum_{i,j} w_i e_{ij}(\delta_j-\delta_i)^T\Gamma(\delta_j-\delta_i)} \\ & + \alpha\textstyle\sum_{i,j} w_i e_{ij}(\delta_j-\delta_i)^T\Gamma(\delta_j-\delta_i) \\ & - \textstyle\sum_i \frac{w_i}{c_i^2}(\delta_i^T P\delta_i)\sum_j e_{ij}(\delta_j-\delta_i)^T\Gamma(\delta_j-\delta_i) \\ & + \textstyle\sum_i \frac{w_i}{c_i^2}(\delta_i^T P\delta_i)\beta_i(c_i-\kappa_i) - \alpha\sum_i w_i\beta_i(c_i-\kappa_i). \end{aligned} \tag{4.42}$$

As $PA+A^TP+Q-\Gamma=0$, we can use $PA+A^TP=-Q+\Gamma$ in the first term of (4.42), yielding

$$\begin{aligned}\dot{V} = {} & \textstyle\sum_i \frac{w_i}{c_i}\delta_i^T(-Q+\Gamma)\delta_i - (1-\alpha)\sum_{i,j} w_i e_{ij}(\delta_j-\delta_i)^T\Gamma(\delta_j-\delta_i) \\ & - \textstyle\sum_i \frac{w_i}{c_i^2}(\delta_i^T P\delta_i)\sum_j e_{ij}(\delta_j-\delta_i)^T\Gamma(\delta_j-\delta_i) \\ & + \textstyle\sum_i \frac{w_i}{c_i^2}(\delta_i^T P\delta_i)\beta_i c_i - \sum_i \frac{w_i}{c_i^2}(\delta_i^T P\delta_i)\beta_i\kappa_i - \alpha\sum_i w_i\beta_i(c_i-\kappa_i), \end{aligned} \tag{4.43}$$

$$\begin{aligned}\dot{V} = {} & \textstyle\sum_i \delta_i^T\left[\frac{w_i}{c_i}(\Gamma-Q+P\beta_i) - \frac{w_i}{c_i^2}P\beta_i\kappa_i\right]\delta_i \\ & - (1-\alpha)\textstyle\sum_{i,j} w_i e_{ij}(\delta_j-\delta_i)^T\Gamma(\delta_j-\delta_i) \\ & - \textstyle\sum_i \frac{w_i}{c_i^2}(\delta_i^T P\delta_i)\sum_j e_{ij}(\delta_j-\delta_i)^T\Gamma(\delta_j-\delta_i) - \alpha\sum_i w_i\beta_i(c_i-\kappa_i). \end{aligned} \tag{4.44}$$

Since Γ is symmetric positive semi-definite matrix, the second term in (4.44) can be upper-bounded as

$$\begin{gathered} -(1-\alpha)\textstyle\sum_{i,j} w_i e_{ij}(\delta_j-\delta_i)^T\Gamma(\delta_j-\delta_i) = \\ -(1-\alpha)\delta^T\left[(WL+L^TW)\otimes\Gamma\right]\delta = \\ -(1-\alpha)\delta^T\left[(WL+L^TW)\otimes I_n\right](I_N\otimes\Gamma)\delta = \\ -(1-\alpha)\delta^T(I_N\otimes\sqrt{\Gamma})^T\left[(WL+L^TW)\otimes I_n\right](I_N\otimes\sqrt{\Gamma})\delta \le \\ -(1-\alpha)\lambda_{\min}\left((WL+L^TW)\otimes I_n\right)\|(I_N\otimes\sqrt{\Gamma})\delta\|^2 = \\ -(1-\alpha)\lambda_{\min}(WL+L^TW)\textstyle\sum_i \delta_i^T\Gamma\delta_i. \end{gathered} \tag{4.45}$$

Let us denote $M = (WL + L^T W)$, which is positive semi-definite by Lemma 4. Then the upper bound on the Lyapunov function time-derivative has the form

$$\begin{aligned}\dot{V} \leq \textstyle\sum_i \delta_i^T \Big[\frac{w_i}{c_i} \overbrace{(\Gamma - Q + \beta_i P)}^{A^T P + PA + \beta_i P} - \frac{w_i}{c_i^2} P \beta_i \kappa_i - (1-\alpha)\lambda_{\min}(M)\Gamma \Big] \delta_i \\ - \textstyle\sum_i \frac{w_i}{c_i^2} (\delta_i^T P \delta_i) \sum_j e_{ij} (\delta_j - \delta_i)^T \Gamma (\delta_j - \delta_i) - \alpha \sum_i w_i \beta_i (c_i - \kappa_i).\end{aligned} \tag{4.46}$$

The time-derivative of the Lyapunov function (4.46) consists of three terms. The first is the only possibly indefinite term quadratic in δ_i, then follows the negative term quartic in δ_i, and finally the linear term in c_i, which is negative for $c_i > \kappa_i$ and positive otherwise. In order to proceed with the stability analysis of (4.31, 4.32) we first bring two technical results regarding (4.46), stated as Lemma 9 and Proposition 3.

Lemma 9. *The term* $\sum_i \frac{w_i}{c_i^2} (\delta_i^T P \delta_i) \sum_j e_{ij} (\delta_j - \delta_i)^T \Gamma (\delta_j - \delta_i)$ *in the time-derivative of the Lyapunov function (4.46) is zero, i.e.,* $\sum_i \frac{w_i}{c_i^2} (\delta_i^T P \delta_i) \sum_j e_{ij} (\delta_j - \delta_i)^T \Gamma (\delta_j - \delta_i) = 0$, *iff* $\forall i, \delta_i \in \ker(\Gamma)$.

Proof. It is straightforward that

$$\forall i, \delta_i \in \ker(\Gamma) \Rightarrow \textstyle\sum_i \frac{w_i}{c_i^2} (\delta_i^T P \delta_i) \sum_j e_{ij} (\delta_j - \delta_i)^T \Gamma (\delta_j - \delta_i) = 0. \tag{4.47}$$

To show that converse is also true,

$$\textstyle\sum_i \frac{w_i}{c_i^2} (\delta_i^T P \delta_i) \sum_j e_{ij} (\delta_j - \delta_i)^T \Gamma (\delta_j - \delta_i) = 0 \Rightarrow \forall i, \delta_i \in \ker(\Gamma), \tag{4.48}$$

we proceed with a proof by contradiction. Since $w_i > 0, \forall i$, by Assumption 11 and Lemma 3, $P \succ 0$, $\Gamma \succeq 0$, and $c_i > 0, \forall i$, it holds that

$$\begin{aligned}\textstyle\sum_i \frac{w_i}{c_i^2} (\delta_i^T P \delta_i) \sum_j e_{ij} (\delta_j - \delta_i)^T \Gamma (\delta_j - \delta_i) = 0 \Leftrightarrow \\ \forall i, w_i (\delta_i^T P \delta_i) \textstyle\sum_j e_{ij} (\delta_j - \delta_i)^T \Gamma (\delta_j - \delta_i) = 0.\end{aligned} \tag{4.49}$$

Let us consider the case when

$$\forall i, w_i (\delta_i^T P \delta_i) \textstyle\sum_j e_{ij} (\delta_j - \delta_i)^T \Gamma (\delta_j - \delta_i) = 0 \quad \text{and yet} \quad \exists j, \delta_j \notin \ker(\Gamma). \tag{4.50}$$

Since $P \succ 0$ and $\delta_j \notin \ker(\Gamma) \implies \delta_j \neq 0$, one has $\delta_j^T P \delta_j > 0$ and thus for the jth summand,

$$w_j (\delta_j^T P \delta_j) \textstyle\sum_k e_{jk} (\delta_k - \delta_j)^T \Gamma (\delta_k - \delta_j) = 0, \tag{4.51}$$

to be zero it must hold that $(\delta_k - \delta_j) \in \ker(\Gamma), \forall k \in \mathcal{V}_j$. If $\delta_j \notin \ker(\Gamma)$ then also such $\delta_k \notin \ker(\Gamma)$ because $\delta_k = \delta_j + v$ and $v \in \ker(\Gamma) \Rightarrow \delta_k \notin \Gamma$. In

other words, every neighbor k of agent j has its $\delta_k \notin \ker(\Gamma)$. Applying the same principle successively to all neighbors of the agent k, their neighbors and so on, by Assumption 11, all δ_i in the graph are not in the kernel of Γ, i.e., $\forall i, \delta_i \notin \ker(\Gamma)$. It follows then, that (4.51) is zero for every i with $\forall i, \delta_i \notin \ker(\Gamma)$ meaning $\forall i, \delta_i^T P \delta_i > 0$ implying

$$\forall i, w_i \textstyle\sum_j e_{ij}(\delta_j - \delta_i)^T \Gamma(\delta_j - \delta_i) = 0, \tag{4.52}$$

which further leads to the sum over i being equal to zero

$$\textstyle\sum_i w_i \sum_j e_{ij}(\delta_j - \delta_i)^T \Gamma(\delta_j - \delta_i) = 0. \tag{4.53}$$

This can happen iff either $\forall i, \delta_i \in \ker(\Gamma)$ or $\forall (i,j), \delta_i = \delta_j$, but in the later case $\delta_i = 0 \in \ker(\Gamma), \forall i$, leading to the contradiction to (4.50), thereby completing the proof. □

Proposition 3. *Given* $0 < \alpha < 1$ *and* $0 < \beta_i < \frac{\lambda_{\min}(Q)}{\lambda_{max}(P)}$. *Let* $\delta_i \notin \ker(\Gamma), \forall i$, *then the first term of (4.46) is negative, i.e.*

$$\textstyle\sum_i \delta_i^T \Big[\frac{w_i}{c_i}(\Gamma - Q + \beta_i P) - \frac{w_i}{c_i^2} P \beta_i \kappa_i - (1-\alpha)\lambda_{\min}(M)\Gamma \Big] \delta_i \leq 0, \tag{4.54}$$

on the domain $\mathcal{D}$ *if all* κ_i*s are sufficiently large.*

Proof. The first term of (4.46), expression (4.54), is bounded from above by

$$\begin{aligned} \textstyle\sum_i \delta_i^T \Big[\frac{w_i}{c_i} & \left(\lambda_{\max}(\Gamma) - \lambda_{\min}(Q) + \beta_i \lambda_{\max}(P)\right) \\ & - \frac{w_i}{c_i^2} \lambda_{\min}(P) \beta_i \kappa_i - (1-\alpha)\lambda_{\min}(M)\lambda_{\min>0}(\Gamma) \Big] \delta_i. \end{aligned} \tag{4.55}$$

Each square bracket term in (4.55), has the form of a quadratic polynomial in c_i^{-1} given by a function

$$f_i(c_i) = \frac{1}{c_i^2} s_i + \frac{1}{c_i} q_i + z, \tag{4.56}$$

with $s_i = -w_i \lambda_{\min}(P)\beta_i \kappa_i$, $q_i = w_i(\lambda_{\max}(\Gamma) - \lambda_{\min}(Q) + \beta_i \lambda_{\max}(P))$, and $z = -(1-\alpha)\lambda_{\min}(M)\lambda_{\min>0}(\Gamma)$. Choose some $0 < \alpha < 1$, $0 < \beta_i < \frac{\lambda_{\min}(Q)}{\lambda_{max}(P)}$, then $s_i \leq 0$, $q_i \in \mathbb{R}$, $z < 0$, and $f_i(c_i)$ depends only on the value of $\kappa_i > 0$ as depicted in Figure 4.2. Let $c_i^* \in \mathbb{R}$ be such that

$$f_i(c_i^*) = \max_{c_i} f_i(c_i), \tag{4.57}$$

then the maximizing c_i^* and the maximum value are

$$c_i^* = -\frac{2s_i}{q_i}, \quad f_i(c_i^*) = -\frac{q_i^2}{4s_i} + z. \tag{4.58}$$

It follows, that c_i^* scales with κ_i and $f_i(c_i^*)$ scales as $1/\kappa_i$. Hence for all κ_is sufficiently large, $f_i(c_i^*) < 0, \forall i$, which implies that (4.54) is negative. This concludes the proof. □

Remark 26. The behaviour of $f_i(c_i)$ in dependence of κ_i is depicted on Figure 4.2 for clarity. The bound on κ_i, obtained from the condition $f_i(c_i^*) < 0, \forall i$, for which Proposition 3 holds, reads

$$\kappa_i > \kappa_i^* = \frac{w_i(\lambda_{\max}(\Gamma) - \lambda_{\min}(Q) + \beta_i\lambda_{\max}(P))^2}{4\beta_i(1-\alpha)\lambda_{\min}(M)\lambda_{\min}(P)\lambda_{\min>0}(\Gamma)}, \quad \forall i. \tag{4.59}$$

For definiteness, let us chose $\alpha = 1/2$, $\beta_i = \frac{\lambda_{\min}(Q)}{\lambda_{max}(P)}$ for the numerator, and $\beta_i = \frac{\lambda_{\min}(Q)}{2\lambda_{max}(P)}$ for the denominator of (4.59), then (4.59) is certainly satisfied if a simpler, albeit more conservative, condition holds

$$\kappa_i > \kappa_i^* > \kappa^* = \frac{w_{\max}\lambda_{\max}(P)(\lambda_{\max}(\Gamma))^2}{\lambda_{\min}(Q)\lambda_{\min}(M)\lambda_{\min}(P)\lambda_{\min>0}(\Gamma)}, \quad \forall i. \tag{4.60}$$

4.4.3 Stability analysis

Starting from the expression for $\dot{V}(\delta, c)$, (4.46), Proposition 3, and Lemma 9 we bring here the main result on dynamics (4.31, 4.32).

Theorem 12. *Consider a network of p agents with the general LTI dynamics (4.23) satisfying Assumption 11. Let each agent implement the control input (4.24) with the coupling gain dynamics (4.25) and let* $0 < \beta_i < \frac{\lambda_{\min}(Q)}{\lambda_{max}(P)}, \forall i$. *Then the agents reach consensus within some bounded region, i.e., their trajectories are UUB, on domain* $\mathcal{D}$, *if all* κ_i*s are sufficiently large, satisfying the bound*

$$\sum_{i=3}^{p}\left[\frac{w_i}{c_i^*}(\Gamma - Q + \beta_i P) - \frac{w_i}{c_i^{*2}}P\beta_i\kappa_i\right] < (p-1)(1-\alpha)\lambda_{\min}(M)\Gamma. \tag{4.61}$$

Proof. Consider the Lyapunov function (4.37) with its time-derivative (4.46). The UUB of the solution of the network error dynamics (4.31, 4.32) is proved by showing that, for κ_is sufficiently large, satisfying (4.61), there exists a closed and bounded region $\mathcal{J} = \{\delta, c | \dot{V}(\delta, c) \geq 0\} \subset \mathcal{D}$ outside of which $\dot{V}(\delta, c) < 0$ on $\mathcal{D}$, in accordance with Remark 23. To that end, we analyze $\dot{V}(\delta, c)$ for several different cases:

1. $\forall i, \delta_i \in \ker(\Gamma)$; The terms containing Γ in (4.46) vanish and the time-derivative of the Lyapunov function (4.46) simplifies into

$$\dot{V} \leq \sum_i \delta_i^T\left[\frac{w_i}{c_i}(-Q + \beta_i P) - \frac{w_i}{c_i^2}P\beta_i\kappa_i\right]\delta_i - \alpha\sum_i w_i\beta_i(c_i - \kappa_i). \tag{4.62}$$

It is obvious that (4.62) is negative definite, i.e., $\dot{V}(\delta, c) < 0$, for $c_i > \kappa_i, \forall i$. If $c_i \leq \kappa_i$, for any i, the positive contribution of terms linear in c_i is bounded and finite, therefore there exists δ_i sufficiently large, such that the contribution of the ith summand in (4.62) is negative definite and thereby $\dot{V}(\delta, c) < 0$. Hence $\dot{V}(\delta, c) \geq 0$ only on a closed and bounded region $\mathcal{J}$.

2. $\forall i, \delta_i \notin \ker(\Gamma)$; The time-derivative of the Lyapunov function is given by the full expression (4.46). Note, that the existence of negative definite terms in $\dot{V}(\delta, c)$, which are quartic in δ_i, is guaranteed by Lemma 9. Let us split the analysis of its sign-dependence into the following three situations:

2.a) one or more δ_is grow with $\nu \in [1, \infty\rangle$, i.e., $\delta_i = \delta_c \nu$, and the remaining $\delta_i = \delta_c$, with all $c_i = c_i^*$ fixed at the value that maximizes the positive contribution of the first term quadratic in δ_i, as in (4.57). Increasing a single δ_i while keeping other $\delta_i = \delta_c$ and all $c_i = c_i^*$ fixed leads to a single indefinite term increasing quadratically in δ_i, few negative definite terms increasing quadratically in δ_i and a single negative definite term which increases quartically with δ_i, hence for some finite value of $\|\delta_i\|$, the negative definite quartic term dominates the contribution of all the positive definite terms and $\dot{V}(\delta, c)$ is necessarily negative definite. This negative definite term certainly exists as per Lemma 9.

For multiple δ_is growing simultaneously, let us consider the worst case scenario, where there arises a minimum number of negative definite terms in $\dot{V}(\delta, c)$, which are quartic in δ_i. The constraint (4.30) implies, that the minimum number of negative definite terms quartic in δ_i, on strongly connected graphs, is 2 and the network is then composed of $p - 1$ agents having $\delta_i = \delta_a \nu$ except one agent which has $\delta_1 = \delta_b \nu$, both δ_a and $\delta_b \in \ker(\Gamma)^{\perp}$. This worst case scenario is depicted in Figure 4.3a. Note, that all agents are considered to have their $c_i = c_i^*$ fixed. For δ_i sufficiently large, the resulting 2 negative definite terms, quartic in δ_i, dominate p indefinite terms quadratic in δ_i, thus $\dot{V}(\delta, c)$ is rendered negative for a finite value of ν.

2.b) one or more c_is grow with $\nu \in [1, \infty\rangle$, i.e., $c_i = c_i^* \nu$, and the remaining $c_i = c_i^*$, with all $\delta_i = \delta_c$ fixed, where c_i^* is given by (4.57). By increasing any c_i above κ_i, the negative contribution of the last term linear in c_i increases with c_i while the contribution of the indefinite term decreases with $1/c_i$. Therefore there exists a value of $c_i > \kappa_i$ such that the increasing negative definite term dominates the indefinite term and $\dot{V}(\delta, c)$ is rendered negative definite. If several c_is are considered to grow simultaneously, then there likewise exists growing $c_i > \kappa_i$ sufficiently large, such that $\dot{V}(\delta, c) < 0$.

2.c) both δ_is and c_is grow with $\nu \in [1, \infty\rangle$, i.e., $\delta_i = \delta_c \nu$ and $c_i = c_i^* \nu$. We analyze the worst case scenario, where there arises a minimum number of negative definite terms, quartic in δ_i, and their corresponding δ_i and c_i increase simultaneously. From the constraint (4.30) on δ_is it follows, that the minimum number of such terms is 2, see Figure 4.3b, and for this worst case scenario

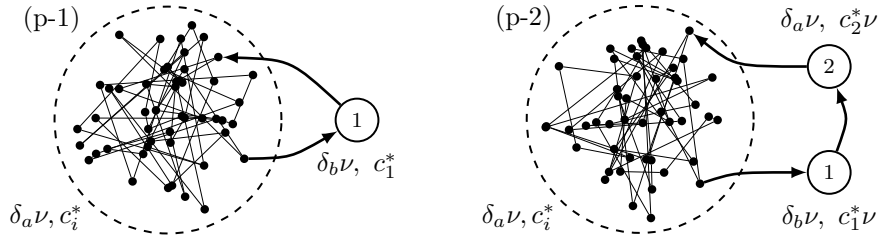

(a) more δ_is grow and c_is are constant (b) both δ_i and c_i grow

Figure 4.3: Network topology of the worst-case scenario for Case 1, $\forall i, \delta_i \notin \ker(\Gamma)$.

the network is composed of $p-1$ agents with $\delta_i = \delta_a\nu$ and one agent with $\delta_1 = \delta_b\nu$, both δ_a and $\delta_b \in \ker(\Gamma)^\perp$. Label the 1st agent's child with index 2. To maximize positive definite contribution of the first term in $\dot{V}(\delta, c)$, all those agents having fixed c_i, have their $c_i = c_i^*$, whereas the 1st and the 2nd agent have $c_1 = c_1^*\nu$ and $c_2 = c_2^*\nu$. Scaling of c_i simultaneously with δ_i makes the negative definite quartic term in δ_i effectively scale only quadratically in ν: comparable to the growth of quadratic indefinite terms. Note however, that the first quadratic terms in $\dot{V}(\delta, c)$, which correspond to the 1st and the 2nd agent, are no longer indefinite with increasing c_is. By scaling c_1 and c_2 they are rendered negative semidefinite for a finite value of ν. The time-derivative of the Lyapunov function is composed of 3 parts corresponding to the agent 1, the agent 2 and the rest of the network

$$\begin{aligned}
\dot{V} \leq & \textstyle\sum_{i=3}^{p} \delta_a^T \left[\frac{w_i}{c_i^*}(\Gamma - Q + \beta_i P) - \frac{w_i}{c_i^{*2}} P\beta_i\kappa_i - (1-\alpha)\lambda_{\min}(M)\Gamma \right] \delta_a\nu^2 \\
& - \alpha \textstyle\sum_{i=3}^{p} w_i\beta_i(c_i^* - \kappa_i) \\
& - \delta_b^T \left[(1-\alpha)\lambda_{\min}(M)\Gamma\right] \delta_b\nu^2 - \frac{w_1}{c_1^{*2}}(\delta_b^T P\delta_b)(\delta_b - \delta_a)^T\Gamma(\delta_b - \delta_a)\nu^2 \\
& - \alpha w_1\beta_1(c_1^*\nu - \kappa_i) \\
& - \delta_a^T \left[(1-\alpha)\lambda_{\min}(M)\Gamma\right] \delta_a\nu^2 - \frac{w_2}{c_2^{*2}}(\delta_a^T P\delta_a)(\delta_a - \delta_b)^T\Gamma(\delta_a - \delta_b)\nu^2 \\
& - \alpha w_2\beta_2(c_2^*\nu - \kappa_i).
\end{aligned} \tag{4.63}$$

If the following bound is satisfied, the first indefinite quadratic terms in (4.63) are dominated by the resulting negative definite quadratic terms alone and $\dot{V}(\delta, c)$ is rendered negative definite,

$$\begin{aligned}
\delta_a^T \textstyle\sum_{i=3}^{p} \left[\frac{w_i}{c_i^*}(\Gamma - Q + \beta_i P) - \frac{w_i}{c_i^{*2}} P\beta_i\kappa_i - (1-\alpha)\lambda_{\min}(M)\Gamma \right] \delta_a\nu^2 < \\
\delta_a^T[(1-\alpha)\lambda_{\min}(M)\Gamma]\delta_a\nu^2,
\end{aligned} \tag{4.64}$$

$$\sum_{i=3}^{p}\left[\frac{w_i}{c_i^*}(\Gamma - Q + \beta_i P) - \frac{w_i}{{c_i^*}^2}P\beta_i\kappa_i\right] - (p-2)(1-\alpha)\lambda_{\min}(M)\Gamma < (1-\alpha)\lambda_{\min}(M)\Gamma, \tag{4.65}$$

$$\sum_{i=3}^{p}\left[\frac{w_i}{c_i^*}(\Gamma - Q + \beta_i P) - \frac{w_i}{{c_i^*}^2}P\beta_i\kappa_i\right] < (p-1)(1-\alpha)\lambda_{\min}(M)\Gamma. \tag{4.66}$$

This leads to the final bound (4.61). Note, that by assuming a common $\beta = \beta_i$, $\forall i$, the inequality (4.61) can be unified for all agents as

$$\frac{w_{\max}}{c_{\min}^*}(\Gamma - Q + \beta P) - \frac{w_{\min}}{{c_{\max}^*}^2}P\beta\kappa_{\min} < \frac{(p-1)}{(p-2)}(1-\alpha)\lambda_{\min}(M)\Gamma. \tag{4.67}$$

Moreover, taking $p \to \infty$, it can be generalized for any number of agents

$$\frac{w_{\max}}{c_{\min}^*}(\Gamma - Q + \beta P) - \frac{w_{\min}}{{c_{\max}^*}^2}P\beta\kappa_{\min} < (1-\alpha)\lambda_{\min}(M)\Gamma. \tag{4.68}$$

The three above investigated situations cover all possible scenarios, which can occur on domain $\mathcal{D}$, for the case when $\forall i, \delta_i \notin \ker(\Gamma)$. They imply, under condition $\forall i, \delta_i \notin \ker(\Gamma)$, that, for all κ_is satisfying (4.61), there always exists a closed and bounded region $\mathcal{J}$, such that $\dot{V}(\delta, c) \geq 0$ in the interior of $\mathcal{J}$ and $\dot{V}(\delta, c) < 0$ in the exterior of $\mathcal{J}$.

3. $\exists i, \delta_i \in \ker(\Gamma) \wedge \exists k, \delta_k \notin \ker(\Gamma)$; Let us denote $\mathcal{S}_\Gamma$ as the set of nodes for which $\delta_i \in \ker(\Gamma)$ and the complementary set $\bar{\mathcal{S}}_\Gamma = \mathcal{V}\backslash\mathcal{S}_\Gamma$ for which $\delta_k \notin \ker(\Gamma)$. Then the time-derivative of the Lyapunov function can be split into two sums over $\mathcal{S}_\Gamma$ and $\bar{\mathcal{S}}_\Gamma$ respectively

$$\begin{aligned}\dot{V} \leq & \sum_{i\in\mathcal{S}_\Gamma}\delta_i^T\left[\frac{w_i}{c_i}(-Q + \beta_i P) - \frac{w_i}{c_i^2}P\beta_i\kappa_i\right]\delta_i - \alpha\sum_{i\in\mathcal{S}_\Gamma} w_i\beta_i(c_i - \kappa_i) \\ & + \sum_{k\in\bar{\mathcal{S}}_\Gamma}\delta_k^T\left[\frac{w_k}{c_k}(\Gamma - Q + \beta_k P) - \frac{w_k}{c_k^2}P\beta_k\kappa_k - (1-\alpha)\lambda_{\min}(M)\Gamma\right]\delta_k \\ & - \sum_{k\in\bar{\mathcal{S}}_\Gamma}\frac{w_k}{c_k^2}(\delta_k^T P\delta_k)\sum_j e_{kj}(\delta_j - \delta_k)^T\Gamma(\delta_j - \delta_k) \\ & - \alpha\sum_{k\in\bar{\mathcal{S}}_\Gamma} w_k\beta_k(c_k - \kappa_k).\end{aligned} \tag{4.69}$$

The first part of (4.69) with sum over $\mathcal{S}_\Gamma$, being identical to (4.62), shares the same conclusion with Case 1, $\forall i, \delta_i \in \ker(\Gamma)$. It is negative definite if, for all i, either $\|\delta_i\|$ or c_i exceeds certain finite value while its maximum positive contribution is bounded for $\|\delta_i\|$ or c_i below that value.

If condition (4.61) derived in Case 2 is satisfied for a network consisting of p agents then it also holds for a smaller number of agents, $p_s = |\bar{\mathcal{S}}_\Gamma| < p$. Hence, the results of Case 2, $\forall i, \delta_i \notin \ker(\Gamma)$, apply to the second part of (4.69) with sum running over $\bar{\mathcal{S}}_\Gamma$.

Because positive contributions of both parts of (4.69) are bounded and $V(\delta, c)$ is radially unbounded, increasing either $\|\delta_i\|$ or c_i or $\|\delta_k\|$ or c_k, the

growing negative definite contribution of one part of (4.69) always eventually dominates the bounded positive definite contribution of the other part. This translates into existence of the bounded region $\mathcal{J}$. Thus, for the case when $\exists i, \delta_i \in \ker(\Gamma) \wedge \exists k, \delta_k \notin \ker(\Gamma)$, for all κ_is satisfying (4.61), there also always exists a closed and bounded region $\mathcal{J}$, such that $\dot{V}(\delta, c) \geq 0$ in its interior and $\dot{V} < 0$ on its exterior.

All the above investigated cases lead to the same conclusion, i.e., for all κ_is satisfying (4.61), there always exists a closed and bounded set $\mathcal{J} \subset \mathcal{D}$, such that $\dot{V}(\delta, c) \geq 0$ on its interior and $\dot{V} < 0$ on its exterior. Since the union of these three cases covers the whole domain $\mathcal{D}$ and $V(\delta, c)$ is radially unbounded on $\mathcal{D}$, this bounded set $\mathcal{J}$ guaranties uniform ultimate boundedness (UUB) of the solution of the network dynamics (4.31, 4.32), for all κ_is sufficiency large. □

Theorem 13. *Consider Theorem 12 and in addition assume that all κ_i satisfy the bound (4.59), then the states of agents fully synchronize, i.e., $\lim_{t\to\infty} \|x_i(t) - x_j(t)\| = 0, \forall(i, j)$. Moreover every $c_i(t)$ converges to κ_i.*

Proof. Following the analysis of $\dot{V}(\delta, c)$ in Section 4.4.2 and by Proposition 3, for sufficiency large κ_i satisfying (4.59), the first two terms in (4.46), quadratic and quartic in δ_i, are both negative definite and the third term, linear in c_i, is negative definite for $c_i > \kappa_i$. Hence if $c_i > \kappa_i, \forall i$ then $\dot{V}(\delta, c) < 0$. On the other hand, if any $c_i < \kappa_i$, then there exists $\|\delta_i\| > 0$, for any i, sufficiently large, such that the negative contribution of the first two terms dominates the bounded positive contribution of the third term in the ith summand of $\dot{V}(\delta, c)$. Therefore $\dot{V}(\delta, c) < 0$ for $\|\delta_i\|$ or c_i sufficiently large. This means that the set $\mathcal{J} = \{\delta, c | \dot{V}(\delta, c) \geq 0\} \subset \mathcal{D}$ is closed and bounded and $\dot{V}(\delta, c) < 0$ on its exterior, thus the solution of the system (4.31, 4.32) is certainly UUB.

Furthermore, the coupling gain dynamics (4.32) has a consequence that $c_i < \kappa_i \Rightarrow \dot{c}_i > 0$. As $V(\delta, c)$ is radially unbounded by Remark 25, there is no escape to infinity in finite time while $c_i < \kappa_i$, so the solution of (4.31, 4.32) always ends in a set $\Omega = \{\delta, c | c_i \geq \kappa_i, \forall i\}$. The set Ω is positively invariant with respect to (4.31, 4.32) and, under (4.59), $\dot{V}(\delta, c) \leq 0$ in its interior. Wherever the solution first enters the region Ω it will be contained, for all future times, in a well defined sub-level set $\Psi = \{\delta, c | V(\delta, c) \leq g\}$, which is bounded on $\mathcal{D}$ by the fact that $V(\delta, c)$ is radially unbounded, and since $\dot{V}(\delta, c) \leq 0$ on the whole Ω the solution has to stay within this set Ψ for all future times. Thus the solution eventually ends in a positively invariant compact set $\Phi = \Psi \cap \Omega$ where $\dot{V}(\delta, c) \leq 0$. Let E be the set of all points where $\dot{V}(\delta, c) = 0$ in Φ and let M be the largest invariant set in E. Then, $M = \{\delta, c | \delta_i = 0, c_i = \kappa_i, \forall i\}$ contains only the equilibrium point and by LaSalle's invariance principle [32], every solution in Φ approaches M as $t \to \infty$. Therefore the system (4.31, 4.32) converges to the equilibrium point $(\delta_i = 0, c_i = \kappa_i, \forall i)$ while being UUB. □

Remark 27. Note that the given Lyapunov proofs provide only sufficient conditions, not necessary ones. It may very well happen that the bounds there are too conservative and one in fact has UUB and convergence to the equilibrium point even for lower values of κ_is. Nevertheless, certainly if all κ_is exceed the given lower bounds one can no longer have limit cycles but only convergence to the target equilibrium point $\{\delta = 0,\, c_i = \kappa_i,\, \forall i\}$, which is the main result here and serves as a justification for the κ_i update process proposed in Section 4.6.

4.5 Adaptive leader-following consensus protocol

The following adaptive consensus protocol is proposed to solve the cooperative tracker problem

$$u_i(t) = c_i(t) K \Big[\textstyle\sum_j e_{ij} \left(x_j(t) - x_i(t) \right) + g_i \left(x_0(t) - x_i(t) \right) \Big], \tag{4.70}$$

$$\begin{aligned} \dot{c}_i(t) = & \textstyle\sum_j e_{ij} \left(x_j(t) - x_i(t) \right)^T \Gamma \left(x_j(t) - x_i(t) \right) \\ & + g_i \left(x_0(t) - x_i(t) \right)^T \Gamma \left(x_0(t) - x_i(t) \right) - \beta_i \left(c_i(t) - \kappa_i \right), \end{aligned} \tag{4.71}$$

where K and Γ are given by (4.26) and (4.27), respectively, and P is the positive definite solution of the ARE, (4.28). Define the tracking error of an agent with respect to the leader, $\delta_i = x_i - x_0$. Then the synchronization error dynamics is

$$\dot{\delta}_i = A\delta_i + c_i B K \Big[\textstyle\sum_j e_{ij} \left(\delta_j - \delta_i \right) - g_i \delta_i \Big], \tag{4.72}$$

$$\dot{c}_i = \textstyle\sum_j e_{ij} (\delta_j - \delta_i)^T \Gamma (\delta_j - \delta_i) + g_i (\delta_i^T \Gamma \delta_i) - \beta_i (c_i - \kappa_i). \tag{4.73}$$

Remark 28. Note that, from the single-agent perspective, the adaptive consensus protocol (4.70, 4.71) is equivalent to the protocol (4.24, 4.25) applied to communication graphs satisfying Assumption 12. The only difference are the pinning terms contained in (4.70, 4.71) which is a matter of notation; hence Remark 24 applies also to (4.70, 4.71). Furthermore, note that the adaptive consensus protocol (4.70, 4.71) contains no additional nonlinearities in contrast to the proposal found in the literature [47].

In the following we derive the time-derivative of the Lyapunov function (4.37), with δ_is as defined in this section, for (4.72, 4.73) and then use it to show UUB and convergence of the adaptive consensus protocol (4.70, 4.71) solving the cooperative tracker problem.

4.5.1 Lyapunov function candidate

Consider the same Lyapunov function as in (4.37) with $\alpha > 0$ and $w_i > 0$, $\forall i$, to be determined later. Let us emphasize, that different from the definition of

vector w in Lemma 3, in this case w is some convenient positive vector to be chosen later. The time-derivative of the Lyapunov function (4.38), under the dynamics (4.72, 4.73), then equals

$$\begin{aligned}\dot{V} = {} & 2\textstyle\sum_i \frac{w_i}{c_i}\delta_i^T P\Big[A\delta_i + c_i BK\Big[\sum_j e_{ij}(\delta_j-\delta_i) - g_i\delta_i\Big]\Big] \\ & - \textstyle\sum_i \frac{w_i}{c_i^2}(\delta_i^T P\delta_i)\Big[\sum_j e_{ij}(\delta_j-\delta_i)^T\Gamma(\delta_j-\delta_i) + g_i(\delta_i^T\Gamma\delta_i) - \beta_i(c_i-\kappa_i)\Big] \\ & + \alpha\textstyle\sum_i w_i\Big[\sum_j e_{ij}(\delta_j-\delta_i)^T\Gamma(\delta_j-\delta_i) + g_i(\delta_i^T\Gamma\delta_i) - \beta_i(c_i-\kappa_i)\Big], \end{aligned} \tag{4.74}$$

$$\begin{aligned}\dot{V} = {} & 2\textstyle\sum_i \frac{w_i}{c_i}\delta_i^T PA\delta_i + 2\sum_i \frac{w_i}{c_i}\delta_i^T Pc_i BK\Big[\sum_j e_{ij}(\delta_j-\delta_i) - g_i\delta_i\Big] \\ & - \textstyle\sum_i \frac{w_i}{c_i^2}(\delta_i^T P\delta_i)\sum_j e_{ij}(\delta_j-\delta_i)^T\Gamma(\delta_j-\delta_i) \\ & - \textstyle\sum_i \frac{w_i}{c_i^2}(\delta_i^T P\delta_i)g_i(\delta_i^T\Gamma\delta_i) + \sum_i \frac{w_i}{c_i^2}(\delta_i^T P\delta_i)\beta_i(c_i-\kappa_i) \\ & + \alpha\textstyle\sum_{i,j} w_i e_{ij}(\delta_j-\delta_i)^T\Gamma(\delta_j-\delta_i) + \alpha\sum_i w_i g_i(\delta_i^T\Gamma\delta_i) \\ & - \alpha\textstyle\sum_i w_i\beta_i(c_i-\kappa_i), \end{aligned} \tag{4.75}$$

$$\begin{aligned}\dot{V} = {} & \textstyle\sum_i \frac{w_i}{c_i}\delta_i^T(PA + A^T P)\delta_i + 2\sum_{i,j} w_i e_{ij}\delta_i^T \overbrace{PBK}^{=\Gamma}(\delta_j-\delta_i) \\ & - 2\textstyle\sum_i w_i g_i\delta_i^T\Gamma\delta_i + \alpha\sum_{i,j} w_i e_{ij}(\delta_j-\delta_i)^T\Gamma(\delta_j-\delta_i) \\ & - \textstyle\sum_i \frac{w_i}{c_i^2}(\delta_i^T P\delta_i)\sum_j e_{ij}(\delta_j-\delta_i)^T\Gamma(\delta_j-\delta_i) \\ & - \textstyle\sum_i \frac{w_i}{c_i^2} g_i(\delta_i^T P\delta_i)(\delta_i^T\Gamma\delta_i) + \sum_i \frac{w_i}{c_i^2}(\delta_i^T P\delta_i)\beta_i(c_i-\kappa_i) \\ & + \alpha\textstyle\sum_i w_i g_i(\delta_i^T\Gamma\delta_i) - \alpha\sum_i w_i\beta_i(c_i-\kappa_i). \end{aligned} \tag{4.76}$$

Let $\alpha = 1$, then four terms of the above yield

$$\begin{aligned} & 2\textstyle\sum_{i,j} w_i e_{ij}\delta_i^T\Gamma(\delta_j-\delta_i) - 2\sum_i w_i g_i(\delta_i^T\Gamma\delta_i) \\ & + \textstyle\sum_{i,j} w_i e_{ij}(\delta_j-\delta_i)^T\Gamma(\delta_j-\delta_i) \\ & + \textstyle\sum_i w_i g_i(\delta_i^T\Gamma\delta_i) = 2\sum_{i,j} w_i e_{ij}\delta_i^T\Gamma(\delta_j-\delta_i) - \sum_i w_i g_i(\delta_i^T\Gamma\delta_i) \\ & \qquad + \textstyle\sum_{i,j} w_i e_{ij}(\delta_j-\delta_i)^T\Gamma(\delta_j-\delta_i) \\ & \qquad = \textstyle\sum_{i,j} w_i e_{ij}(\delta_j+\delta_i)^T\Gamma(\delta_j-\delta_i) - \sum_i w_i g_i(\delta_i^T\Gamma\delta_i) \\ & \qquad = \textstyle\sum_{i,j} w_i e_{ij}(\delta_j^T\Gamma\delta_j + \delta_i^T\Gamma\delta_i) - \sum_i w_i g_i(\delta_i^T\Gamma\delta_i) \\ & \qquad = -w^T(L+G)v, \end{aligned} \tag{4.77}$$

where v is a vector composed of elements $v_i = \delta_i^T\Gamma\delta_i \geq 0$. Choosing the positive vector $w > 0$ such that $(L+G)^T w > 0$, which is possible by the properties of nonsingular M-matrices [61], makes this expression (4.77) certainly negative semi-definite in δ, $-w^T(L+G)v \leq 0$; the expression (4.77) being zero iff $v = 0$.

Hence

$$\begin{aligned}\dot{V} = &\textstyle\sum_i \frac{w_i}{c_i}\delta_i^T(PA + A^TP)\delta_i + \delta_i^T\Gamma\delta_i) - \sum_i w_i g_i(\delta_i^T\Gamma\delta_i)\\ &- \textstyle\sum_i \frac{w_i}{c_i^2}(\delta_i^TP\delta_i)\sum_j e_{ij}(\delta_j - \delta_i)^T\Gamma(\delta_j - \delta_i)\\ &- \textstyle\sum_i \frac{w_i}{c_i^2} g_i(\delta_i^TP\delta_i)(\delta_i^T\Gamma\delta_i) + \sum_i \frac{w_i}{c_i^2}(\delta_i^TP\delta_i)\beta_i(c_i - \kappa_i)\\ &- \textstyle\sum_i w_i\beta_i(c_i - \kappa_i).\end{aligned} \tag{4.78}$$

Substituting $PA + A^TP = -Q + \Gamma$ in the first term of (4.78), yields

$$\begin{aligned}\dot{V} = &\textstyle\sum_i \frac{w_i}{c_i}\delta_i^T\Gamma\delta_i - \sum_i \frac{w_i}{c_i^2}(\delta_i^TP\delta_i)\sum_j e_{ij}(\delta_j - \delta_i)^T\Gamma(\delta_j - \delta_i)\\ &- \textstyle\sum_i \frac{w_i}{c_i^2} g_i(\delta_i^TP\delta_i)(\delta_i^T\Gamma\delta_i)\\ &- w^T(L + G)v + \textstyle\sum_i \frac{w_i}{c_i}(\delta_i^TP\delta_i)\beta_i - \sum_i \frac{w_i}{c_i}\delta_i^TQ\delta_i\\ &- \textstyle\sum_i \frac{w_i}{c_i^2}(\delta_i^TP\delta_i)\beta_i\kappa_i - \sum_i w_i\beta_i(c_i - \kappa_i),\end{aligned} \tag{4.79}$$

$$\begin{aligned}\dot{V} = &\textstyle\sum_i \frac{w_i}{c_i}\delta_i^T\Gamma\delta_i - \sum_i \frac{w_i}{c_i^2}(\delta_i^TP\delta_i)\sum_j e_{ij}(\delta_j - \delta_i)^T\Gamma(\delta_j - \delta_i)\\ &- \textstyle\sum_i \frac{w_i}{c_i^2} g_i(\delta_i^TP\delta_i)(\delta_i^T\Gamma\delta_i)\\ &- w^T(L + G)v - \textstyle\sum_i \frac{w_i}{c_i}\delta_i^T(Q + \beta_iP)\delta_i\\ &- \textstyle\sum_i \frac{w_i}{c_i^2}(\delta_i^TP\delta_i)\beta_i\kappa_i - \sum_i w_i\beta_i(c_i - \kappa_i),\end{aligned} \tag{4.80}$$

which for the choice of w so that $w^T(L + G) = \mathbf{1}_p^T$, (i.e., $w^T = \mathbf{1}_p^T(L + G)^{-1}$), simplifies to $w^T(L + G)v = \mathbf{1}_p^Tv = \sum_i \delta_i^T\Gamma\delta_i$, so

$$\begin{aligned}\dot{V} = &\textstyle\sum_i \frac{w_i}{c_i}\delta_i^T\Gamma\delta_i - \sum_i \frac{w_i}{c_i}\delta_i^T(Q + \beta_iP)\delta_i - \sum_i \frac{w_i}{c_i^2}(\delta_i^TP\delta_i)\beta_i\kappa_i\\ &- \textstyle\sum_i \delta_i^T\Gamma\delta_i - \sum_i \frac{w_i}{c_i^2}(\delta_i^TP\delta_i)\sum_j e_{ij}(\delta_j - \delta_i)^T\Gamma(\delta_j - \delta_i)\\ &- \textstyle\sum_i \frac{w_i}{c_i^2} g_i(\delta_i^TP\delta_i)(\delta_i^T\Gamma\delta_i) - \sum_i w_i\beta_i(c_i - \kappa_i),\end{aligned} \tag{4.81}$$

$$\begin{aligned}\dot{V} = &\textstyle\sum_i \delta_i^T\left[\frac{w_i}{c_i}(\Gamma - Q + \beta_iP) - \frac{w_i}{c_i^2}P\beta_i\kappa_i - \Gamma\right]\delta_i - \sum_i w_i\beta_i(c_i - \kappa_i)\\ &- \textstyle\sum_i \frac{w_i}{c_i^2}(\delta_i^TP\delta_i)\sum_j e_{ij}(\delta_j - \delta_i)^T\Gamma(\delta_j - \delta_i)\\ &- \textstyle\sum_i \frac{w_i}{c_i^2} g_i(\delta_i^TP\delta_i)(\delta_i^T\Gamma\delta_i).\end{aligned} \tag{4.82}$$

Lemma 10. *All terms in the time-derivative of the Lyapunov function (4.82), which are quartic in δ_i, vanish iff $\delta_i \in \ker(\Gamma), \forall i$.*

Proof. Assume that all the quartic terms in (4.82) vanish; that includes the summands of the last term in (4.82) containing the pinning gains g_i. Particularly for those to vanish, nodes that are pinned by the leader need to have their $\delta_i \in \ker(\Gamma)$. Further, these nodes subsequently pin to other nodes in the rest

of the graph, which need to have their δ_j such that $(\delta_j - \delta_i) \in \ker(\Gamma)$, making those $\delta_j \in \ker(\Gamma)$ as well, and so on, by Assumption 12, until the ending leafs of all the pinned trees in the spanning forest. Hence necessarily $\delta_i \in \ker(\Gamma)$ for all agents in the entire graph. The converse implication is obvious. □

Proposition 4. *Given* $0 < \beta_i < \frac{\lambda_{\min}(Q)}{\lambda_{max}(P)}$. *Let* $\delta_i \notin \ker(\Gamma), \forall i$, *then the first term of (4.82) is negative, i.e.*

$$\sum_i \delta_i^T \left[\frac{w_i}{c_i}(\Gamma - Q + \beta_i P) - \frac{w_i}{c_i^2} P \beta_i \kappa_i - \Gamma \right] \delta_i \leq 0, \tag{4.83}$$

on the domain $\mathcal{D}$ *if all* $\kappa_i s$ *are sufficiently large.*

Remark 29. The proof of Proposition 4 follows along similar lines as the proof of Proposition 3, hence we omit it here for brevity and only introduce the resulting bound on κ_i for which condition (4.83) is satisfied; that is

$$\kappa_i > \kappa_i^* = \frac{w_i(\lambda_{\max}(\Gamma) - \lambda_{\min}(Q) + \beta_i \lambda_{\max}(P))^2}{4\beta_i \lambda_{\min}(P)\lambda_{\min>0}(\Gamma)}, \quad \forall i. \tag{4.84}$$

4.5.2 Stability analysis

Starting from expression (4.82), Lemma 10 and Proposition 4 we bring here the main results on dynamics (4.72, 4.73).

Theorem 14. *Consider a network of* p *agents with the general LTI dynamics (4.23) satisfying Assumption 12. Let each agent implement the control input (4.70) with the coupling gain dynamics (4.71) and let* $0 < \beta_i < \frac{\lambda_{\min}(Q)}{\lambda_{max}(P)}, \forall i$. *Then the agents' states reach an agreement with the leader's state within some bounded region, i.e., their trajectories are UUB, on domain* $\mathcal{D}$, *if all* $\kappa_i s$ *are sufficiently large, satisfying the bound*

$$\sum_{i=2}^{p} \left[\frac{w_i}{c_i^*}(\Gamma - Q + \beta_i P) - \frac{w_i}{{c_i^*}^2} P \beta_i \kappa_i \right] < p\Gamma. \tag{4.85}$$

Remark 30. Note, that by assuming one common $\beta = \beta_i, \forall i$, inequality (4.85) can be stated uniformly for all agents as

$$\frac{w_{\max}}{c_{\min}^*}(\Gamma - Q + \beta P) - \frac{w_{\min}}{{c_{\max}^*}^2} P \beta \kappa_{\min} < \frac{p}{(p-1)}\Gamma. \tag{4.86}$$

Theorem 15. *Consider Theorem 14 and in addition assume that all* $\kappa_i s$ *satisfy the bound (4.84), then the agents' states fully synchronize with the leader's, i.e.,* $\lim_{t\to\infty} \|x_i(t) - x_0(t)\| = 0, \forall i$. *Moreover every* $c_i(t)$ *converges to* κ_i.

The proofs of Theorems 14 and 15 proceed from the time-derivative of the Lyapunov function (4.82), Lemma 10, and Proposition 4 along similar lines as in the irreducible graph case for Theorems 12 and 13, respectively, by examining the pertinent worst-case scenarios. Here the role of non-vanishing quartic terms is taken by the quartic terms containing the pinning gain, g_i, or the terms stemming from the leaf nodes. We omit the proofs for brevity. Note, that the comments of Remark 27 on the network stability apply here as well.

4.6 Reference estimation mechanism

Building on results of previous sections which guarantee that for κ_is sufficiently large one has convergence and for other κ_is only UUB, this section brings the κ_i estimation mechanism based on real-time observation of the actual behavior of the network. The estimation of κ_is determines the stability of the network of agents implementing the adaptive consensus protocol. Each agent runs an estimation algorithm to obtain its κ_i. Since c_i is pushed to κ_i by the c_i dynamics, each agent seemingly estimates its c_i. This applies to both developments in Sections 4.4 and 4.5, addressing cooperative regulator and tracker problems.

Remark 31. From the proposed Lyapunov analysis in Sections 4.4.3 and 4.5.2, it follows that any choice of constant c_is would lead to a more conservative bound for those c_is, than the bound for pertaining κ_is; as in that case, the beneficial effect of c_i dynamics on the time-derivative of the Lyapunov function would be absent.

To estimate the value of such κ_is, previous results [36, 37] introduce two algorithms: the interval-halving estimation algorithm [36] applicable to both directed and undirected graphs and the eigenvalue estimation algorithm [37] appropriate for undirected graphs. They are briefly summarized in the following two sections. The reader is pointed to [36, 37], for more details.

4.6.1 Interval-halving estimation algorithm

The interval-halving mechanism for estimation of κ_i is stated in Algorithm 4.1. It updates the value of κ_i as long as the trajectory of the network dynamics exhibits oscillations, i.e., as long as it is only UUB. From a single-agent perspective, the oscillating trajectory implies oscillating coupling gain, therefore the coupling gain c_i is sampled at a sampling frequency f_s and recorded in a time window Δt. The highest and the lowest recorded values are averaged and this average is then used as a new value of κ_i. This process is periodically repeated. The coupling gains, c_is, stop oscillating when the κ_is get sufficiently large and the trajectory of the network dynamics converges. The κ_is then also reach their steady-state values.

Algorithm 4.1 Interval-halving algorithm for determination of κ_i

- **Parameters:** sampling frequency f_s and time windows $\triangle t$.
- **Variables:** sampling buffer c_B of size $\triangle t \cdot f_s$.
- **Initialization:** Fill c_B with samples of c_i, sampled at f_s.

1: Record a sample of c_i into c_B at the sampling frequency f_s.
2: Calculate the new $\kappa_i = (\max(c_B) + min(c_B))/2$.
3: Repeat from 1.

Remark 32. Note, that the interconnection of Algorithm 4.1 and the adaptive consensus protocol creates a hybrid system. To handle changes of the network topology, e.g., of adding or dropping an agent, Algorithm 4.1 is reinitialized and c_is are set to their initial values after each network change. Since an agent can detect changes in its neighborhood and forward this information to other agents in the network, the reinitialization is fully distributed. A dead-zone is used in updating κ_is to handle measurement noise.

4.6.2 Eigenvalue estimation algorithm

The eigenvalue estimation algorithm is based on the estimation of Laplacian eigenvalues in multi-agent systems [17, 18], applicable only to undirected graphs. Each agent estimates the Laplacian eigenvalues by performing an algorithm with the following updating rule

$$\begin{aligned} \dot{r}_i(t) &= -\xi \textstyle\sum_j e_{ij}(t)\left(q_i(t) - q_j(t)\right), \\ \dot{q}_i(t) &= \xi \textstyle\sum_j e_{ij}(t)\left(r_i(t) - r_j(t)\right), \end{aligned} \tag{4.87}$$

where $\xi > 0$ is a constant parameter and $r_i, q_i \in \mathbb{R}$ are artificial states of the ith agent eigenvalue estimator. Following from [17], each pair of states r_i, q_i oscillates as a linear combination of sinusoids with frequencies $f_k = \xi\lambda_k(L), k \in \{1, 2, \ldots, p\}$. Using the Fast Fourier Transformation, each agent can independently estimate these frequencies f_k and thereby the non-zero eigenvalues of Laplacian matrix $\lambda_k(L)$. The new κ_i value is then calculated as

$$\kappa_i = \frac{1}{2\lambda_{\min>0}(L)}, \tag{4.88}$$

where $\lambda_{\min>0}(L)$ is the smallest non-zero estimated eigenvalue of L. This formula is adopted from the stability condition of a static consensus protocol. [76] In summary, to estimate the value of κ_i, each agent performs steps given in Algorithm 4.2.

Remark 33. If the agents correctly estimate the smallest non-zero eigenvalue of the Laplacian matrix the network of agents should reach convergence. On the

Algorithm 4.2 Eigenvalue estimation algorithm for determination of κ_i

- **Parameters:** constant $\xi > 0$, sampling frequency f_s, time windows $\triangle t$.
- **Variables:** sampling buffer c_B of size $\triangle t \cdot f_s$, estimated frequencies f_k.
- **Initialization:** Generate the initial conditions $r_i(0), q_i(0) \in \{-1, 1\}$.

1: Perform the state updating rule (4.87).
2: In a time window $\triangle t$, estimate the frequencies f_k of sinusoids of agent's artificial state r_i or q_i.
3: Calculate the smallest non-zero estimated eigenvalue of L as $\lambda_{\min>0}(L) = \min_k(f_k)/\xi$.
4: Use $\lambda_{\min>0}(L)$ to calculate the new κ_i from (4.88).
5: Repeat from 1.

other hand, if this eigenvalue is unobservable for some agents and they estimate different eigenvalue instead of the smallest non-zero one, the adaptive control protocol still guarantees UUB.

Remark 34. Algorithm 4.2 is found robust to changes of the network topology and to measurement noise, while Algorithm 4.1 requires an additional detection of a change in the network topology and a dead-zone to handle measurement noise. Moreover, different from Algorithm 4.1, Algorithm 4.2 decouples the κ_i estimator from the control law, hence they can be designed separately. Nevertheless, on large-scale networks, Algorithm 4.2 leads to higher κ_is and thereby c_is than Algorithm 4.1. Thus, for a special case of undirected graphs, Algorithm 4.2 outperforms Algorithm 4.1 on small networks only. For a thorough comparison of the both approaches see simulations in the following section.

4.7 Numerical simulations

This section brings simulations of the proposed adaptive consensus protocol solving both cooperative control problems on directed and undirected graphs. The agents are double-integrators, described by a general LTI dynamics (4.23), with

$$A = \begin{bmatrix} 0 & 1 \\ 0 & 0 \end{bmatrix}, \quad B = \begin{bmatrix} 0 \\ 1 \end{bmatrix}, \quad x_i = \begin{bmatrix} x_{i_1} \\ x_{i_2} \end{bmatrix}, \quad \forall i, \tag{4.89}$$

where x_{i_1} and x_{i_2} represent respectively the position and velocity of the ith agent. Design matrices Q and R are chosen as identity matrices of appropriate dimension. Each κ_i is initialized to $c_i(0)$, $\forall i$. Initial conditions of the agents are chosen as follows

$$x_{i_1}(0) \in \langle -10, 10 \rangle, \quad x_{i_2}(0) = 0, \quad c_i(0) = 0.01, \quad \forall i, \tag{4.90}$$

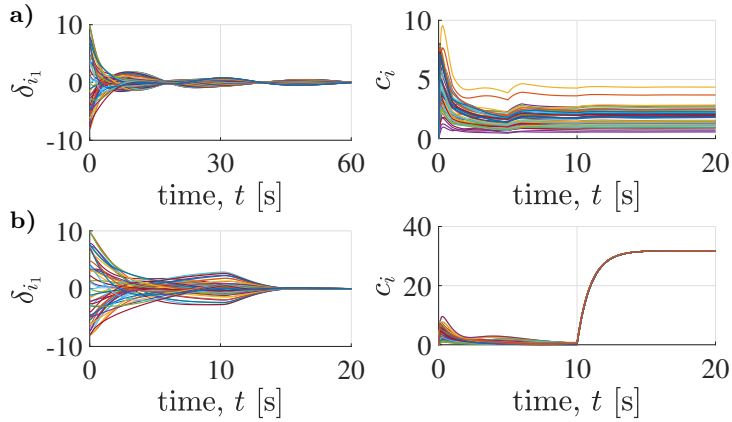

Figure 4.4: Simulations of the proposed protocol (4.24, 4.25) with **a)** Algorithm 4.1 and **b)** Algorithm 4.2 on an undirected circle consisting of 50 agents.

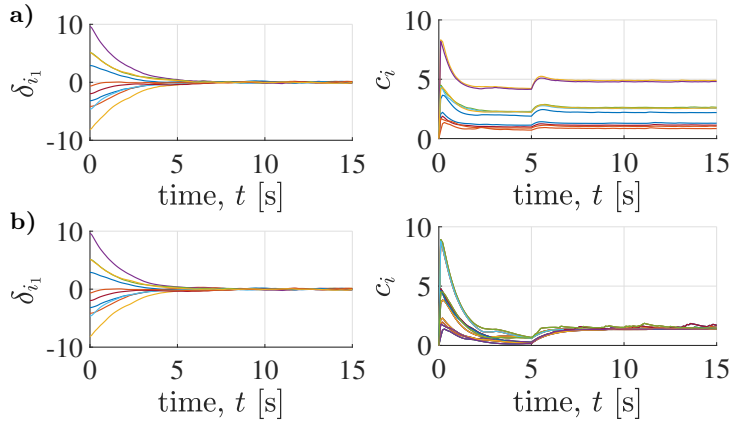

Figure 4.5: Simulations of the proposed protocol (4.24, 4.25) with **a)** Algorithm 4.1 and **b)** Algorithm 4.2 on an undirected circle consisting of 10 agents with noise in state measurements.

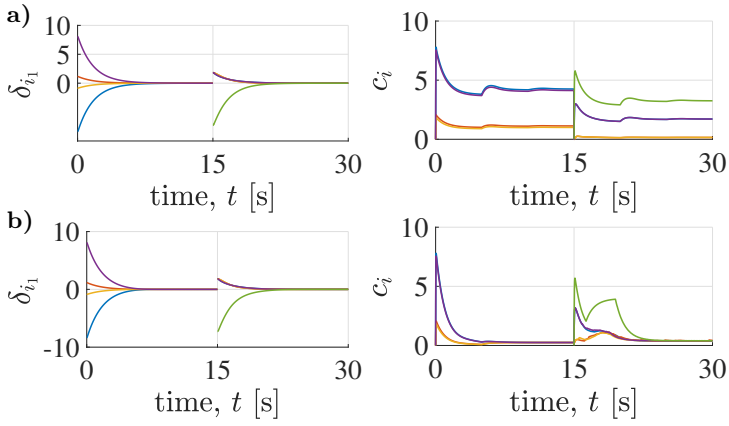

Figure 4.6: Simulations of the proposed protocol (4.24, 4.25) with **a)** Algorithm 4.1 and **b)** Algorithm 4.2 for a change in the graph topology as depicted in Figure 4.8.

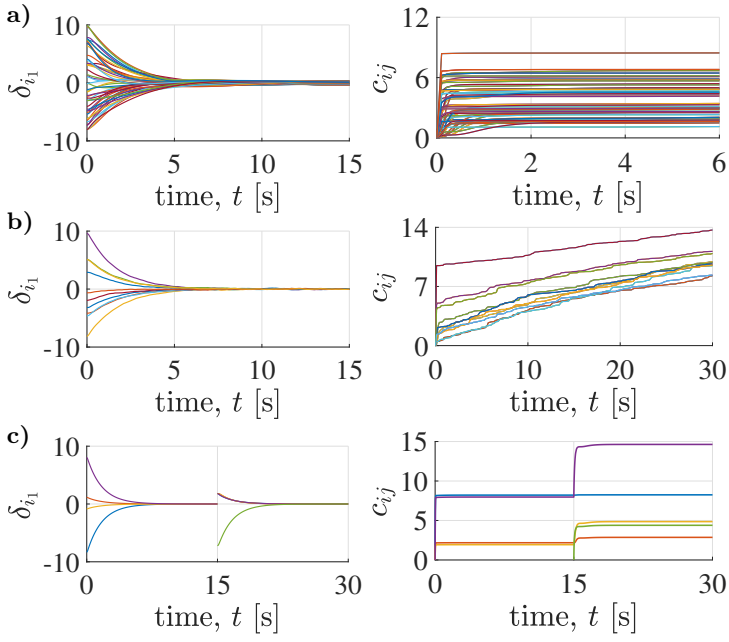

Figure 4.7: Simulation of an existing adaptive consensus protocol from the literature [46] on an undirected circle consisting of **a)** 50 agents; **b)** 10 agents with noise in state measurements **c)** 5 agents with a change in the graph topology, (see Figure 4.8).

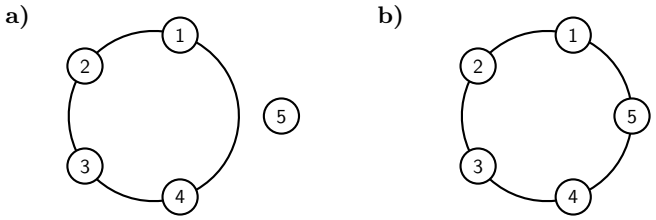

Figure 4.8: Change of the topology from **a)** to **b)** at $t = 15$ s.

where states x_{i_1} are chosen randomly in the range $\langle -10, 10 \rangle$. In figures, δ_{i_1} denotes the position error corresponding to the state x_{i_1}. The positive constants β_i are set to

$$\beta_i = \beta = 0.9 \frac{\lambda_{\min}(Q)}{\lambda_{max}(P)}, \quad \forall i. \tag{4.91}$$

Simulations of the adaptive consensus protocol (4.24, 4.25) solving the cooperative regulator problem on undirected circular communication graphs are depicted in Figures 4.4, 4.5, and 4.6. The protocol uses both Algorithm 4.1 and 4.2 from Section 4.6. For their comparison, each figure shows two simulations a) and b) corresponding to these estimation algorithms. Algorithm 4.1 is configured to the time window $\triangle t = 5$ s and the sampling frequency $f_{s1} = 10$ Hz. Algorithm 4.2 is configured to $f_{s1} = 50$ Hz. Figure 4.4 shows the simulations on an undirected circle consisting of 50 agents. In this simulation, Algorithm 4.2 uses $\triangle t = 10$ s. Assuming noise acting on state measurements, the responses of 10 agents in an undirected circular topology are plotted in Figure 4.5. Figure 4.6 shows the responses of 5 agents to a change in the network topology. At the time instant of 15 seconds the graph topology is switched from an undirected circle of 4 synchronized agents to an undirected circle of 5 agents, as depicted in Figure 4.8. In simulations shown on Figure 4.5 and 4.6, Algorithm 4.2 uses the estimation period $\triangle t = 5$ s. Simulations of an existing adaptive consensus protocol from the literature [46] are shown in Figure 4.7, for comparison.

Remark 35. Comparison of Figure 4.4 and 4.5, demonstrates that Algorithm 4.1 attains lower c_i values, than Algorithm 4.2 while preserving stability on large-scale networks. Thereby Algorithm 4.2 outperforms Algorithm 4.1 only on smaller networks. Furthermore, from Figures 4.5 and 4.6 follows, that the proposed protocol (4.24, 4.25) implemented with both Algorithm 4.1 and 4.2 is found to be robust to measurement noise and changes of the network topology. Moreover, by comparison to the simulations shown in Figure 4.7, at least in some situations, it attains lower c_i values than the existing adaptive consensus protocol from the literature [46].

Figures 4.9 and 4.10 show simulations solving the cooperative regulator and tracker problems, respectively, on directed communication graphs. The

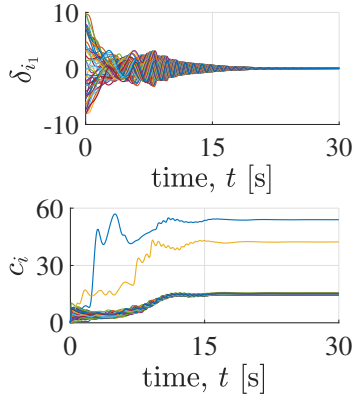

Figure 4.9: Simulation of the proposed protocol (4.24, 4.25) with Algorithm 4.2 on a directed graph consisting of two interconnected circles as depicted in Figure 4.10.

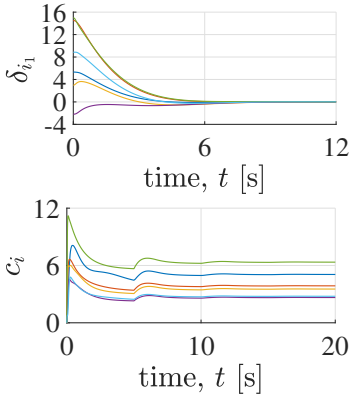

Figure 4.11: Simulation of the proposed protocol (4.70, 4.71) with Algorithm 4.2 on a directed graph consisting of 6 agents following a leader as depicted in Figure 4.12.

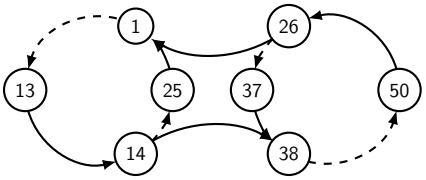

Figure 4.10: A directed graph consisting of two interconnected circles, each having 25 agents.

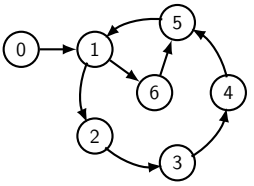

Figure 4.12: A directed graph consisting of 6 agents $\{1, 2, \ldots, 6\}$ and a leader $\{0\}$.

graph topologies are depicted correspondingly in Figures 4.11 and 4.12. For the cooperative regulator problem, the adaptive consensus protocol (4.24, 4.25) uses Algorithm 4.1 configured to $f_{s1} = 25$ Hz, $\triangle t = 2$ s, while for the cooperative tracker problem the adaptive consensus protocol (4.70, 4.71) uses Algorithm 4.1 with $f_{s1} = 10$ Hz, $\triangle t = 5$ s.

Remark 36. Although it has been proven that UUB is guaranteed for κ_is sufficiently large, satisfying the bound (4.61) for cooperative regulator problem or the bound (4.85) for cooperative tracker problem, simulations show that UUB is found, in fact, for any choice of κ_is. The bounds (4.61) and (4.85) are only sufficient but not necessary. In considered examples, using any positive κ_is one achieves UUB or even convergence for κ_i values lower than required by the Theorem 12 and 14.

4.8 Concluding remarks

This chapter introduced a novel distributed adaptive consensus protocol for multi-agent systems that solves the cooperative regulator and tracker problems on general directed graphs. The protocol incorporates a novel coupling gain dynamics allowing feedback coupling gains to decay to some estimated reference values. These reference values are updated on-line, in real-time, by one of the two proposed estimation algorithms. Due to decay, the coupling gains in some situations attain lower values than in existing adaptive consensus protocols proposed in the literature. Moreover, the presented adaptive protocol design provides a unified approach to both cooperative control problems on undirected as well as on directed communication networks. Agents in the network design and implement their controls in a fully distributed manner based only on their local information and information from their neighbors. Additionally, in combination with the estimation algorithms, the proposed protocol exhibits robustness to measurement noise and changes of the network topology. A thorough stability analysis of the adaptive control law is provided. The uniform ultimate boundedness and convergence of the agents' trajectories are thus rigorously proven. Numerical simulations validate the theoretical results.

5

Final conclusion

This thesis brings two complementary approaches for distributed control and estimation in networked multi-agent systems. They are originally introduced in our previous work, [38, 39]. Both approaches consider agents with general LTI dynamics and communication networks given by a general directed graph.

The first distributed approach, presented in Chapter 3, brings a distributed Luenberger-like observer [39], similar to [80], which considers process noises acting on the plant's states and measurement noises corrupting the sensors' measurements, similarly as the general Kalman filter [42] and DKF in [55] do. Thereby, the observer achieves some required properties of both DLO and DKF designs. The observer does not aim for optimality of the Kalman filter but rather for a suboptimal albeit easier to implement distributed Luenberger-like observer design that achieves reasonable sensor fusion by taking into account precision of available measurements. It primarily addresses state estimation of large-scale systems represented by flexible structures. To avoid difficulties of DKFs with large communication load, especially on large-scale networks, it does not directly communicate the covariance matrices between nodes. Each node in the sensor network implements a local micro-Kalman filter to achieve sensor fusion. Only partial observability from a single-node perspective is assumed by the observer. Moreover, the observer allows for existence of nodes that do not measure anything but contribute to sensor fusion. In addition, it allows for insertion of redundant nodes into the network. This increases robustness to node and communication link failures. Structured Lyapunov functions are used to prove stability of the distributed observer. The functionality and required properties of the distributed observer design are validated by simulations.

The second distributed approach, given in Chapter 4, presents a novel DACP [38] proposing a simple, unified framework for the cooperative regulator and tracker problems. The protocol implements an adaptive control law that

adapts coupling gains and allows them to decay to lower values. To be more specific, coupling gains are being adapted by a modified coupling gain dynamics containing an additional decay term, which pushes the coupling gains to their reference values. These coupling gains' references are estimated on-line from the network trajectories by one of the two proposed estimation algorithms: Algorithm 4.2, based on estimation of Laplacian eigenvalues, [17, 18], and Algorithm 4.1, based on interval halving. Algorithm 4.1 applies to both undirected and directed graphs, while Algorithm 4.2 works on undirected graphs only. Benefit of Algorithm 4.2, in contrast to Algorithm 4.1, is that it fully decouples the adaptation of coupling gains from estimation of their references. The decay of coupling gains to their references solves the problems of existing DACPs, [69, 75, 46, 47], with unbounded or overly large coupling gain values. Moreover, the estimation of coupling gain references with an estimation algorithm improves robustness of the DACP to noise or disturbances. Nonetheless, different from the celebrated static consensus protocols, [45, 76, 77], the proposed DACP does not require any centralized information for its design, similarly as other DACPs; hence, it is fully distributed. Thorough stability analysis of the DACP is carried out and the stability of the network is proven using Lyapunov function techniques. Provided numerical simulations validate the functionality of the DACP and compare its performance with an existing DACP [46] from the literature.

5.1 Fulfillment of the goals

Goal 1 of this thesis, stated in Section 1.2, is fulfilled by the distributed Luenberger-like observer design for sensor networks, [39], presented in Sections 3.3, 3.4, and 3.5. According to the design procedure detailed in Section 3.5, the distributed observer considers process disturbance acting on the plat state and measurement noises corrupting the sensors' measurements. Thereby, the distributed observer satisfies requirement 1a. Furthermore, under Assumption 9 in Section 3.3, it provides robustness to node or communication link failures; hence it fits requirement 1b. Since the proposed estimation approach does not communicate covariance-related matrices, it provides lower communication burden than existing distributed estimation approaches, as discussed in Section 3.2. The overall performance of the communication was not further analyzed; therefore, the proposed approach only partially satisfies the last requirement 1c.

Goal 2 of this thesis, stated in Section 1.2, is fulfilled by the DACP, [38], presented in Section 4.4. According to the adaptive law for adaptation of coupling gains (4.25), the coupling gains can decay to their reference values; thereby, the DACP satisfies requirement 2c. The DACP design provides a unified approach to both cooperative regulator and tracker problems, as presented in Section 4.4 and 4.5, respectively, thus satisfying requirement 2b. Since

this approach does not require any centralized information for its design and implementation, it is fully distributed; hence it meets requirement 2a. The lack of the centralized information is compensated by its estimation. For this purpose, two estimation algorithms are developed, which is done beyond the main requirements. These algorithms are described in Section 4.6.

Further details on the fulfillment of this thesis's goals from Section 1.2 are given by the main contributions in Sections 3.2 and 4.2.

5.2 Future research

One of the tasks for future research is to derive the UUB bound on the synchronization error for the DACP in Chapter 4, and compare this bound with those existing in the literature, [50, 11]. The existing DACP designs [50, 11] suffer from a drawback stemming from one common static reference for coupling gains. This causes the UUB bound on the synchronization error to depend on network properties, which are considered as centralized information. Hence, one expects the performance of the DACPs in [50, 11] to vary with the network configuration, which is usually not required. According to the DACP design in Chapter 4, each agent has its own coupling gain's reference value, which might avoid the above-mentioned drawback of existing DACPs; however, this was not verified yet, and, therefore, it is a task for future research.

A further extension of the proposed distributed Luenberger-like observer in Chapter 3 is offered by DACPs. Namely, the adaptive law in Chapter 4 can be used for the adaptation of network feedback coupling gains to achieve a fully distributed observer design. Following this scenario, each node adapts its coupling gain given by a positive scalar γ_i, which replaces the current design parameter γ common for all nodes. The design of the distributed observer summarized in Algorithm 3.2 assumes γ sufficiently large to satisfy the lower bounds (3.83) and (3.84). Since both bounds depend on network properties, which need to be known at least to a certain extent, the design of the observer is not fully distributed. The adaptation of coupling gains solves this problem. Extending the distributed observer in Chapter 3 with the distributed adaptive law in Chapter 4 leads to a fully distributed adaptive Luenberger-like observer. The main tasks for the future research are to investigate stability of such a distributed observer, prove its convergence, and validate its performance in numerical simulations.

Note that there already exist results on decentralized/distributed estimators incorporating the adaptation of coupling gains. For example, the authors in [15] propose a design of adaptive consensus filters for estimation of distributed parameter systems using a sensor network. The sensor network consists of groups of sensors, where each group of sensors belongs to a filter implementing a local Luenberger observer. Each consensus filter implements an adaptive law

for adaptation of the feedback weighting gains. The sensor fusion is used to fuse the estimates of all filters in the network with appropriate weighting. The plant has to be fully observable by each filter individually; therefore, every filter can fully estimate states of the plant. Moreover, the proposed approach considers an all to all coupling of filters, which requires a full communication graph. This is different from distributed estimator in Chapter 3, which assumes only partial observability by each single agent on general directed communication graphs.

Bibliography

[1] I. Akyildiz, Weilian Su, Y. Sankarasubramaniam, and E. Cayirci, "A survey on sensor networks," *IEEE Communications Magazine*, vol. 40, no. 8, pp. 102–114, 2002.

[2] P. J. Antsaklis and A. N. Michel, *A Linear Systems Primer*. Boston, MA: Birkhäuser, 2007.

[3] M. Arcak, "Passivity as a design tool for group coordination," *IEEE Transactions on Automatic Control*, vol. 52, no. 8, pp. 1380–1390, 2007.

[4] R. Baheti and H. Gill, "Cyber-physical Systems, The Impact of Control Technology," *IEEE Control Systems Society*, 2011.

[5] S. Barbarossa, S. Sardellitti, and P. D. Lorenzo, "Chapter 7. Distributed Detection and Estimation in Wireless Sensor Networks," in *Academic Press Library in Signal Processing*, 2013, pp. 329–408.

[6] A. Bemporad, M. Heemels, and M. Johansson, *Networked Control Systems, Lecture Notes in Control and Information Sciences*. London: Springer, 2010.

[7] A. Bidram, F. L. Lewis, and A. Davoudi, "Distributed control systems for small-scale power networks: Using multiagent cooperative control theory," *IEEE Control Systems*, 2014.

[8] N. Biggs, *Algebraic graph theory*. Cambridge, UK: Cambridge University Press, 1974.

[9] J. W. Brewer, "Kronecker Products and Matrix Calculus in System Theory," *IEEE Transactions on Circuits and Systems*, vol. 25, no. 9, pp. 772–781, 1978.

[10] Y. Cao, W. Yu, W. Ren, and G. Chen, "An overview of recent progress in the study of distributed multi-agent coordination," *IEEE Transactions on Industrial Informatics*, vol. 9, no. 1, pp. 427–438, 2013.

[11] B. Cheng and Z. Li, "Fully Distributed Event-Triggered Protocols for Linear Multi-agent Networks," *IEEE Transactions on Automatic Control*, vol. 64, no. 4, pp. 1655–1662, 2018.

[12] N. Chopra and M. W. Spong, "Passivity-Based Control of Multi-Agent Systems," in *Advances in Robot Control, from everyday physics to human-like movements*. Urbana, IL: Coordinated Science Laboratory, University of Illinois at Urbana-Champaign, 2006, pp. 107–134.

[13] G. Cooray, "The Kuramoto Model," Tech. Rep., 2008.

[14] A. Das and F. L. Lewis, "Distributed adaptive control for synchronization of unknown nonlinear networked systems," *Automatica*, vol. 46, no. 12, pp. 2014–2021, 2010.

[15] M. A. Demetriou, "Design of consensus and adaptive consensus filters for distributed parameter systems," *Automatica*, vol. 46, no. 2, pp. 300–311, 2010.

[16] J. Fax and R. Murray, "Information Flow and Cooperative Control of Vehicle Formations," *IEEE Transactions on Automatic Control*, vol. 49, no. 9, pp. 1465–1476, 2004.

[17] M. Franceschelli, A. Gasparri, A. Giua, and C. Seatzu, "Decentralized laplacian eigenvalues estimation for networked multi-agent systems," *Proceedings of the IEEE Conference on Decision and Control*, pp. 2717–2722, 2009.

[18] M. Franceschelli, A. Gasparri, A. Giua, and C. Seatzu, "Decentralized estimation of Laplacian eigenvalues in multi-agent systems," *Automatica*, vol. 49, no. 4, pp. 1031–1036, 2013.

[19] F. Garin and L. Schenato, *A Survey on Distributed Estimation and Control Applications Using Linear Consensus Algorithms*. London, UK: Springer, 2010.

[20] W. K. Gawronski, *Advanced Dynamics and Active Control of Structures*. New York, NY: Springer, 2004.

[21] C. Godsil and G. Royle, *Algebraic Graph Theory*. New York, NY: Springer, 2001.

[22] K. Hengster-Movric and F. L. Lewis, "Cooperative observers and regulators for discrete-time multiagent systems," *International Journal of Robust and Nonlinear Control*, vol. 23, no. 14, pp. 1545–1562, 2013.

[23] K. Hengster-Movric, M. Sebek, and S. Celikovsky, "Structured Lyapunov Functions for Synchronization of Identical Affine-in-control Agents – Unified Approach," *Journal of the Franklin Institute*, vol. 353, no. 14, pp. 3457–3486, 2016.

[24] I. Herman, Š. Knotek, V. Prajzner, S. Knotek, J. Dostal, and V. Prajzner, "Stability of hydronic networks with independent zone controllers," *IEEE Transactions on Control Systems Technology*, 2017.

[25] R. A. Horn and C. R. Johnson, *Matrix Analysis*. Cambridge, UK: Cambridge University Press, 1985.

[26] R. A. Horn and C. R. Johnson, *Topics in matrix analysis*. Cambridge, UK: Cambridge University Press, 1991.

[27] A. Jadbabaie and A. Morse, "Coordination of groups of mobile autonomous agents using nearest neighbor rules," *IEEE Transactions on Automatic Control*, vol. 48, no. 6, pp. 988–1001, 2003.

[28] A. H. Jazwinski, *Stochastic Processes and Filtering Theory*. New York, NY, and London, UK: Academic Press, 1970.

[29] H. Ji, F. L. Lewis, Z. Hou, and D. Mikulski, "Distributed information-weighted Kalman consensus filter for sensor networks," *Automatica*, vol. 77, pp. 18–30, 2017.

[30] R. E. Kalman, "On the general theory of control systems," *IEEE Transactions on Automatic Control*, vol. 4, no. 3, pp. 110 – 110, 1959.

[31] S. K. Khaitan and J. D. McCalley, "Design techniques and applications of cyberphysical systems: A survey," *IEEE Systems Journal*, vol. 9, no. 2, pp. 350–365, 2015.

[32] H. Khalil, *Nonlinear Systems*, 2nd ed. Upper Saddle River, NJ: Prentice-Hall, 1996.

[33] J. Kim, H. Shim, and J. Wu, "On distributed optimal Kalman-Bucy filtering by averaging dynamics of heterogeneous agents," *Proceedings of the IEEE Conference on Decision and Control*, 2016.

[34] T. Kim, H. Shim, and D. D. Cho, "Distributed Luenberger observer design," *Proceedings of the IEEE Conference on Decision and Control*, 2016.

[35] S. Knotek, "Fully distributed adaptive consensus protocol with bounded gains," *Proceedings of the International Student Conference on Electrical Engineering*, 2016.

[36] S. Knotek, K. Hengster-Movric, and M. Sebek, "Distributed adaptive consensus protocol with decaying gains on directed graphs," *Proceedings of the IFAC Workshop on Distributed Estimation and Control in Networked Systems*, vol. 49, no. 22, 2016.

[37] S. Knotek, K. Hengster-Movric, and M. Sebek, "Distributed adaptive consensus protocol with Laplacian eigenvalues estimation," *Proceedings of the 21st International Conference on Process Control*, pp. 269–273, 2017.

[38] S. Knotek, K. Hengster-Movric, and M. Sebek, "Distributed adaptive consensus protocol with decaying gains," *International Journal of Robust and Nonlinear Control*, vol. 30, no. 15, pp. 6166– 6188, 2020.

[39] S. Knotek, K. Hengster-Movric, and M. Sebek, "Distributed Estimation on Sensor Networks with Measurement Uncertainties," *IEEE Transactions on Control Systems Technology*, pp. 1–15, 2020.

[40] J. Lee, B. Bagheri, and H. A. Kao, "A Cyber-Physical Systems architecture for Industry 4.0-based manufacturing systems," *Manufacturing Letters*, vol. 3, pp. 18–23, 2015.

[41] N. Levinson, "The Wiener (Root Mean Square) Error Criterion in Filter Design and Prediction," *Journal of Mathematics and Physics*, vol. 25, no. 1-4, pp. 261–278, apr 1946.

[42] F. L. Lewis, L. Xie, and D. Popa, *Optimal and Robust Estimation: With an Introduction to Stochastic Control Theory, Second Edition.* Boca Raton, FL: CRC Press, 2007.

[43] F. L. Lewis, H. Zhang, K. Hengster-Movric, and A. Das, *Cooperative Control of Multi-Agent Systems.* London, UK: Springer, 2014.

[44] Z. Li, M. Z. Chen, and Z. Ding, "Distributed adaptive controllers for cooperative output regulation of heterogeneous agents over directed graphs," *Automatica*, vol. 68, pp. 179–183, 2016.

[45] Z. Li, Z. Duan, G. Chen, and L. Huang, "Consensus of Multiagent Systems and Synchronization of Complex Networks: A Unified Viewpoint," *IEEE Transactions on Circuits and Systems I: Regular Papers*, vol. 57, no. 1, pp. 213–224, 2010.

[46] Z. Li, W. Ren, X. Liu, and M. Fu, "Consensus of Multi-Agent Systems With General Linear and Lipschitz Nonlinear Dynamics Using Distributed Adaptive Protocols," *IEEE Transactions on Automatic Control*, vol. 58, no. 7, pp. 1786–1791, 2013.

[47] Z. Li, G. Wen, Z. Duan, and W. Ren, "Designing fully distributed consensus protocols for linear multi-agent systems with directed graphs," *IEEE Transactions on Automatic Control*, vol. 60, no. 4, pp. 1152–1157, 2015.

[48] D. G. Luenberger, "Observing the State of a Linear System," *IEEE Transactions on Military Electronics*, vol. 8, no. 2, pp. 74–80, 1964.

[49] J. Lunze, *Control theory of digitally networked dynamic systems*. Heidelberg: Springer, 2014.

[50] Y. Lv, Z. Li, Z. Duan, and J. Chen, "Distributed adaptive output feedback consensus protocols for linear systems on directed graphs with a leader of bounded input," *Automatica*, vol. 74, pp. 308–314, 2016.

[51] H. Min, F. Sun, S. Wang, and H. Li, "Distributed adaptive consensus algorithm for networked Euler-Lagrange systems," *IET Control Theory & Applications*, vol. 5, no. 1, pp. 145–154, 2011.

[52] W. Ni and D. Cheng, "Leader-following consensus of multi-agent systems under fixed and switching topologies," *Systems & Control Letters*, vol. 59, no. 3-4, pp. 209–217, 2010.

[53] K. K. Oh, M. C. Park, and H. S. Ahn, "A survey of multi-agent formation control," *Automatica*, vol. 53, pp. 424–440, 2015.

[54] R. Olfati-Saber, "Distributed Kalman Filter with Embedded Consensus Filters," *Proceedings of the IEEE Conference on Decision and Control*, vol. 2005, pp. 8179–8184, 2005.

[55] R. Olfati-Saber, "Distributed Kalman filtering for sensor networks," *Proceedings of the IEEE Conference on Decision and Control*, pp. 5492–5498, 2007.

[56] R. Olfati-Saber, "Kalman-Consensus filter: Optimality, stability, and performance," *Proceedings of the IEEE Conference on Decision and Control*, pp. 7036–7042, 2009.

[57] R. Olfati-Saber, J. A. Fax, and R. M. Murray, "Consensus and Cooperation in Networked Multi-Agent Systems," *Proceedings of the IEEE*, vol. 95, no. 1, pp. 215–233, 2007.

[58] R. Olfati-Saber and R. M. Murray, "Consensus problems in networks of agents with switching topology and time-delays," *IEEE Transactions on Automatic Control*, vol. 49, no. 9, pp. 1520–1533, 2004.

[59] R. Olfati-Saber and J. S. Shamma, "Consensus Filters for Sensor Networks and Distributed Sensor Fusion," *Proceedings of the IEEE Conference on Decision and Control*, pp. 6698–6703, 2005.

[60] L. Orihuela, P. Millán, C. Vivas, and F. R. Rubio, "Distributed Control and Estimation Scheme With Applications to Process Control," *IEEE Transactions on Control Systems Technology*, vol. 23, no. 4, pp. 1563–1570, 2015.

[61] Z. Qu, *Cooperative Control of Dynamical Systems*. London, UK: Springer, 2008.

[62] B. Rao and H. Durrant-Whyte, "Fully decentralised algorithm for multisensor Kalman filtering," in *IEEE Proceedings D - Control Theory and Applications*, 1991, vol. 138, no. 5, pp. 413–420.

[63] B. Rao, H. Durrant-Whyte, and J. Sheen, "A Fully Decentralized Multi-Sensor System For Tracking and Surveillance," *International Journal of Robotics and Research*, vol. 12, no. 1, pp. 20–24, 1993.

[64] W. Ren, R. W. Beard, and E. M. Atkins, "Information Consensus in Multivehicle Cooperative Control," *IEEE Control Systems Magazine*, vol. 27, no. 2, pp. 71–82, 2007.

[65] D. Simon, *Optimal State Estimation: Kalman, H∞, and Nonlinear Approaches*. Hoboken, NJ: John Wiley & Sons, 2006.

[66] J.-J. E. Slotine and W. Li, *Applied Nonlinear Control*. Englewood Cliffs, NJ: Prentice hall, 1991.

[67] D. P. Spanos, R. Olfati-saber, and R. M. Murray, "Dynamic consensus on mobile networks," *Proceedings of the IFAC World Congress*, 2005.

[68] J. L. Speyer, "Computation and Transmission Requirements for a Decentralized Linear-Quadratic-Gaussian Control Problem," *IEEE Transactions on Automatic Control*, vol. 24, no. 2, pp. 266–269, 1979.

[69] H. Su, G. Chen, X. Wang, and Z. Lin, "Adaptive second-order consensus of networked mobile agents with nonlinear dynamics," *Automatica*, vol. 47, no. 2, pp. 368–375, 2011.

[70] S. Sun, H. Lin, J. Ma, and X. Li, "Multi-sensor distributed fusion estimation with applications in networked systems: A review paper," *Information Fusion*, vol. 38, pp. 122–134, 2017.

[71] J. W. Tukey and N. Wiener, "The Extrapolation, Interpolation and Smoothing of Stationary Time Series with Engineering Applications." *Journal of the American Statistical Association*, vol. 47, no. 258, pp. 319–321, 1952.

[72] F.-Y. Wang and D. Liu, *Networked Control Systems*. London, UK: Springer, 2008.

[73] S. Wasserman and K. Faust, *Social network analysis: methods and applications*. Cambridge, UK: Cambridge University Press, 1994.

[74] H. Yu and X. Xia, "Adaptive consensus of multi-agents in networks with jointly connected topologies," *Automatica*, vol. 48, no. 8, pp. 1783–1790, 2012.

[75] W. Yu, W. Ren, W. X. Zheng, G. Chen, and J. Lü, "Distributed control gains design for consensus in multi-agent systems with second-order nonlinear dynamics," *Automatica*, vol. 49, no. 7, pp. 2107–2115, 2013.

[76] H. Zhang, F. L. Lewis, and A. Das, "Optimal Design for Synchronization of Cooperative Systems: State Feedback, Observer and Output Feedback," *IEEE Transactions on Automatic Control*, vol. 56, no. 8, pp. 1948–1952, 2011.

[77] H. Zhang, F. L. Lewis, and Z. Qu, "Lyapunov, Adaptive, and Optimal Design Techniques for Cooperative Systems on Directed Communication Graphs," *IEEE Transactions on Industrial Electronics*, vol. 59, no. 7, pp. 3026–3041, 2012.

[78] H. Zhang, Z. Li, Z. Qu, and F. L. Lewis, "On constructing Lyapunov functions for multi-agent systems," *Automatica*, vol. 58, pp. 39–42, 2015.

[79] X. Zhang, K. Hengster-Movric, and M. Šebek, "Distributed Observer and Controller Design for Spatially Interconnected Systems," *IEEE Transactions on Control Systems Technology*, vol. 27, no. 1, pp. 1–13, 2019.

[80] X. Zhang, K. Hengster-Movric, M. Sebek, W. Desmet, and C. Faria, "Consensus-based distributed sensor fusion over a network," *Proceedings of the IEEE Conference on Control Technology and Applications*, 2017.

Publications and awards

Papers directly related to this thesis

Journal papers

Š. Knotek, K. Hengster-Movric, M. Šebek, "Distributed Estimation on Sensor Networks with Measurement Uncertainties," *IEEE Transactions on Control Systems Technology*, accepted in Sept. 2020.

Š. Knotek, K. Hengster-Movric, M. Šebek, "Distributed adaptive consensus protocol with decaying gains," *International Journal of Robust and Nonlinear Control*, vol. 30, no. 15, pp. 6166– 6188, July 2020.

Conference papers

Š. Knotek, "Fully distributed adaptive consensus protocol with bounded gains," *Proceedings of the 20th International Student Conference on Electrical Engineering (POSTER)*, May 2016.

Š. Knotek, K. Hengster-Movric, M. Šebek, "Distributed adaptive consensus protocol with decaying gains on directed graphs," *Proceedings of the 6th IFAC Workshop on Distributed Estimation and Control in Networked Systems (NecSys)*, vol. 49, no. 22, pp. 355-360, Sept. 2016.

Š. Knotek, K. Hengster-Movric, M. Šebek, "Distributed adaptive consensus protocol with Laplacian eigenvalues estimation," *Proceedings of the 21st International Conference on Process Control (PC)*, pp. 269-273, June 2017.

Papers not directly related to this thesis

Journal papers

I. Herman, Š. Knotek, J. Dostál and V. Prajzner, "Stability of Hydronic Networks With Independent Zone Controllers," *IEEE Transactions on Control Systems Technology*, vol. 26, no. 6, pp. 2214-2222, Nov. 2018.

Conference papers

R. Balogh, Š. Knotek, J. Šturcel, "Automated Testbed for Measurements and Evaluation of the Position Sensors Characteristics," *Proceedings of the 28th Conference Cybernetics & Informatics (K&I)*, Feb. 2016.

Awards

- Winner of the Best Poster Award on the *20th International Student Conference on Electrical Engineering (POSTER)* in May 2016.